Calcium-regulated transcription in plant innate immunity: interplay between CAMTA3 and MAPKs and CDPKs

Dissertation

Zur Erlangung des
Doktorgrades der Naturwissenschaften (Dr. rer. nat.)

der

Naturwissenschaftlichen Fakultät I – Biowissenschaften –

der Martin-Luther-Universität

Halle-Wittenberg

Vorgelegt

Von Frau Xiyuan Jiang

geb. am 31/12/1986 in Xi'an (China)

Gutachter:

Prof. Dr. Dierk Scheel – Leibniz-Institut für Pflanzenbiochemie

Prof. Dr. Klaus Humbeck – Martin-Luther-Universität Halle-Wittenberg

Prof. Dr. Hillel Fromm – Tel Aviv University

Verteidigungsdatum: 01. 07. 2019

Index

List of Abbreviations I
1 Introduction 1
1.1 Plant innate immunity 1
1.2 PAMP-Triggered Immunity (PTI) 2
1.2.1 Pathogen-Associated Molecular Patterns (PAMPs) 2
1.2.2 Pattern Recognition Receptors (PRRs) 2
1.2.3 PRR complex formation and activation 3
1.2.4 Cellular immune signaling activation 4
1.3 MAPK cascades in PTI 5
1.3.1 RLCKs link PRR complexes and MAPK cascade activation 5
1.3.2 MAPK cascades in PTI 6
1.3.3 MAPK substrates 7
1.4 Ca^{2+} signaling in PTI 8
1.4.1 Ca^{2+}/CaM regulate plant immunity 8
1.4.2 Calcium-dependent protein kinases (CDPKs) 9
1.5 Effector-triggered immunity 10
1.5.1 Pathogen effectors sabotage signaling components of PTI 10
1.5.2 ETI activation 10
1.6 CAMTA3: a Calmodulin-binding transcription factor involved in plant innate immunity 12
1.6.1 CAMTAs exist widely in eukaryotes and possess conserved functional domains 12
1.6.2 CAMTAs function as transcription factor by directly binding to a conserved motif in the promoters of target genes 13
1.6.3 *Arabidopsis* CAMTA3: a multi-functional regulator 13
1.6.3.1 CAMTA3 is a negative regulator of plant immunity 14
1.6.3.2 CAMTA3 is a transcriptional activator in cold stress and early general stress responses 16
1.6.3.3 CAMTA3 regulates other response pathways 17
1.6.3.4 CAMTA3 is guarded by two NLRs 18
1.6.4 CAMTA3 is a potential pathogen-responsive MAPK substrate 18
1.7 Aim of the present work 19
2 Materials and Methods 21

Index

2.1 Materials 21
2.1.1 Chemicals 21
2.1.2 Media 21
2.1.3 Bacteria 22
2.1.4 Plant materials and growth conditions 22
2.1.5 Plasmids 23
2.2 Methods 24
2.2.1 Molecular cloning 24
2.2.1.1 Gateway cloning 24
2.2.1.2 Classical cloning for promoter activity assay 25
2.2.1.3 Site-directed mutagenesis (SDM) 25
2.2.2 Plasmid preperation 26
2.2.3 Transformations 26
2.2.3.1 *E.coli* heat-shock transformation 26
2.2.3.2 *Agrobacterium tumefaciens* cold-shock transformation 27
2.2.3.3 *Agrobacterium-mediated* plant stable transformation 27
2.2.3.4 Isolation and transient transformation of *A. thaliana* mesophyll protoplasts 27
2.2.4 Identification of CAMTA3 overexpression homozygous line 27
2.2.4.1 Genomic DNA isolation and genotyping CAMTA3 overexpression line 27
2.2.4.2 Southern blot 28
2.2.4.3 Segregation analysis 28
2.2.5 Real-time PCR analysis 29
2.2.5.1 Total RNA extraction 29
2.2.5.2 cDNA synthesis 29
2.2.5.3 real-time PCR 29
2.2.6 Protoplast assays 29
2.2.6.1 Reporter activity assay 29
2.2.6.2 Protein stability assay 30
2.2.6.3 Protein phosphorylation-mediated mobility shift assay 30
2.2.6.4 Microscopy 31
2.2.7 Protein immunoprecipitation from plant materials 31
2.2.7.1 From protoplasts 31
2.2.7.2 Protein extraction from seedlings and adult plants 32

2.2.8 Western Blot 32
2.2.8.1 Phos-Tag™-based Western blot 32
2.2.8.2 Quantitative Western blot 32
2.2.9 Protein-protein interaction assays 34
2.2.9.1 Bimolecular fluorescence complementation 34
2.2.9.2 Split luciferase assay 34
2.2.9.3 Yeast two-hybrid 34
2.2.10 *In vitro* kinase assay with recombinant proteins 35
2.2.10.1 Expression of recombinant proteins in *E. coli* 35
2.2.10.2 Protein purification 35
2.2.10.3 *In vitro* phosphorylation assay 36
2.2.11 Phosphorylation site mapping 37
3 Results 39
3.1 CAMTA3 negatively regulates defense-related gene expression 39
3.1.1 Growth phenotypic comparison of Col-0, *camta3* mutants, and CAMTA3 overexpression lines 39
3.1.2 CAMTA3 expression is PAMP inducible 40
3.1.3 CAMTA3 negatively regulates expression of defense related genes 40
3.2 flg22 induces CAMTA3 phosphorylation and destabilization *in vivo* 44
3.2.1 flg22 induces a proteasome-mediated CAMTA3 degradation *in vivo* 44
3.2.2 CAMTA3 is phosphorylated upon flg22 elicitation *in vivo* 45
3.3 CAMTA3 interacts with and is phosphorylated by PAMP-responsive MAPKs 46
3.3.1 CAMTA3 interacts with PAMP-responsive MAPKs *in vivo* 46
3.3.2 CAMTA3 is phosphorylated by PAMP-responsive MAPKs *in vitro* 48
3.3.3 CAMTA3 is phosphorylated by MPK3 and MPK6 *in vivo* 48
3.4 CAMTA3 is phosphorylated by pathogen-regulated MPK3/6 at multiple sites, which mediate CAMTA3 protein destabilization 50
3.4.1 CAMTA3 is phosphorylated by MPK3 and MPK6 at multiple sites 50
3.4.2 MPK3/6-induced phosphorylation of CAMTA3 causes its destabilization 53
3.5 Potential mechanism of CAMTA3 destabilization mediated by phosphorylation 55
3.5.1 The reported interaction between CAMTA3 and SR1IP1 cannot be reproduced 55
3.5.2 CAMTA3 and SR1IP1 localize in different cell compartment 57
3.5.3 Phosphorylation induces CAMTA3 subcellular localization change 58

3.6 Additional kinases may be involved in flg22-mediated phosphorylation of CAMTA3 60
3.6.1 Additional flg22-responsive kinases may phosphorylate CAMTA3, and CPK5 is one of the candidates 60
3.6.2 CPKs, mainly from subfamily I, affected CAMTA3 phosphorylation status and stability mostly 61
3.7 CAMTA3 is an indirect target for CPK5 63
3.7.1 CAMTA3 interacts with CPK5 *in vivo* 63
3.7.2 CPK5 does not phosphorylate CAMTA3 *in vitro* 64
4 Discussion 67
4.1 CAMTA3: a hub in MAPK- and CDPK-mediated defense responses 67
4.2 CAMTA3 acts as either transcriptional repressor or activator 68
4.3 CAMTA3 is a crucial regulator for both PTI and ETI in *Arabidopsis* 70
4.4 Working model for the function of CAMTA3 in PTI regulation 73
5 Summary 75
6 Zusammenfassung 76
7 Bibliography 77
8 Appendix 91
8.1 Tables 91
8.2 Figures 96
Acknowledgements 97
Curriculum Vitae 99
Declaration 101

List of Abbreviations

3-AT	3-amino-1,2,4-triazole
µM	micromolar
A. thaliana	*Arabidopsis thaliana*
ABA	abscisic acid
ACS	1-aminocyclopropane-1-carboxylic acid synthase
AD	acivation domain
AEBSF	4-(2-Aminoethyl) benzenesulfonyl fluoride hydrochloride
ANK	ankyrin repeat
ATP	adenosine triphosphate
AVP	*Arabidopsis* V-PPase gene
Avr	avirulence
B. cinerea	*Botrytis cinerea*
BAK1	brassinosteroid insensitive 1-associated kinase 1
BiFC	bimolecular fluorescence complementation
BIK1	botrytis-induced kinase 1
BKK1	BAK1-LIKE1
bp	base pair
BR	brassinosteroid
BRI1	brassinosteroid-insensitive 1
BSK1	brassinosteroid-signaling kinase 1
CA	constitutively active
Ca^{2+}	calcium
CaM	calmodulin
CaMBD	CaM-binding domain
CAMTA	Calmodulin-binding transcription activator
CBB	coomassie brilliant blue
CBF/DREB	C-repeat-binding factor/dehydration responsive element-binding factor
CBL	calcineurin B-like protein
CC	coiled-coil
CDPK	calcium-dependent protein kinase
CEBiP	chitin-elicitor binding protein
CERK1	chitin-elicitor receptor kinase 1
CFP	cyan fluorescent protein
ChIP	chromatin immunoprecipitation
CHX	cycloheximide
CML	calmodulin and CaM-like protein
co-IP	co-immunoprecipitation
Col-0	wild-type *Arabidopsis* ecotype Columbia-0
CRCK3	calmodulin-binding receptor-like cytoplasmic kinase 3
CTAB	cetyltrimethylammonium bromide
CUL3	cullin3
DBD	DNA binding domain
DEX	dexamethasone
DNA	deoxyribonucleic acid
DSC	dominant suppressor of CAMTA3
DTT	dithiothreitol
E. coli	*Escherichia coli*
E3	ubiquitin ligase
EDR2	enhanced disease resistance 2
EDS1	enhanced disease susceptibility 1
EDTA	ethylenediaminetetraacetic acid
EFR	EF-Tu receptor
EF-Tu	translation elongation factor Tu
EGF	epidermal growth factor
EGTA	Ethylene-bis(oxyethylenenitrilo)tetraacetic acid
EIN3	ethylene insensitive 3
elf18	18 amino acid peptide derived from translation elongation factor Tu
EMSA	electrophoretic mobility shift assay
ERF104	ethylene response factor 104
ET	ethylene
ETI	effector-triggered immunity
ETS	effector-triggered susceptibility
EV	empty vector
FL	full length
flg22	22 amino acid peptide derived from flagellin
FLS2	flagellin sensing 2
GFP	green fluorescent protein
Glu-C	endoproteinase GluC
GO	gene ontology
GSR	general stress response
GST	glutathione-S-transferase
GUS	β-Glucuronidase
h	hour
HA	hemagglutinin
HEPES	4-(2-hydroxyethyl)-1-piperazineethanesulfonic acid
HHP2	heptahelical protein 2
His	histidine
HR	hypersensitive response
HRP	horsereadish peroxidase
IP	immunoprecipitation
IPTG	isopropyl β-D-1-thiogalactopyranoside
IR	insect regurgitant
JA	jasmonic acid
Kb	kilobase

kDa	kilodalton
LPS	lipopolysaccharide
LRR	leucine-rich repeat
LUC	luciferase
LYK5	LysM-containing receptor-like kinase 5
LysM	lysin motif
M	molar
m	meter
MAPK	mitogen-activated protein kinase
MAPKK/ MAP2K	MAPK kinase
MAPKKK/ MAP3K	MAPKK kinase
MBP	myelin basic protein
MEK	MAPK and ERK kinase
MEKK	MEK kinase
MES	2-(N-morpholino)ethanesulfonic acid
MG115	26S-proteasome inhibitor
min	minute
MKS1	MPK4 substrate 1
Mn^{2+}	manganese
MS	mass spectrometry
MS	Murashige-Skoog
NADPH	nicotinamide adenine dinucleotide phosphate
NB	nucleotide binding
NDR1	non-race-specific disease resistance 1
NHL10	NDR1/HIN1-like protein 10
NLR	nucleotide-binding leucine-rich repeat domain receptor
NLS	nuclear localization signal
nM	nanomolar
nm	nanometer
NRM	N-terminal repression module
OD_{600}	optical density at 600 nm
OE	overexpression
OGA	oligogalacturonic acid
OsCBT	Oryza sativa CaM-binding transcription factor
P. syringae	*Pseudomonas syringae*
PAD	phytoalexin deficient
PAGE	polyacrylamide gel electrophoresis
PAMP/ MAMP	pathogen- or microbe-associated molecular pattern
PAT1	protein associated with topoisomerase II 1
PBL1	*avr*PphB sensitive 1-like 1
Pc	*Petroselinum crispum*
PCR	polymerase chain reaction
PCRK1/2	PTI compromised receptor-like cytoplasmic kinase 1/2
PR gene	pathogenesis related gene
PRR	pattern recognition receptor
Pst	*Pseudomonas syringae* pv. t*omato*
PTI	PAMP-triggered immunity
R gene	resistance gene
RBOHD	respiratory burst oxidase homologue D
RIN4	RPM1-interacting protein 4
RLCK	receptor-like cytoplasmic kinase
RLK	receptor-like kinase
RLP	receptor-like protein
RNA	ribonucleic acid
ROS	reactive oxygen species
RSRE	rapid stress response element
RT	room temperature
RT-qPCR	quantitative reverse transcription PCR
SA	salicylic acid
SAR	systemic acquired resistance
SD	standard deviation
SD medium	synthetic defined dropout medium
SD-LW	SD medium-Leu-Trp
SD-LWAH	SD medium-Leu-Trp-Ade-His
SDM	site-directed mutagenesis
SDS	sodium dodecyl sulfate
SERK	somatic embryogenesis receptor kinase
SR	signal response
SR1IP1	SR1 interaction protein 1
SUMM	suppressor of mkk1 mkk2
T3SS	type III secretion system
TIR	Toll-interleukin 1 receptor
UBQ10	polyubiquitin 10
UT	untreat
WT	wild type
YFP	yellow fluorescent protein

1 Introduction

Plants need to resist harsh environmental conditions such as extreme temperatures, drought stress, flood, salt stress etc. On the other hand, there are constant threats from diseases/damage caused by a wide range of pathogens, which can cause an approximately 40% decrease of potential global crop yield (Schwessinger and Ronald 2012). For these reasons, our growing population will face food shortage in the future. Therefore, it is an important task in the field to develop by breeding or modern molecular tools crops with enhanced resistance to diseases to improve agricultural production. To achieve this goal, it is necessary to first understand the mechanisms of plant-pathogen interactions and plant immunity systems, which could help us develop more resistant plants.

1.1 Plant innate immunity

Unlike animals, plants are sessile, and do not possess a circulatory adaptive immune system. Therefore, plants develop and rely on an efficient innate immunity of each cell to defend against various pathogens invasion. The first line of plant innate immunity is initiated by perception of pathogen- or microbe-associated molecular patterns (PAMPs/MAMPs) via direct recognition by plant transmembrane pattern recognition receptors (PRRs). This recognition results in PAMP-triggered immunity (PTI) in the infected plant tissue. To overcome PTI and establish successful infection, pathogens evolve virulence effectors to interfere with host immune system components to suppress PTI, thus leading to effector-triggered susceptibility (ETS). In some resistant cultivars, effectors may be directly or indirectly recognized by intracellular nucleotide-binding (NB) leucine-rich repeat (LRR) domain receptors (NLRs) from host plant, resulting in stronger plant defense responses to inhibit growth of pathogens, typically referred to as effector-triggered immunity (ETI). ETI is usually accompanied by a hypersensitive cell death response (HR) at the infection site. Pathogens may subsequently gain additional effectors to counter ETI while plants may also acquire new NLRs for another round of ETI. A so-called “zigzag model” has been proposed to describe this evolutionary change of the immunity status (Jones and Dangl 2006).

1.2 PAMP-Triggered Immunity (PTI)

1.2.1 Pathogen-Associated Molecular Patterns (PAMPs)

In its natural habitat, plants face a wide range of biotic stresses from bacteria, fungi, oomycetes, and viruses. To defend against pathogenic microorganisms, plants need to recognize non-self which is mediated by PRR recognition of conserved PAMPs. PAMPs are conserved molecular structures derived from microorganisms, which are sufficient to trigger plant immune responses. Numerous PAMPs have already been shown to trigger plant defense responses. For instance, a well-studied bacterial PAMP is flg22, a 22-amino-acid epitope in the N terminal region of flagellin. Flg22 can be perceived by many plant species, such as *Arabidopsis*, tobacco, potato, and tomato (Felix et al. 1999). The ligand flg22 and its receptor flagellin sensing 2 (FLS2) is the first PAMP-PRR pair identified to initiate plant immune response (Gómez-Gómez and Boller 2000; Chinchilla et al. 2006). And interestingly, besides flg22, another flagellin epitope (flgII-28) was discovered and recognized by some solanaceous species, such as tomato, potato and pepper. Another receptor, FLS3, was recently discovered in tomato that recognizes this flgII-28 epitope (Hind et al. 2016). It also indicates that the pairs of PRR-PAMP are very specific. Elf18 is an 18 amino acid peptide derived from the conserved N-terminus of the translation elongation factor Tu (EF-Tu), one of the most abundant protein of bacteria. In *Arabidopsis* and some other plant species, this EF-Tu epitope is efficient to initiate defense responses such as production of reactive oxygen species (ROS), biosynthesis of stress hormone ethylene, and so on (Zipfel et al. 2006; Kunze et al. 2004). A well-studied fungal PAMP is chitin, a major component of fungal cell wall, which triggers defense responses in a wide range of plant species (Cao et al. 2014; Newman et al. 2013; Shibuya and Minami 2001). Similarly, the oomycete-derived Pep13 also acts as a PAMP in parsley and potato (Brunner et al. 2002).

1.2.2 Pattern Recognition Receptors (PRRs)

Plant genomes encode many PRRs that recognize diverse PAMPs. Receptor-like kinases (RLKs) and receptor-like proteins (RLPs) both function as plant PRRs. RLKs possess a ligand-binding ectodomain, a transmembrane domain, and an intracellular kinase domain, while RLPs lack the intracellular kinase domain. Based on their ligand-binding ectodomain, plant PRRs can be divided into mainly four different subgroups. For example, leucine-rich repeat (LRR)-containing PRRs, which is likely to bind peptides or proteins such as bacterial flagellin and elongation factor Tu (EF-Tu), lysin motifs (LysM) PRRs binding fungal

chitin or bacterial peptidoglycan, lectin-type PRRs recognizing extracellular ATP or bacterial lipopolysaccharides (LPS), and epidermal growth factor (EGF)-like PRRs recognizing oligogalacturonides derived from plant cell wall (Couto and Zipfel 2016; Boutrot and Zipfel 2017; Saijo, Loo, and Yasuda 2018). In *Arabidopsis*, one of the best-studied PRRs, flagellin sensing 2 (FLS2) is the receptor for flagellin or PAMP flg22. FLS2 is an LRR receptor-like kinase; it recognizes and physically interacts with flg22. *Arabidopsis fls2* mutant plants are impaired in flg22 binding and not able to induce defense responses such as ROS production, MAPK cascade activation, defense gene expression (Chinchilla et al. 2006; Gómez-Gómez and Boller 2000). Besides *Arabidopsis* (*Brassicaceae*), tomato (a *Solanaceae* plant) was also reported to recognize and respond to flg22, and tomato even responded to a shortened version of flg22, flg15, which is inactive in *Arabidopsis* (Chinchilla et al. 2006). Later, *LeFLS2* was also identified in tomato genome encoding the tomato flagellin receptor, which is the first functionally characterized *Arabidopsis* AtFLS2 ortholog (Robatzek et al. 2007). Similar to FLS2, EF-Tu receptor (EFR) is also a plant receptor-like kinase that acts as a PRR for EF-Tu in the plant innate immunity system. Unlike FLS2, EFR is only found in *brassicaceous* plants (Zipfel et al. 2006). The rice chitin-elicitor binding protein (OsCEBiP) plays a key role in perception and transduction of chitin signaling. OsCEBiP is a PRR containing extracellular lysin motif (LysM) domain for chitin binding, a transmembrane region and lacks an intracellular kinase domain (Kaku et al. 2006). Chitin-elicitor receptor kinase 1 (OsCERK1), which is a LysM-containing PRR with an intracellular kinase domain, was reported to form a receptor complex with OsCEBiP for chitin perception in rice (Hayafune et al. 2014). *Arabidopsis* AtCERK1 was first reported as a key chitin receptor for chitin perception (Miya et al. 2007). But AtLYK5 (LysM-containing receptor-like kinase 5) was later reported as the primary receptor for chitin with a much higher chitin binding affinity and forms a complex with AtCERK1 for chitin perception (Cao et al. 2014).

1.2.3 PRR complex formation and activation

Plant PRRs transduce signal from the extracellular to the intracellular side by forming complexes with a co-receptor to initiate downstream defense responses. Brassinosteroid insensitive 1-associated kinase 1 (BAK1) (also known as somatic embryogenesis receptor kinase 3, SERK3) is such a co-receptor that associates with LRR-type PRRs for PAMP perception. It was first known as a co-receptor for a plant hormone receptor brassinosteroid-insensitive 1 (BRI1) that is involved in developmental regulation through brassinosteroids (BRs) (Sun, Han, et al. 2013). For example, perception of bacterial flagellin (flg22)

and EF-Tu (elf18) by *Arabidopsis* LRR-receptor kinases FLS2 and EFR, respectively, induces a heteromerization with BAK1/SERK3 and other related proteins from SERK family, such as BAK1-LIKE1/SERK4 (BKK1/SERK4), to initiate plant defense (Sun, Li, et al. 2013; Chinchilla et al. 2007; Schulze et al. 2010; Roux et al. 2011). Analogous to the role of BAK1 and BKK1, CERK1 was also reported as a regulatory receptor kinase that form a chitin-dependent complex with LysM-containing PRRs, such as CEBiP in rice and LYK5 in *Arabidopsis* (Hayafune et al. 2014; Cao et al. 2014).

Receptor-like cytoplasmic kinases (RLCKs) that lack extracellular ectodomains, especially members from subfamily VII, were reported to play crucial rule in PTI and provide a link between extracellular ligand perception and downstream signaling (Couto and Zipfel 2016; Rao et al. 2018). The RLCK-VII family member BOTRYTIS-INDUCED KINASE 1 (BIK1) was reported to directly interact with FLS2 and BAK1 in an inactive state in the absence of flg22. Flg22-induced FLS2-BAK1 association and phosphorylation cause phosphorylation of BIK1, which in turn further phosphorylates the FLS2-BAK1 complex and dissociates from the complex to activate downstream signaling. For instance, BIK1 phosphorylates the NADPH oxidase respiratory burst oxidase homologue D (RBOHD) to activate ROS production. BIK1's closest homolog *avrPphB* sensitive 1-like 1 (PBL1) was also reported to interact with FLS2 and BIK1. Both are also required for signaling elicited by flg22, elf18 and chitin (Lu et al. 2010; Saijo, Loo, and Yasuda 2018; Zhang et al. 2010; Li et al. 2014; Ranf et al. 2014). Brassinosteroid-signaling kinase 1 (BSK1) and PTI compromised receptor-like cytoplasmic kinase 1/2 (PCRK1/2) also physically interact with FLS2, and are also regulators of PTI (Kong et al. 2016; Shi, Yan, et al. 2013; Shi, Shen, et al. 2013). The RLCK PBL27 associates with CERK1 and MAPKKK5. In response to chitin treatment, PBL27 phosphorylates MAPKKK5, which subsequently disassociates from PBL27 to interact and activate downstream MAPKKs and MPKs. This discovery provides the missing link between cell surface receptor and downstream intracellular responses (Yamada et al. 2016).

1.2.4 Cellular immune signaling activation

Upon ligand binding and PRR complex activation, RLCKs transmit immune signals to intracellular compartments and initiate several of the following signaling events within minutes. Production of extracellular reactive oxygen species (ROS) is one of the earliest events controlled by the NADPH oxidase RBOHD. As mentioned before, BIK1 (and the related PBL1) directly interacts with and phosphorylates RBOHD on specific sites upon PAMP elicitation in a calcium-independent manner. It is required and critical

for PAMP-induced ROS burst, which in turn controls stomata closure and restrict entry of bacteria into leaf tissues in *Arabidopsis* (Li et al. 2014; Kadota et al. 2014).

Rise of cytosolic Ca^{2+} level is another first output after PAMP perception. Besides directly activating RBOHD, BIK1 and PBL1 are also required for PAMP-induced cytosolic Ca^{2+} burst, which in turn promotes ROS production as well (Li et al. 2014; Ranf et al. 2014). Ca^{2+} burst also activates calcium-dependent protein kinases (CDPKs), which can also directly phosphorylate RBOHD at sites distinct from those targeted by BIK1 and activate RBOHD to trigger ROS production (Dubiella et al. 2013). Besides these, activation of mitogen-activated protein kinase (MAPK) cascades is also involved into inducing transcriptional changes to establish PTI (Couto and Zipfel 2016).

1.3 MAPK cascades in PTI

1.3.1 RLCKs link PRR complexes and MAPK cascade activation

Mitogen-activated protein kinase (MAPK) cascades are conserved signaling transduction modules in eukaryotes (yeasts, animals, and plants). MAPK cascades transduce extracellular stimuli into intracellular biochemical and physiological responses. During PTI, MAPK cascades are quickly activated within a few minutes upon pathogens or PAMPs perception, but the link between PRR complexes and MAPK cascade activation is, until recently, largely unknown. The first evidence was reported in rice. OsRLCK185 interacts with and is phosphorylated by chitin receptor OsCERK1 upon chitin perception. Loss of OsRLCK185 inhibits chitin-induced activation of OsMPK3/6, but not OsMPK4, which indicates that OsRLCK185 is required for chitin-induced MAPK activation in rice (Yamaguchi et al. 2013). However, this result didn't prove that RLCK185 is a direct upstream kinase of MAP3K in the MAPK cascade. The first direct evidence was reported in *Arabidopsis*. As mentioned in last chapter, PBL27 was reported to associate with both receptor CERK1 and MAPKKK5, and phosphorylates MAPKKK5. Chitin perception triggers disassociation between PBL27 and MAPKKK5, which in turn interacts with and activates downstream MAP2Ks and MPKs (Yamada et al. 2016). And more recently, another *Arabidopsis* RLCK BSK1, which interacts with FLS2 and important for PTI activation, was also reported to interact with and phosphorylate MAPKKK5, and positively regulates plant immunity (Yan et al. 2018). Recently, it was also reported that RLCK VII-4 family members, which act downstream of PRRs, directly phosphorylate MAPKKK5 and MEKK1 at specific sites to mediate

MPK3/MPK6 and MPK4 activation, respectively (Bi et al. 2018). These results provide the link between the cell surface receptor complexes and the activation of the MAPK cascade.

1.3.2 MAPK cascades in PTI

A MAPK cascade module consists of three kinases that are activated by successive phosphorylation. MAPKK kinases (MAP3Ks) phosphorylate MAPK kinases (MAP2Ks) through the conserved serine and/or threonine residues in their activation T-loop, which in turn phosphorylate and activate MAPKs through conserved threonine and tyrosine in the T×Y motif located in T-loop. Phosphorylated and activated MAPKs further phosphorylate their downstream substrates (e.g. transcription factors) to regulate their activity, stability or localization. In plants, MAPK cascades are associated with various developmental, growth, hormonal, and defense responses. (Group et al. 2002; Rasmussen et al. 2012). The current work will focus only on MAPK cascades implicated in plant innate immunity.

Arabidopsis genome encodes 20 MAPKs, 10 MAP2Ks, and approximate 60 MAP3Ks. Perception of PAMPs by PRRs activate at least two MAPK cascades. The best studied pathogen/PAMP responsive MAPKs are MPK3, MPK4, and MPK6, which are known to be activated during pathogens infection or PAMPs elicitation, such as flg22 and elf18. Subsequently, an MPK4 paralog, MPK11, was identified as the fourth PAMP-activated MAPK (Group et al. 2002; Pitzschke, Schikora, and Hirt 2009; Bethke et al. 2011; Felix et al. 1999; Zipfel et al. 2006). The first "complete" MAPK cascade, MEKK1-MKK4/5-MPK3/6, in *Arabidopsis* innate immunity was discovered by Asai *et al.*, which acts downstream of FLS2 (Asai et al. 2002). However, subsequent genetic evidence showed that in the *mekk1* knockout mutant, MPK3/6 is activated at a similar level to wild type upon flg22 treatment, while MPK4 is not activated. This indicates that MEKK1 acts upstream of MPK4 instead of MPK3/6 (Suarez-Rodriguez et al. 2007). Interestingly, two highly related MAP3K, MAPKKK3/5, were recently reported to form a kinase cascade with MKK4/5 and MPK3/6 to transduce defense signals from multiple PRRs, conferring resistance to bacterial and fungal pathogens in *Arabidopsis* (Bi et al. 2018; Sun et al. 2018). The other MAPK cascade, which is also activated in response to pathogen infection, is MEKK1-MKK1/2-MPK4. MEKK1 interacts with MKK1/MKK2, which in turn interact with MPK4 (Ichimura et al. 1998). And MEKK1, MKK1/MKK2 are required for flg22-triggered MPK4 activity, and they function together to regulate innate immune responses (Suarez-Rodriguez et al. 2007; Gao et al. 2008). The fourth PAMP/MAMP-activated MAPK MPK11 may also be involved in the same cascade,

because both MKK1 and MKK2 interact with and weakly phosphorylate MPK11 (Lee et al. 2008; Bethke et al. 2011).

1.3.3 MAPK substrates

The two *Arabidopsis* MAPK modules described above play diverse roles in plant defense against various pathogens. After activating MAPK cascades in response to PAMPs perception, activated MAPKs phosphorylate a variety of substrates to transduce upstream signals to trigger further defense responses. These substrates could be transcription factors or key biosynthetic enzymes. It may change target proteins properties such as protein stability, localization, enzyme activity, or the ability to bind to other partners, which can in turn change downstream processes such as a change of defense-related gene expression, secondary metabolic compounds biosynthesis, and so on (Zhang, Chen, and Harmon 2016). Therefore, it is important to identify the MAPK targets responsible for the numerous cellular processes that they are involved in.

The first *in vivo* identified MPK6 substrates are 1-aminocyclopropane-1-carboxylic acid synthase-2/6 (ACS2/6), which are the rate-limiting enzymes of ethylene biosynthesis (Liu and Zhang 2004), and later the same research group also identified ACS2/6 as the substrate of MPK3 (Han et al. 2010). Ethylene is a plant stress hormone and the production in plants is increased after biotic challenges via MPK3/6-mediated phosphorylation of ACS2/6 that stabilizes and elevates ACS2/6 activity. A mutation in *mpk6* partially blocks flg22-induced ethylene production, and in *mpk3 mpk6* double mutant, ethylene production is largely reduced in response to *Botrytis cinerea* inoculation (Liu and Zhang 2004; Han et al. 2010). Interestingly, MPK3/6 not only stabilize ACS2/6 protein level by phosphorylation but also promote *ACS2/6* expression through WRKY33 phosphorylation, which is a pathogen-inducible transcription factor that directly binds W-boxes in the *ACS2/6* promoter to positively regulate their transcription (Li et al. 2012). Besides regulating *ACS2/6* expression, phosphorylation of WRKY33 by MPK3/6 cascade is also required for camalexin biosynthesis in response to *B. cinerea* by promoting the expression of camalexin biosynthetic genes, such as *PAD3*. (Mao et al. 2011). MPK4 and one of its substrates, MKS1 (MPK4 substrate 1), are also involved in regulating *PAD3* expression through a trimeric WRKY33-MPK4-MKS1 complex. Pathogen infection triggers the phosphorylation of MKS1 by MPK4, and the MKS1-WRKY33 complex is released from MPK4. This may be coordinated with a subsequent or possibly parallel MPK3/6-mediated WRKY33 phosphorylation that promotes *PAD3* transcription and subsequently camalexin

biosynthesis (Mao et al. 2011; Rasmussen et al. 2012; Qiu et al. 2008; Andreasson et al. 2005). The MPK6 substrate ERF104 (Ethylene response factor) is a transcription factor and flg22-induced phosphorylation by MPK6 triggers ERF104 release from MPK6, thus allowing ERF104 to target downstream genes (Bethke et al. 2009). Another MPK4 substrate PAT1 (protein associated with topoisomerase II) plays a role in mRNA decapping and regulates immune response (Roux et al. 2015). While some pathogen-responsive MAPK substrates have been identified in plants, these are just the tip of the iceberg and there is a need to identify further substrates.

1.4 Ca^{2+} signaling in PTI

1.4.1 Ca^{2+}/CaM regulate plant immunity

Plants use calcium as a secondary messenger to control diverse developmental processes and to respond to diverse environmental stimuli such as light, drought, temperature, salt stress, pathogens and so on (Cheval et al. 2013; Galon, Finkler, and Fromm 2010). Ca^{2+} plays a crucial role in both PTI and ETI. As mentioned in the previous chapter, Ca^{2+} influx is one of the earliest signaling events after pathogens/PAMPs perception (Lecourieux, Ranjeva, and Pugin 2006). Virulent pathogens and PAMPs typically induce a rapid and transient increase of cytosolic Ca^{2+} level, while avirulent pathogen strains induce a second and sustained Ca^{2+} response (Cheval et al. 2013). Perception of PAMPs or other elicitors elevates Ca^{2+} levels not only in the cytosol, but also in nuclear and other cellular compartments. These stimulus-specific, rapid and transient patterns with spatio-temporal features of Ca^{2+} signals are referred to as Ca^{2+} signatures (Cheval et al. 2013). Ca^{2+} sensor proteins decode the Ca^{2+} signatures by directly binding Ca^{2+} with their EF-hand motifs and transduce the Ca^{2+} signals into downstream cellular responses. The plant Ca^{2+} sensor proteins are classified into three subfamilies: Calmodulin and CaM-like proteins (CMLs), Ca^{2+}-dependent protein kinases (CDPKs) and calcineurin B-like proteins (CBLs) (DeFalco, Bender, and Snedden 2010). Among these, involvement in pathogen or PAMP response has so far mostly been associated with CaMs and CDPKs.

CaM is highly conserved in eukaryote, and seven CaM isoforms are encoded in *Arabidopsis* genome (Ranty, Aldon, and Galaud 2006). A conformational change of CaM induced by Ca^{2+} binding results in an interaction with downstream targets that contain CaM-binding domain (CaMBD), such as transcription

factors, kinases or metabolic enzymes (DeFalco, Bender, and Snedden 2010; Cheval et al. 2013). An example of CaM-regulated transcription factor is CAMTA3 (for a detailed description, see Chapter 1.6).

1.4.2 Calcium-dependent protein kinases (CDPKs)

CDPKs (also abbreviated as CPKs) are calcium-regulated serine/threonine kinases and unique to plants. They have both Ca^{2+} sensing and signaling (i.e. phosphorylation) function in a single protein. Five domains can be defined in a CDPK: (i) an N-terminal variable domain, (ii) a conserved catalytic serine/threonine kinase domain, (iii) a pseudosubstrate-containing autoinhibitory junction domain that inhibits kinase activity by interaction with the active site, (iv) a CaM-like domain with four functional Ca^{2+}-binding EF-hands, and (v) a C-terminal variable domain (DeFalco, Bender, and Snedden 2010). 34 CDPKs are encoded in the *Arabidopsis* genome, and divided into four subgroups according to sequence similarity. CDPKs localize to plasma membrane, cytosol, nucleus and other subcellular compartments, which may change dynamically in response to diverse stimuli (Boudsocq and Sheen 2013).

Multiple *Arabidopsis* CDPKs are transiently activated upon perception of PAMPs such as flg22, including CPK4, CPK5, CPK6 and CPK11 from subgroup I, and are required for inducing the expression of the flg22-inducible *NHL10* gene. Kinase activities induced by flg22 treatment are minimal in an *fls2* mutant or in the presence of Ca^{2+} channel blocker, suggesting that the CDPKs are activated downstream of FLS2 and requires Ca^{2+} (Boudsocq et al. 2010). Comparison of microarray data showed considerable overlap of genes regulated by overexpressing constitutively-active CPK5/CPK11 with early PAMP-regulated genes, indicating that these CDPKs play a role in PAMP-induced transcriptional reprogramming. CDPKs and MAPKs differentially as well as coordinately regulate flg22-responsive gene expression; the regulation may be MAPK-specific, CDPK-specific or synergistically controlled by both MAPK/CDPK (Boudsocq and Sheen 2013; Boudsocq et al. 2010). CPK4/5/6/11 are reported to be positive regulators in PAMP signaling. Besides regulating expression of flg22-induced genes, CDPKs also affect ROS production. In *Arabidopsis*, CPK5 is reported to directly phosphorylate the NADPH oxidase RBOHD to regulate ROS production in response to flg22 (Dubiella et al. 2013). Moreover, the *cpk* mutants are impaired in both basal and flg22-induced resistance to bacterial pathogen (Boudsocq et al. 2010). Only very few substrates of the indicated CDPKs are known. Besides RBOHD, the WRKY8/28/48 transcription factors have been shown to be phosphorylated by CPK4/5/6/11 (Gao et al. 2013).

1.5 Effector-triggered immunity

1.5.1 Pathogen effectors sabotage signaling components of PTI

The above chapters describes several key elements of PTI. However, PTI can be overcome by successful pathogens that have evolved virulence factors, so-called effectors, to dampen basal defenses. Effectors are directly delivered into host cells. For example, Gram-negative pathogenic bacteria use a type III secretion system (T3SS) to inject effector proteins into host cells (Galán et al. 2014). The delivered effector proteins target and change the characteristics of host immune system components at multiple levels. For example, effectors may target PRR complex components. *Pseudomonas. syringae* effector AvrPto was reported as a kinase inhibitor that interacts with and dephosphorylates receptor kinases like FLS2 and EFR (Xiang et al. 2008). AvrPto and AvrPtoB also bind to BAK1, the co-receptor of multiple PRRs, and to disrupt the ligand-dependent association of BAK1 with PRRs during infection (Shan et al. 2008). The *Xanthomonas campestris* effector AvrAC inhibits PTI by targeting BIK1 and reducing its kinase activity after adding uridine 5'-monophosphate to phosphorylation sites of the BIK1 activation loop (Feng et al. 2012). Some effectors target elements of the MAPK cascades. For instance, the *P. syringae* effector HopAI1 is a phosphothreonine lyase that inactivates MPK3, 4, 6 by removing the phosphate moiety (Zhang et al. 2007; Zhang et al. 2012) or AvrRpt2 that prevents flg22-induced activation of MPK4/11 (Eschen-Lippold et al. 2016). Other targets of effectors include disruption of immunity-associated vesicle trafficking (Xin and He 2013). Pathogens also produce small molecule effectors such as coronatine that mimics jasmonic acid (JA) to overcome salicylic acid (SA)-dependent defenses and induce stomatal opening (BROOKS, BENDER, and KUNKEL 2005).

1.5.2 ETI activation

While originally functioning as virulence factors, effector proteins may "betray" pathogens through the evolution of disease resistance (*R*) genes in host plants. Such *R* genes encode intracellular nucleotide-binding (NB) leucine-rich repeat (LRR) domain receptors (NLRs) that recognize the pathogen effectors or the modifications they generate. The recognized effector is termed an avirulence (Avr) protein. Plant NLRs are classified into two groups based on their N-terminal domains: those with a Toll-interleukin 1 receptor (TIR) domain are called TIR-NLRs, and others with a coiled-coil (CC) domain are called CC-NLRs (Takken and Tameling 2009; Elmore, Lin, and Coaker 2011). Two ways of effector recognition exist, either direct

physical interaction between NLR and the effector or in most cases, indirect interaction mediated by effector-induced modifications of another host protein (Elmore, Lin, and Coaker 2011). This host target monitored by NLR is often called a “guardee” and the indirect recognition concept as “guard hypothesis” (van der Hoorn and Kamoun 2008). Such intracellular perception induces a stronger resistance response termed effector-triggered immunity (ETI), which is often associated with a local programmed cell death (known as the hypersensitive response, HR) that restricts pathogen growth at the infection site (Jones and Dangl 2006).

An example of host target of effectors that is guarded by NLRs is RIN4 (RPM1-interacting protein 4), which is manipulated by three bacterial effectors (AvrRpm1, AvrB, and AvrRpt2) and guarded by two Arabidopsis NLRs (RPM1 and RPS2). AvrRpm1 and AvrB associate with and cause RIN4 phosphorylation, and this modification activates RPM1-mediated immunity (Mackey et al. 2002). AvrRpt2, on the other hand, cleaves and causes RIN4 degradation by its cysteine protease activity (Axtell et al. 2003). Cleavage of RIN4 activates RPS2-mediated immunity (Mackey et al. 2003; Axtell and Staskawicz 2003). Thus, loss of RIN4 can result in an RPS2-dependent autoimmune phenotype, including dwarfism, spontaneous dead cell lesion formation, constitutive expression of *PR* genes, and enhanced resistance to pathogen infection (Mackey et al. 2002).

Similar to RIN4, another example of the guard hypothesis is the monitoring of components of the MEKK1-MKK1/2-MPK4 cascade. An autoimmune phenotype is also shown in *mekk1*, *mkk1 mkk2*, and *mpk4* mutants and is dependent on the NLR SUMM2 (suppressor of mkk1 mkk2 2). The *P. syringae* effector HopAI1 targets MPK4 cascade by inhibiting MPK4 kinase activity and triggers SUMM2 activity. Thus, disruption of MPK4 cascade can induce the activation of SUMM2-mediated immune responses (Zhang et al. 2012; Thulasi Devendrakumar, Li, and Zhang 2018). However, SUMM2 does not interact with MPK4, but senses the disruption of MPK4 cascade via the phosphorylation status of CRCK3/SUMM3 (calmodulin-binding receptor-like cytoplasmic kinase 3) (Zhang et al. 2017). Hence, this last example shows that besides roles in PTI, calcium signaling is also involved in ETI. Recently, one of the calcium/CaM-regulated transcription factor, CAMTA3, was shown to be also a “guardee” (Lolle et al. 2017). CAMTA3 is subject of this thesis and is described in details below.

1.6 CAMTA3: a Calmodulin-binding transcription factor involved in plant innate immunity

1.6.1 CAMTAs exist widely in eukaryotes and possess conserved functional domains

Calmodulin-binding transcription activators (CAMTAs) exist in various eukaryotes but not in prokaryotes. In humans, HsCAMTA2 acts as a transcriptional coactivator together with another transcription factor to promote expression of cardiac growth and remodeling genes, and to induce cardiac hypertrophy (Song et al. 2006). HsCAMTA1 is also involved in human tumor suppression (Barbashina et al. 2005). And in flies, *DmCAMTA* encodes a transcription activator important for eye functions, where CaM binding stimulates DmCAMTA activity and is crucial for deactivation of rhodopsin, and phototransduction in response to light signals (Han et al. 2006). In plants, a CAMTA homolog, NtER1, was firstly reported in *Nicotiana tabacum*. CaM binds with high affinity to NtER1 in a calcium-dependent manner. *NtER1* expression is rapidly induced by ethylene and during senescence (Yang and Poovaiah 2000). A rice homolog, designated as OsCBT (Oryza sativa CaM-binding transcription factor) has transcriptional activity (Choi et al. 2005) and acts as a negative regulator of disease resistance against *Xanthomonas oryzae* and *Magnaporthe grisea* (Koo et al. 2009). In *Arabidopsis*, six AtCAMTAs are known. They are involved in many different signaling pathways induced by environmental stimuli/signals such as extreme temperatures, high salt, drought, UV, or some plant hormones (e.g. ABA, ethylene, SA) and also biotic stresses (Fig. 1-1) (Finkler, Ashery-Padan, and Fromm 2007).

The CAMTA proteins share similar functional domain organization: (i) there is a highly conserved CG-1 domain in the N-terminus of the protein, which is a sequence-specific DNA-binding domain and also includes a predicted nuclear localization signal (NLS). (ii) The TIG domain is thought to be involved in non-specific DNA contacts and also protein dimerization. (iii) The Ankyrin (ANK) repeats are present, which typically participate in protein-protein interactions. (iv) As calmodulin-binding proteins, CAMTAs also contain one or more Ca^{2+}-dependent CaM-binding domains and variable number of IQ motifs, which are also involved in binding Ca^{2+}/CaM and CaM-like proteins (Fig. 1-1) (Finkler, Ashery-Padan, and Fromm 2007).

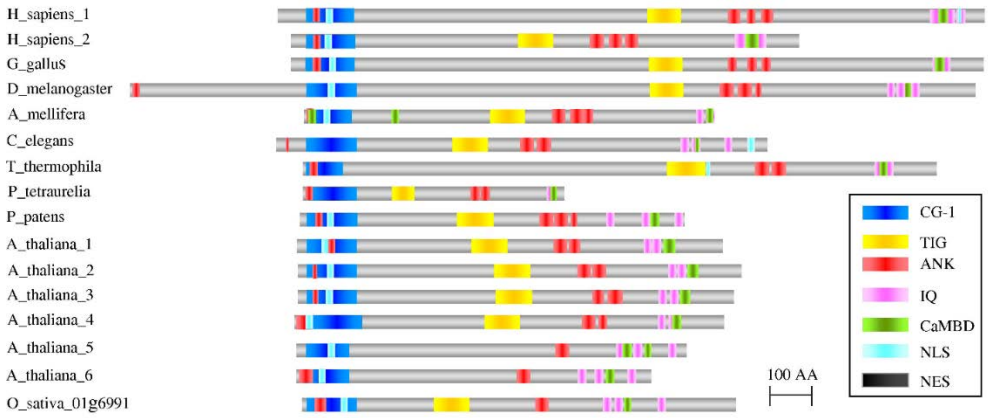

Fig 1-1. Schematic representation of CAMTAs domains. CAMTAs exist widely in eukaryotes and possess conserved functional domains. (Finkler, Ashery-Padan, and Fromm 2007).

1.6.2 CAMTAs function as transcription factor by directly binding to a conserved motif in the promoters of target genes

Both subcellular fractionation (Bouché et al. 2002) and microscopy studies (Yang and Poovaiah 2002) show CAMTAs to localize in the nucleus. The first evidence that CAMTAs function as transcription factors came from experiments where *Arabidopsis* AtCAMTA1 and two human CAMTAs (HsCAMTA1/2) were able to activate transcription in yeast (Bouché et al. 2002). Further, *in vitro* gel retardation assay shows that *Arabidopsis* AtCAMTA3 targets a specific DNA element via the CG-1 domain. This specific *cis*-element is a 6-bp conserved motif with the sequence (A/C/G)CGCG(G/T/C) (Yang and Poovaiah 2002). *In vivo* transcription activation function of CAMTAs was subsequently supported in plant-based studies. In a GUS reporter assay, rice CAMTA homolog OsCBT activates a synthetic promoter (containing the CGCG element) in protoplasts (Choi et al. 2005). In suspension *Arabidopsis* cells, CAMTA1 activates *AVP1* (*Arabidopsis* V-PPase gene) expression by binding to its CGCG box region and this is the first identification of a downstream gene directly regulated by CAMTA (Mitsuda, Isono, and Sato 2003).

1.6.3 *Arabidopsis* CAMTA3: a multi-functional regulator

The six *Arabidopsis* CAMTA proteins AtCAMTA1-6 (previously named Signal Response 1-6, AtSR1-6) have 43-78% sequence similarities and are especially conserved (> 90% similarity) in the N-terminal CG-1 DNA binding region and C-terminal CaM-binding region. Besides expression in different developmental stages,

some *CAMTAs* respond rapidly to various abiotic and biotic challenges (Yang and Poovaiah 2002). For example, *AtCAMTA1* was reported to respond to drought (Pandey et al. 2013), salt and heat shock stresses (Galon et al. 2010). It was also reported that AtCAMTA1- 3 repress SA biosynthesis at warm temperatures and they function together to positively regulate freezing tolerance by inducing *CBF1-3* and other early cold-induced genes (Kim et al. 2013; Doherty et al. 2009). AtCAMTA3 and 5 also function in different cold-signaling pathway in response to rapid temperature decrease (Kidokoro et al. 2017). Additionally, AtCAMTAs were also reported to respond to wounding, abscisic acid, ethylene and methyl jasmonate (Yang and Poovaiah 2002).

1.6.3.1 CAMTA3 is a negative regulator of plant immunity

AtCAMTA3 (AT2G22300) is one of best-studied CAMTAs. The basal expression level of *CAMTA3* is low but can be induced by different stress signals (Yang and Poovaiah 2002). CAMTA3 is thought to be a suppressor of defense responses in *Arabidopsis*. Transcriptomics analysis of two T-DNA insertion knockout mutants (*camta3-1* and *camta3-2*) revealed 99 up-regulated genes in comparison to Col-0, of which a large portion (32 genes) are defense-related genes (e.g. *PRs*, *NDR1*, *PAD4*, *ZAT10* and various *WRKYs*) (Galon et al. 2008). Both *camta3* mutants show temperature-dependent autoimmune phenotypes, which disappear when grown at higher temperature (25-27^{o}C). At 19-21^{o}C, *camta3* mutants display reduced growth, chlorotic lesions, and constitutive expression of *PR* genes (systemic acquired resistance-associated marker genes). Hypersensitive response- and SAR-related features such as accumulation of SA, ROS and autofluorescent compounds are also increased. Furthermore, *camta3* mutants show enhanced resistance against virulent *Pseudomonas syring*ae pv. *tomato* DC3000 (*Pst* DC3000), avirulent *Pst* DC3000 (*AvrRpt2*), and the fungal pathogens *Botrytis cinerea* and powdery mildew *Golovinomyces cichoracearum* (Fig. 1-2 A) (Galon et al. 2008; Du et al. 2009; Nie et al. 2012).

CAMTA3 negatively regulates plant defense by directly binding to the promoter of targeted defense-related genes at specific “CGCG”-containing *cis*-elements. An example is *Enhanced Disease Susceptibility 1* (*EDS1*), a positive regulator of SA biosynthesis and required for TIR-NLR-mediated resistance. *In vitro* electrophoretic mobility shift assay (EMSA) and *in vivo* chromatin immunoprecipitation (ChIP) assay indicated a direct interaction between CAMTA3 and *EDS1* promoter fragment covering the CGCG box. Promoter-luciferase-reporter assay showed that CAMTA3 represses *EDS1* expression, which would negatively regulate SA-mediated plant immunity (Du et al. 2009). Besides *EDS1*, CAMTA3 also negatively regulate expression of *NDR1* (*non-race-specific disease resistance 1*) and *EIN3* (*ethylene insensitive 3*) by

interacting with CGCG *cis*-elements in their promoters (Fig. 1-2 B) (Nie et al. 2012). NDR1 is required for CC-NLR-mediated resistance while EIN3 is a key component of ET signaling.

Interestingly, two independent genetic screens led to an identical gain-of-function mutant, *camta3-3D*, with an A855V amino acid exchange located in the first IQ motif (Nie et al. 2012; Jing et al. 2011). One screen was searching for suppressors of *edr2*-mediated resistance to powdery mildew (Nie et al. 2012), while the second screen was for SAR deficient mutants (Jing et al. 2011). This *camta3-3D* mutation fully suppresses *edr2*-mediated dramatic necrotic lesion formation, cell death, H_2O_2 accumulation and induced *PR* genes expression upon mildew infection and *edr2*-mediated ET-induced senescence (Nie et al. 2012), and it also displays strong SAR defects (Jing et al. 2011). Notably, this gain-of-function mutant differs phenotypically from the *camta3* null allele. It is larger than *camta3* and Col-0 and do not show spontaneous chlorotic lesions. *PR* genes expression and SA levels are also lower in *camta3-3D* than in *camta3* and Col-0. Opposite to the *camta3* knock-out, *camta3-3D* displays enhanced susceptibility to virulent and avirulent bacterial strains and fungal pathogen compared to *camta3* and Col-0. (Nie et al. 2012). Thus, multiple lines of evidence demonstrate that CAMTA3 is a negative regulator of plant immune responses.

In agreement to its role as a negative regulator, virulent *Pst* DC3000 and avirulent *Pst* DC3000 (containing *avrRpt2* or *avrRPS4*) induce CAMTA3 degradation (Fig. 1-2 C) (Zhang et al. 2014). This removal of a defense suppressor requires SR1IP1 (SR1 interaction protein 1; note that SR1 is the alternative name for CAMTA3). SR1IP1 is thought to act as a substrate adaptor for CAMTA3 to cullin3 (CUL3)-based E3 ubiquitin ligase. It triggers CAMTA3 ubiquitination, thus leading to degradation via the 26S proteasome pathway, and thereby positively regulates plant defense.

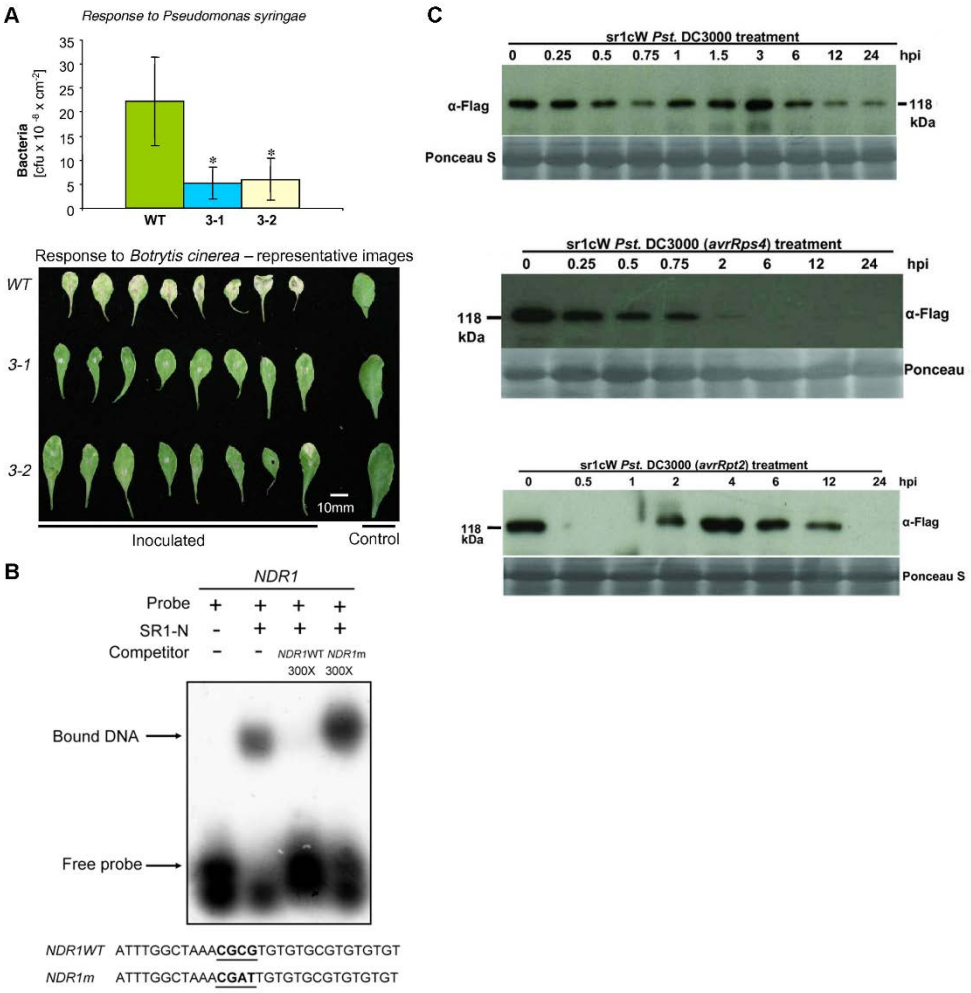

Fig 1-2. CAMTA3 is a negative regulator of plant immunity and destabilized upon pathogen infection. A. *camta3* mutants (*3-1* and *3-2* stand for *camta3-1* and *camta3-2*) show enhanced resistance to bacterial pathogen (*Pseudomonas syringae* pv. *tomato* DC3000) after spray infection of plants with a bacterial suspension of 5×10^7 cfu ml^{-1}, and fungal pathogen (*Botrytis cinerea*) after inoculation with spores (Galon et al. 2008). **B.** CAMTA3 directly binds to the promoter fragment of *NDR1* by *in vitro* EMSA (Nie et al. 2012). **C.** CAMTA3 is degraded specifically induced by pathogen challenge (SR1 stands for CAMTA3) (Zhang et al. 2014).

1.6.3.2 CAMTA3 is a transcriptional activator in cold stress and early general stress responses

In contrast to CAMTA3's negative role in defense gene expression described above, CAMTA3 was initially reported to act as transcriptional activator in cold stress response. The *Arabidopsis CBF* cold response pathway is the central regulatory pathway in cold acclimation, and three *Arabidopsis* transcription factor encoding *CBF* genes are rapidly induced by low temperature (Gilmour et al. 1998). *ZAT12* is also a cold-responsive-gene (Vogel et al. 2005). Notably, CGCG *cis*-elements are present in the promoters of *CBF1*, *CBF2*, and *ZAT12*, but not *CBF3*. Cold-induced transcripts accumulation of *CBF1*, *CBF2* and *ZAT12* are

dramatically decreased in a *camta3* mutant compared to Col-0. A *GUS*-reporter driven by the promoter fragment from *CBF2* (that includes the CGCG box) showed reduced levels of *GUS* transcripts and GUS activity in a *camta3* background. The direct interaction between CAMTA3 and *CBF2* promoter (tested using *in vitro* EMSA) supports the interpretation that CAMTA3 acts as a transcriptional activator to positively induce *CBF2* expression (Doherty et al. 2009).

CAMTA3 was also reported as a transcriptional activator in the *RSRE* (rapid stress response element)-driven general stress response (GSR) (Bjornson et al. 2014; Benn et al. 2014), which is rapid and transient response to various abiotic and biotic stresses. The RSRE *cis*-element deduced from the GSR gene promoters in *Arabidopsis* is *vCGCGb* (Walley et al. 2007) and thus identical to the element recognized by CAMTAs (Yang and Poovaiah 2002). Transgenic *Arabidopsis* plants with a luciferase reporter driven by a synthetic promoter containing four copies of *RSRE* respond to various abiotic stresses (e.g. mechanical wounding and cold treatment) and biotic stresses including biological elicitors (e.g. oligogalacturonic acid (OGA), insect regurgitant (IR) and flg22) or cabbage looper feeding or *Botrytis cinerea* infection (Benn et al. 2014; Walley et al. 2007). Furthermore, CAMTA3 induces reporter activity driven by *RSRE*, and a *camta3-4* mutant (containing a premature stop codon) displays reduced *RSRE*-controlled reporter activity (Benn et al. 2014; Bjornson et al. 2014). All these results indicate that CAMTA3 positively regulates early stress responses

1.6.3.3 CAMTA3 regulates other response pathways

Besides functions described before, CAMTA3 also functions in many other signaling pathways. A recent RNA-seq-based gene expression study identified about 3000 CAMTA3-regulated genes (Prasad et al. 2016), much more than previous microarray study (Galon et al. 2008). Gene ontology (GO) enrichment of up-regulated genes in the *camta3* mutant are mostly associated with plant defense response to biotic factors, but additionally also salt stress-responsive genes. It was also shown that *camta3* mutant are more tolerant to salt stress and *in vivo* ChIP assay suggests that CAMTA3 binds to promoters of the salt-responsive genes that are upregulated in the *camta3* background. Thus, CAMTA3 is a negative regulator in response to salt (Prasad et al. 2016). CAMTA3 also positively regulate herbivore-induced plant response by controlling wound-induced JA biosynthesis, which is modulated by endogenous SA levels (Laluk et al. 2012; Qiu et al. 2012).

1.6.3.4 CAMTA3 is guarded by two NLRs

Recently, the temperature-dependent autoimmune phenotypes of *camta3* was found to be triggered by the activation of two TIR-type NLR proteins, DSC1 (dominant suppressor of CAMTA3 1) and DSC2. This contests the above interpretation that CAMTA3 negatively regulates immune response by directly binding of the gene promoter and suppressing of the downstream target genes (*EDS1*, *NDR1* and *EIN3*). Autoimmunity in *camta3* is suppressed when DSC1 and DSC2 are missing, while overexpressing DSC1/2 triggers strong and rapid HR, which is reduced by co-expression of CAMTA3. DSC1/2 and CAMTA3 associate to form a complex, where DSC1/2 are inactive when CAMTA3 is present and are activated in the absence of CAMTA3. Thus, CAMTA3 is a plant guardee, with DSC1/2 monitoring for malfunction in CAMTA3 caused either by mutations or through yet-to-be discovered modification by pathogen effectors (Lolle et al. 2017; Yuan et al. 2018)

1.6.4 CAMTA3 is a potential pathogen-responsive MAPK substrate

To identify putative MAPK substrates, plants expressing dexamethasone (DEX)-inducible constitutively-active form of the tobacco MEK2 (NtMEK2^{DD}) was used to synthetically activate MPK3/6 and collected for analysis of *in vivo* MAPK substrates. With a combination of phosphopeptide enrichment and MS (mass spectrometry), hundreds of putative MAPK substrates were identified and interestingly, CAMTA3 was detected to be phosphorylated at serine 8 (Hoehenwarter et al. 2013). In addition, five phosphopeptides with motifs typical for MAPK phosphorylation sites (so-called (S/T)P motif) are annotated in the PhosPhAt database for CAMTA3. PhosPhAt is an *Arabidopsis* database for phosphorylation sites identified in published large- and medium-scale phosphoproteomics experimental dataset (Heazlewood et al. 2008). In particular, the CAMTA3 phosphorylation data were taken from a variety of experiments including treatment with flg22 (Benschop et al. 2007), abscisic acid (ABA) (Umezawa et al. 2013) or auxin (Zhang et al. 2013) and DNA damage response through irradiation (Roitinger et al. 2015). Thus, CAMTA3 is potentially phosphorylated by MAPKs after PAMP treatment.

1.7 Aim of the present work

From the studies introduced above, the *Arabidopsis* CAMTA3 appears to function as a transcriptional repressor for genes involved in plant immunity and salt tolerance but acts as a transcriptional activator when bound to promoters of genes involved in cold acclimation or general stress response. How CAMTA3 differentially regulates these signaling response pathways remains unclear. In this work, I will focus on how CAMTA3 negatively regulates plant defense pathways, especially during PTI. Since post-translational modifications may potentially modulate CAMTA3 function(s), the working hypothesis is to investigate if protein phosphorylation plays a role in its regulation. In this study, the major objectives of the current study are:

- To validate phosphorylation of CAMTA3 by MAPKs and other kinases (e.g. CPK5)
- To identify the phosphorylation sites of CAMTA3 by indicated kinases.
- To study the effects of phosphorylation by indicated kinases on CAMTA3.

2 Materials and Methods

2.1 Materials

2.1.1 Chemicals

All chemicals were used in analytical quality, if not specified differently. Chemicals and antibiotics used in this study were ordered from Carl Roth (Karlsruhe, Germany), SIGMA Aldrich (St. Louis, USA), Merck KGaA (Darmstadt, Germany), Serva (Heidelberg, Germany), BioRad (Hercules, USA) and Applichem GmbH (Darmstadt, Germany). Plant, yeast and bacterial media ingredients were ordered from BD (Franklin Lakes, USA), Duchefa (Haarlem, Netherland) and MP Biomedicals (Solon, USA). Enzymes were ordered by Thermo Fisher Scientific (Waltham, USA), New England Biolabs (Ipswich, USA) and Yakult Phamaceuticals (Tokyo, Japan). Antibodies were ordered from Biolegend (San Diego, USA), SIGMA Aldrich (St. Louis, USA), Cell Signaling technology (Danvers, USA), Takara (Kusatsu, Japan) and IBA Lifesciences (Goettingen, Germany). Primers were ordered from Eurofins Genomics (Ebersberg, Germany). Flg22 was synthesized in house by Petra Majovsky (Hoehenwarter group, IPB Halle) using an EPS221 peptide synthesizer (Abimed).

2.1.2 Media

Luria-Bertani Medium (LB Medium):

- Yeast extract (5 g/l), Tryptone (10 g/l), NaCl (5 g/l)
- For solid medium 15 g/l agar was added

Half strength Murashige-Skoog Medium (½ MS Medium)

- MS medium including B5 vitamins (Duchefa Biochemie) (2.2 g/l), sucrose (2.5 g/l), MES (0.2 g/l); pH 5.7 (adjusted with KOH)

YPAD Medium

- Yeast extract (10 g/l), Difco Peptone (20 g/l), Adenine hemisulphate (100 mg/l)
- After autoclaving, filtered sterilized glucose solution was added to the final concentration of 2%
- For solid medium 20 g/l agar was added

Synthetic Defined Dropout Medium (SD-Medium)

- SD Medium-Leu-Trp (SD-LW) (MP Biomedicals) (27.4 g/l)
- SD-Medium-Ade-His-Leu-Trp (SD-LWAH) (MP Biomedicals) (27.4 g/l), for higher stringency. 20-100 mM of 3-Amino-1,2,4-triazole was added
- For solid medium 20 g/l agar was added

2.1.3 Bacteria

The *Escherichia coli* strain DH5α (Thermo) was used for molecular cloning, and the strain KRX (Promega) were used for expression of recombinant fusion proteins. Strain DB3.1 was used for propagation of plasmids containing the *ccd*B gene such as the destination vectors for the Gateway system (Invitrogen). All strains were grown in LB-medium supplemented with the appropriate antibiotics at 37°C if not specified differently. *Agrobacterium tumefaciens* strain GV3101 was used for *Agrobacterium*-mediated stable transformation of *Arabidopsis thaliana* and grown in LB-medium at 28°C supplemented with the appropriate antibiotics.

Antibiotics were used in the following concentrations: Ampicillin (100 µg/ml), Carbenicillin (50 µg/ml) Gentamycin (15 µg/ml), Kanamycin (50 µg/ml), Rifampicin (75 µg/ml) and Spectinomycin (50 µg/ml).

2.1.4 Plant materials and growth conditions

Arabidopsis thaliana ecotype Columbia (Col-0), mutants and overexpression lines for experiments were grown on soil or in phytocabinets and phytochambers under short-day condition (8-hour-light/16-hour-dark photoperiod, at 20-22°C and 60% humidity). Plants for screening or setting seeds were grown in phytocabinets or greenhouse under long day conditions (16-hour-light/8-hour-dark at 20-22°C). The seeds of T-DNA insertion mutants of CAMTA3, *camta3-1* (SALK_001152) and *camta3-2* (SALK_064889) were ordered from NASC, and CAMTA3 overexpression lines were generated by *Agrobacterium*-mediated transformation, see chapter 2.2.3.3. CAMTA3 complementation line C4.6 (in *camta3-2* background) was provided by Prof. Hillel Fromm (Tel Aviv University, Israel). Transgenic plant expressing $MKK5^{DD}$ driven by a dexamethasone (DEX)-inducible promoter was produced by Dr. Ines Lassowskat (Lee lab, IPB Halle) (Lassowskat et al. 2014).

Plants grown in sterile condition were germinated in liquid ½ MS medium. Seeds were vapor-phase sterilized in an exsiccator with a beaker at the bottom with NaOCl solution (12% Cl) and Hydrochlorid acid (3:1, v/v). The seeds were sterilized by chlorine gas for 3 hours, and gas was allowed to completely evaporate. Subsequently, seeds were sowed in liquid ½ MS medium, and first stratified for two days at 4°C in the dark before putting into light room.

2.1.5 Plasmids

For BiFC assay, *pE-SPYNE-MPK3*, *MPK4*, *MPK8*, *pUC-SPYNE-MPK6* plasmids for expression N- or C-terminal cMyc-nYFP fusions were provided by the host laboratory. For expressing GST-MPK3, MPK4, MPK6 using in the *in vitro* kinase assay, *pGEX4T-1-MPK3*, *MPK4* and *MPK6* plasmids (Feilner et al. 2005) were also provided by host laboratory. Plasmids *p2HAGW7-MPK3-WT*, *MPK4-WT* and *MPK6-WT*, and *p2HAGW7-MPK3-CA*, *MPK4-CA* and *MPK6-CA* (Genot et al. 2017; Berriri et al. 2012) for expression of N-terminal hemagglutinin-tag MPK3-WT/CA (constitutively active), MPK4-WT/CA and MPK6-WT/CA were used in the *in vivo* phosphorylation mobility shift assay, and provided by Dr. Jean Colcombet (INRA, France). Plasmids *pRT100myc-MKK5^{KR}* and *MKK5^{DD}* for expression of N-terminally cMyc-tagged *Petroselinum crispum* (*Pc*) MKK5^{KR} and MKK5^{DD} (Lee et al. 2004) were generated by Dr. Justin Lee and provided by the host laboratory. Plasmids *pCambia1300-cLUC-WRKY34* and *pCambia1300-MVQ1-nLUC* for expression of N-terminal cLUC and C-terminal nLUC fusions were generated by Samuel Grimm (master student, Lee lab, IPB Halle) and used as a positive control in slit-luciferase assay. Plasmid *pEXSG-ERF104-CFP* was expressed in protoplast as a nuclear marker protein for co-localization experiment, and provided by host laboratory. Plasmids expressing CPK5-FL, CPK5m-FL, CPK5-VK or CPK5m-VK fused with C-terminal strepII tag were provided by Prof. Tina Romeis (DCPS, Berlin). Plasmids expressing CPK1ac (constitutively active), CPK2ac, CPK3ac, CPK4ac, CPK5ac, CPK6ac, CPK10ac, CPK11ac, CPK28ac, CPK30ac or CPK32ac fused with Flag-tag were provided by Dr. Marie Boudsocq (CNRS-INRA, France). For reporter activity assays, *pUBQ10-GUS* was used as normalization construct, and *p35s-LUC* was used as a control. Both of them were provided by the host laboratory.

2.2 Methods

2.2.1 Molecular cloning

2.2.1.1 Gateway cloning

CAMTA3 and *SR1IP1* coding sequences were PCR amplified from *Arabidopsis thaliana* Col-0 cDNA. *CPK5* and *CPK5-VK* and their kinase-deficient versions were amplified from in constructs *pXCSG-strepII* provided by Prof. Tina Romeis (DCPS, Berlin) (Dubiella et al. 2013) (appendix Table I). Indicated PCR products were cloned into *pENTR/D-TOPO* and *pDONR221* entry clones using the pENTR™/D-TOPO®-Cloning Kit (Invitrogen) and BP Clonase™ II Enzyme mix (Invitrogen). All entry clones were cloned into respective destination vectors (Table 2-1) using LR Clonase™ II enzyme mix (Invitrogen). Reactions were performed according to the manufacturer's protocol.

Table 2-1 Gateway destination vectors used in this study

Name	Selection marker	Structure	Source
pUGW14	Amp^R	p35S-**GW**-3xHA	(Nakagawa et al. 2007)
pUGW18	Amp^R	p35S-4xcMyc-**GW**	(Nakagawa et al. 2007)
pEarleyGate101	Kan^R, Bar^R	p35S-**GW**-YFP-HA-OCS	(Earley et al. 2006)
pUC-SPYCE-GW	Amp^R	p35S-**GW**-HA-cYFP-nosT	(Walter et al. 2004)
pUC-SPYNE-GW	Amp^R	p35S-**GW**-cMyc-nYFP-nosT	(Walter et al. 2004)
pE-SPYCE-GW	Amp^R	p35S-HA-cYFP-**GW**-pA35S	(Walter et al. 2004)
pE-SPYNE-GW	Amp^R	p35S-cMyc-nYFP-**GW**-pA35S	(Walter et al. 2004)
pUBC-YFP	$Spec^R$, Bar^R	pUBQ10-**GW**-YFP-T35	(Grefen et al. 2010)
pUBC-CFP	$Spec^R$, Bar^R	pUBQ10-**GW**-CFP-T35	(Grefen et al. 2010)
pCambia1300-cLUC-CT	Kan^R, Hyg^R	p35S-**GW**-cLUC-Term.RBS	(Chen et al. 2008)
pCambia1300-nLUC-CT	Kan^R, Hyg^R	p35S-**GW**-nLUC-Term.RBS	(Chen et al. 2008)
pCambia1300-cLUC-NT	Kan^R, Hyg^R	p35S-cLUC-**GW**-Term.RBS	(Chen et al. 2008)
pDEST-N110	Amp^R	pT7-lacO-SD-His10-**GW**	(Dyson et al. 2004)
pDEST™22	Amp^R	pADH1-Gal4 AD-**GW**	Invitrogen
pDEST™32	$Gent^R$	pADH1-Gal4 DBD-**GW**	Invitrogen

2.2.1.2 Classical cloning for promoter activity assay

Promoters of *EDS1*, *EIN3*, *ZAT10*, *ZAT12*, *CBF2* and *WRKY33* were amplified from Col-0 genomic DNA using primers introducing a 5'-*Bam*HI (5'-*Pst*I for *pZAT10*) and a 3'-*Nco*I restriction sites. Vector *pNHL10-LUC* was digested by indicated restriction enzymes (Fermentas), and *pNHL10* was substituted by indicated promoter fragments by ligation with T4 ligase (Fermentas). All the primers used for cloning are listed in appendix Table II.

2.2.1.3 Site-directed mutagenesis (SDM)

SDM was performed on *pENTR/D-CAMTA3* entry vector. CAMTA3-mutP1, mutP2, mutP2+ and mutP3 mutants were generated using the mutagenesis method based on Type IIs restriction digestion and the description in (Palm-Forster, Eschen-Lippold, and Lee 2012) (Table 2-2, 2-3), and a *Kas*I or a *Apa*I restriction sites were introduced at the site of mutagenesis. CAMTA3 phospho-mimic was synthesized by Invitrogen (USA).

Table 2-2 SDM PCR mix

Component	Volume [µl]
5×HF buffer	5
DMSO	1.5
dNTP (10 mM)	1.5
Each primer (10 µM)	2.5
Template (100 ng/µl)	1
DNA polymerase[1]	0.5
ddH_2O	30.5

Table 2-3 SDM PCR programme

Temperature [°C]	Duration	Cycles
98	30''	1
98	10''	3
60[2]	10''	3
72	3'	3
98	10''	20
72[3]	3'	20
72	7'	1

After gel electrophoresis and elution with Invisorb® Fragment Cleanup (stratec molecular), DNA was eluted in 20.5 µl of H_2O and digested by *Dpn*I at 37°C overnight. *Dpn*I digested DNA products were digested by *Bsa*I and ligated by T4 DNA ligase in the same reaction as described in Table 2-4 and 2-5.

[1] Use commercial high-fidelity DNA polymerase (e.g. Phusion Hot Start II High Fidelity DNA Polymerase, Thermo Scientific).
[2] Calculate and use the annealing temperature of the complementary sequence of the primer.
[3] Calculate and use the annealing temperature of the complete primer sequence (maximum 72°C).

Table 2-4 SDM restriction and ligation reaction mix

Component	Volume [µl]
***Dpn*I digestion product**	25
***Dpn*I**	0.1
***Bsa*I**	0.4
10× restriction buffer	0.5
T4 DNA ligase	1.5
ATP (20 mM)	0.75
ddH_2O	1.75

Table 2-5 SDM restriction and ligation reaction

Temperature [°C]	Duration	Cycles
37	5’	20
16	5’	20
16	∞	

5 µl of reaction mix was used for *E.coli* transformation. All the primers used for SDM are listed in appendix Table III.

2.2.2 Plasmid preparation

Plasmids were isolated from 4 ml LB Medium cultures using Invisorb® Spin Plasmid Mini Two (stratec molecular) or from 100 ml LB Medium cultures using NucleoBond® Xtra Midi (Macherey Nagel) or 300 ml LB Medium cultures using NucleoBond® Xtra Maxi (Macherey Nagel). Isolation was performed according to the manufacturer’s protocols.

2.2.3 Transformations

2.2.3.1 *E.coli* heat-shock transformation

E. coli strains were transformed using heat shock transformation. Competent cells (50 µl) were thawed on ice and the appropriate plasmid (50 ng) was added. Cells with plasmids were incubated on ice for 15-30 min, and applied for a heat shock at 42°C for 1 min. Cells were subsequently incubated for 1 min on ice and added 500 µl of LB Medium. Cells were incubated with shaking at 37°C for at least 30 min, and plated on LB media plates with respective antibiotics.

2.2.3.2 *Agrobacterium tumefaciens* cold-shock transformation

Agrobacterium strain GV3101 was transformed using cold shock transformation. Competent cells (200 µl) were thawed on ice and added plasmids (1 µg). Cells were incubated on ice for 5-30 min before applying a cold shock by freezing the cells in liquid nitrogen for 1 min. Subsequently, cells were thawed at 37°C for 5 min. 1 ml of LB Medium were added and cells were incubated at 28°C for 2-3 hours with shaking, and placed on LB media plates with respective antibiotics.

2.2.3.3 *Agrobacterium-mediated* plant stable transformation

CAMTA3 was constructed into vector *pEarleyGate101* under control of the *35S* promoter and fused with YFP tag. Transgenic *A. thaliana* lines were generated by *Agrobacterium*-mediated transformation with the floral dip method as described in (Logemann et al. 2006; Zhang et al. 2006).

2.2.3.4 Isolation and transient transformation of *A. thaliana* mesophyll protoplasts

Protoplast isolation and transformation was performed with 8-10 fully expanded leaves from 4-6 week old plants as described in (Yoo, Cho, and Sheen 2007) with following changes. After infiltration of leaf strips with enzyme mix (cellulase R10 and macerzyme R10), leaf strips was digested at 18-20°C for at least 3 hours in the dark. During washing steps, protoplast solution was kept on ice, and 10 µg plasmid DNA was transfected into every 100 µl protoplasts. After transfection, protoplasts were incubated at 18-20°C in the dark for 14-16 hours and used in different assays. For protein expression analysis, aliquoted protoplasts (300 µl) were treated with elicitors or certain chemicals, pelleted and frozen in liquid nitrogen after removal of supernatant. Pellets were suspended by adding 12 µl of 2× loading buffer (125 mM Tris pH 6.8; 4% SDS; 20% Glycerol; 2% β-mercaptoethanol; bromophenol blue), and incubated at 95°C for 10 min. Denatured samples were loaded into SDS-PAGE, and western blot was performed subsequently.

2.2.4 Identification of CAMTA3 overexpression homozygous line

2.2.4.1 Genomic DNA isolation and genotyping CAMTA3 overexpression line

After floral-dip transformation, T1 generation seeds were sowed on soil and selected by BASTA (1:2500) spraying. BASTA resistant plants were collected and genomic DNA was isolated for genotyping and southern blot.

Genomic DNA of Col-0 and T1 CAMTA3 overexpression line were extracted by CTAB method. 50-100 mg grinded leaf tissue was suspended into 600 µl CTAB buffer (2% CTAB; 20 mM EDTA; 100 mM Tris-HCl pH8.0; 1.4 M NaCl; 1% PVP40, filtered sterilization. 0.2% mercaptoethanol was freshly added before 65°C preheating) and incubated at 65°C for 30 min. Lysate was centrifuged and supernatants was harshly mixed with 600 µl chloroform twice. Clear supernatant was mixed gently with equal volume of ice-cold isopropanol and incubated for DNA precipitation at room temperature for at least 30 min. DNA was spun down and washed by 70% ethanol. Dry pellet was dissolved into 50 µl double-distilled H_2O.

Isolated genomic DNA was used for genotyping CAMTA3 overexpression lines. Two pairs of primers were used in one reaction: Basta_F/R and petC_F/R. Primer sequences are listed in appendix Table IV. The lines with stronger *petC* than *Basta* band were picked up for Western blot to check protein expression and Southern blot to screen for lines with single or low copy insertions.

2.2.4.2 Southern blot

The positive T1 generation was selected and Southern blot was performed as described in (Southern 2006). *Basta* resistance gene fragment was used as probe, and amplified with Phusion high fidelity polymerase (Thermo Fisher Scientific) by PCR from *pEarleyGate101* vector. PCR products (403 bp) were separated on an agarose gel and purified with Invisorb® Fragment CleanUp kit (stratec molecular). 25 ng purified DNA fragment was labelled with ^{32}P-α-ATP using the Megaprime DNA labelling kit (GE Healthcare) according to manufacturer's protocol. Genomic DNA was digested with *Eco*RI (Thermo Fisher Scientific) overnight and precipitated (2.5 vol 100% cold ethanol; 0.1 vol NaAc, -80°C for 30 min). DNA was subsequently separated on a 1% agarose gel (4°C, 40 V). Gel was depurinated (0.2 M HCl), denatured (1.5 M NaCl; 0.5 M NaOH) and neutralized (1.5 M NaCl; 0.5 M Tris-HCl) before transferring DNA to Nylon Membrane (positively charged) (Roche). Both prehybridization and hybridization occur at 42°C. After stringency wash steps, membrane was exposed to phosphoimaging plate, which was read by scanning with Typhoon FLA 9500 (GE Healthcare).

2.2.4.3 Segregation analysis

T2 generation was selected again by BASTA, where the surviving plants are homozygous or heterozygous lines. After growing under long day condition, T3 generation seeds were harvested and sowed on soil. 24 seedlings from individual lines were picked for BASTA selection, and homozygous lines were selected based on the survival rate (100%).

2.2.5 Real-time PCR analysis

2.2.5.1 Total RNA extraction

Total RNA was extracted from plant tissues (*Arabidopsis* seedlings or adult leaves) using TRIzol method. 50-100 mg grinded plant tissue was suspended into 1 ml TRIzol (250 ml Phenol saturated; 45.5 g Guanidine Thiocyanate; 15.5 g Ammonium; 17.5 ml 3 M Sodium Acetate pH 5.0; 25 ml Glycerol in 500 ml) and incubated and vortexed at room temperature. Chloroform (200 µl) was added into lysate before vortexing. After centrifuging, supernatant was mixed with Isopropanol (500 µl) for precipitation at room temperature for at least 10 min. Pellet was washing by 70% ethanol and dried, and dissolved into 40 µl RNase free H_2O.

2.2.5.2 cDNA synthesis

2 µg of RNA (adjusted to 8 µl with H_2O) was digested by 1 µl of DNase I with 1 µl of 10× buffer with $MgCl_2$ (37°C for 30 min). 1 µl of 25 mM EDTA was added and incubated at 65°C for 10 min. The reaction of cDNA synthesis included 1 µl of oligo$(dT)_{18}$, 2 µl of 10 mM dNTPs, 1 µl of RiboLock RNase Inhibitor, 1 µl of RevertAid Reverse Transcriptase and 4 µl of 5× reaction buffer for RT (Thermo Fisher scientific) with the program (37°C for 5 min, 42°C for 60 min and 70°C for 10 min).

2.2.5.3 Real-time PCR

Diluted cDNA (1:10) was used for real-time PCR following manufacturer's protocol from 5×QPCR Mix EvaGreen® (ROX) (Bio & Sell). Primers and probes are listed in appendix Table V. The PCR was performed in MX3005P cyclers (Agilent), and the program consisted of an initial activation step (95°C, 15 min) followed by 40 cycles (15 s at 95°C and 60 s at 60°C).

2.2.6 Protoplast assays

2.2.6.1 Reporter activity assay

Luciferase expression was driven by promoters of *EDS1*, *EIN3*, *ZAT10*, *ZAT12*, *CBF2*, *WRKY33* and *35S*. A *pUBQ10-GUS* was co-transfected for normalization. Protoplasts were also transfected with *pUGW14-CAMTA3* or *pUGW15-CFP*. 200 µM luciferin (Invitrogen) was added to protoplast suspension after transfection and overnight incubation. Protoplasts were aliquoted (90 µl) for three biological replicates

by transferring to 96-well microtiter plate (Greiner), and rested for 30-40 min in the dark at room temperature. Subsequently, protoplasts were elicited with 100 nM flg22 or H_2O, and luciferase activity kinetics was monitored by a 96-well plate Luminoscan Ascent plate reader (Thermo) for continues 3 hours.

For normalization, GUS activity of transfected protoplasts was measured. Protoplast extracts were prepared by adding extraction buffer (50 mM $NaPO_4$ pH 7.0; 1 mM EDTA; 0.1% TritonX-100; 10 mM β-mercaptoethanol; proteinase inhibitor) to protoplast suspension, and vortexed. 50 µl of extracts were taken to mix with pre-cooled 10 mM 4-Methylumbelliferyl-β-D-glucuronide (dissolved in 1× extraction buffer), and kept at 4°C, and immediately 20 µl of the mix was transferred to 200 µl stop buffer (0.2 M Na_2CO_3) (T_0), while the rest of the mix was incubated at 37°C for 15 min and subsequently transferred 20 µl to stop buffer (T_{15}). GUS activity for both time points were measured by a Twinkle LB790 plate reader (Berthold), and luminescence was divided by GUS-value (T_{15}-T_0) for normalization.

2.2.6.2 Protein stability assay

After overnight incubation, *pUGW14-CAMTA3* transfected protoplasts (300 µl) were co-elicited by 100 nM flg22 and 1 µM Cycloheximide (CHX) for 1 and 3 hours. 50 µM of MG115 (Serva) was used to pretreat protoplasts for 30 min before flg22 and CHX elicitation. Samples were boiled in loading buffer, and loaded in SDS-PAGE for western blot.

Without any elicitation, *pUGW14-CAMTA3* were also co-transfected with *MKK5^{DD}*, *CPK5-VK* or indicated *CDPKac*, and western blot was performed to analyze protein stability.

2.2.6.3 Protein phosphorylation-mediated mobility shift assay

After overnight incubation, *pUGW14-CAMTA3* transfected protoplasts (300 µl) were elicited by 100 nM flg22 and harvested at different time points. If necessary, λ-phosphatase was used to treat protoplast extracts according to the manufacturer's protocol of Lambda Protein Phosphatase (NEB).

Without any elicitation, *pUGW14-CAMTA3* were also co-transfected with *MKK5^{DD}*, *CPK5-VK* or indicated *CDPKac*. Samples were boiled in loading buffer and a Phos-Tag^{TM}-based western blot was performed to analyze protein mobility shift as described in the chapter 2.2.8.1.

2.2.6.4 Microscopy

For localization studies, *pUBC* plasmids coding CAMTA3-YFP or SR1IP1-CFP were transfected into protoplasts. For co-localization studies, *pUBC* plasmid coding CAMTA3-YFP was co-transfected with the one coding SR1IP1-CFP or pEXSG-ERF104-CFP that served as a nuclear marker. For the experiment in which MPK3 and MPK6 were needed to be activated, plasmid of *pRT100myc-MKK5^{DD}* or *MKK5^{KR}* were co-transfected. After transfection and overnight incubation, protoplasts were either directly analyzed by confocal laser scanning microscopy with an LSM780 (Zeiss) or treated with 100 nM flg22 before analyzing. YFP was excited with a 514 nm laser and emission detected between 500 and 570 nm. CFP was excited with a 458 nm laser and emission recorded from 480 to 520 nm.

2.2.7 Protein immunoprecipitation from plant materials

2.2.7.1 From protoplasts

Plasmids of *pEXSG* coding CPK5-FL-strepII and CPK5m-FL-strepII was used as kinases for *in vitro* phosphorylation assay. Both plasmids were expressed in and proteins were immunoprecipitated from protoplasts. Indicated proteins were extracted with protein extraction buffer modified from (Dubiella et al. 2013) (100 mM Tris pH 8.0; 5 mM EGTA; 5 mM EDTA; 100 mM NaCl; 20 mM DTT; 0.5 mM AEBSF; 2 µg/ml Aprotinin; 2 µg/ml Leupeptin; Protease-Inhibitor Mix P (Serva); 0.5% TritonX-100), and immunoprecipitated based on the manufacturer's protocol of MagStrep "type3" XT beads 5% suspension (IBA Lifesciences).

Plasmids of *p2HAGW7* coding HA-tagged MPK3-WT/CA, MPK4-WT/CA and MPK6-WT/CA were used for *in vivo* phosphorylation experiment, and the indicated protein kinase activities were determined by autoradiography. Indicated proteins were extracted from transfected protoplasts with MAPK extraction buffer (25 mM Tris pH 7.8; 75 mM NaCl; 15 mM EGTA; 15 mM β-Glycerophosphate; 15 mM 4-Nitrophenylphosphate; 10 mM $MgCl_2$; 1 mM NaF; 0.5 mM Na_3VO_4; 1 mM DTT; 0.1% Tween20; 1 mM PMSF; 10 µg/ml Leupeptin; 10 µg/ml Aprotinin) provided by the host laboratory. HA antibody was bonded to the beads of Protein G Sepharose® 4 Fast Flow (GE Healthcare) and immunoprecipitation was based on the manufacturer's protocol.

2.2.7.2 Protein extraction from seedlings and adult plants

YFP-tagged CAMTA3 was extracted from transgenic lines. Grinded plant materials were suspended and proteins were extracted by modified RIPA buffer (10 mM Tris pH 7.5; 150 mM NaCl; 0.5 mM EDTA; 0.1% SDS; 1% TritonX-100; 1% Deoxycholate; 1 mg/ml DNase; 2.5 mM $MgCl_2$; 1 mM NaF; 0.5 mM Na_3VO_4; 1 mM PMSF; Protease-Inhibitor Mix P). Proteins were immunoprecipitated using GFP-Trap®_A (Chromotek) based on the manufacturer's protocol.

2.2.8 Western Blot

2.2.8.1 Phos-Tag™-based Western blot

Phos-Tag™-based Western blot was used for distinguishing phosphorylated proteins from non-phosphorylated proteins. According to the large size of CAMTA3, 6% Phos-Tag™ gel was prepared by polymerized additional 100 µM $MnCl_2$ and 50 µM Phos-Tag™ AAL-107 (NARD). Gel electrophoresis and Western blot were performed based on the manufacturer's protocol. After separating protein samples on Phos-Tag™ SDS-PAGE, elimination of the Mn^{2+} from the gel using chelating agent EDTA is necessary to increase the following transfer efficiency. The gel was washed 3 times 30 min with a transfer buffer containing 10 mM EDTA and one time with 1 mM EDTA. Subsequently, proteins were transferred in wet conditions onto Nitrocellulose member (Macherey Nagel) for 135 min at 100 V, and standard Western blot procedures were performed after that.

2.2.8.2 Quantitative Western blot

Odyssey® CLx multiplex imaging system (Li-COR) was used for Western blot quantification. After blotting, nitrocellulose membrane was stained with REVERT™ Total Protein Stain (Li-COR) according to the manufacturer's protocol. Total proteins for every samples were imaged in the 700 nm channel with Odyssey® imaging system and quantified with Image Studio™ Software (Li-COR) as described in the manufacturer's instruction.

Membrane was blocked with Odyssey® Blocking Buffer (Li-COR) for 1 hour after total protein stain and subsequently incubated with primary antibody diluted in Odyssey™ Blocking Buffer (0.2% Tween 20) for 1 hour. After wash steps, membrane was incubated with secondary antibody IRDye® 800CW Goat anti-Mouse or anti-Rabbit IgG (H+L) (Li-COR) diluted in Odyssey™ Blocking Buffer (0.2% Tween 20) for 1 hour.

After wash steps, target proteins were imaged in the 800 nm channel with Odyssey® imaging system and quantified with Image Studio™ Software.

The target protein signals (800 nm) were normalized by total protein quantification (700 nm), and the calculation was followed REVERT™ Total Protein Stain Normalization Protocol from Odyssey® CLx Application Protocols Manual (Li-COR). Three biological replicate experiments were performed, and the normalized values from individual experiment were normalized by the median of each dataset following by a statistical analysis. All the antibodies used for western blot are listed in Table 2-6 and 2-7.

Table 2-6 List of primary antibodies used in the thesis

Antibody	Producer	Dilution	Secondary antibody
anti-HA	Eurogentec	1:1000	anti-mouse
anti-cMyc	Sigma-Aldrich	1:1000	anti-mouse
anti-luciferase	Sigma-Aldrich	1:5000	anti-rabbit
anti-phospho-p44/43 MAPK	Cell Signaling Technology	1:1000	anti-rabbit
anti-Flag	Stratagene	1:1000	anti-mouse
anti-GFP	Clontech	1:2000	anti-mouse
anti-His	Sigma-Aldrich	1:3000	anti-mouse
Strep-Tactin HRP	IBA lifesciences	1:4000	

Table 2-7 List of secondary antibodies coupled to HRP used in the thesis

Antibody	Producer	Dilution
anti-mouse	Sigma-Aldrich	1:10 000
anti-rabbit	Bio-Rad	1:5000
IRDye® 800CW Goat anti-Mouse IgG	Li-COR	1:10 000
IRDye® 800CW Goat anti-Rabbit IgG	Li-COR	1:10 000

2.2.9 Protein-protein interaction assays

2.2.9.1 Bimolecular fluorescence complementation

Arabidopsis Col-0 protoplasts were co-transfected with constructs of *pE-SPYNE/pUC-SPYNE* or *pE-SPYCE/pUC-SPYCE* (Walter et al. 2004) coding nYFP-MPK3, MPK4, MPK8, CPK5, CPK5m and SR1IP1, cYFP-CAMTA3, MPK6-nYFP, SR1IP1-nYFP and CAMTA3-cYFP, respectively. Transfected protoplasts were analyzed by confocal laser scanning microscopy with an LSM780 (Zeiss) after overnight incubation with or without elicitation (H_2O or 100 nM flg22). Reconstituted YFP was excited with a 514 nm laser and emissions detected between 500 and 570 nm.

2.2.9.2 Split luciferase assay

Split luciferase assay was performed as described in (Furlan et al. 2017) and in *Arabidopsis* protoplasts derived from transgenic plants expressing $MKK5^{DD}$ driven by a dexamethasone (DEX)-inducible promoter. Protoplasts were co-transfected with constructs of *pCambia1300-cLUC-CT*, *pCambia1300-cLUC-NT* and *pCambia1300-nLUC-CT* (Chen et al. 2008) coding CAMTA3-WT/mutP3-cLUC, cLUC-CFP and SR1IP1-nLUC, respectively. Besides, cLUC-WRKY34 and MVQ1-nLUC were constructed and described in the master thesis (Grimm 2017), and co-expressed as a positive control. Construct of *pUBQ10::GUS* was co-transfected for normalization (Sun and Callis 1997). Ethanol or 2 µM of DEX was added directly after transfection as mock treatment or to induce $MKK5^{DD}$ expression. After overnight expression and treatment, three biological replicates were transferred to 96-well microtiter plates (Greiner) and calmed down in room temperature for half-hour. 1 mM of luciferin (Invitrogen) was added and luminescence was monitored in the Luminoscan Ascent plate reader (Thermo Fisher Scientific) for continuous 1 hour. Values are the total luminescence in 1 hour normalized against the GUS assay readings as described in the chapter 2.2.6.1.

2.2.9.3 Yeast two-hybrid

Yeast two-hybrid assay employed the ProQuest™ Two-Hybrid System (Invitrogen) and performed according to the manufacturer's protocol. CAMTA3-WT and phospho-mutant variants were fused with activation domain (AD) cloning into *pDEST22*, and SR1IP1 was fused with DNA binding domain (DBD) cloning into *pDEST32* (Invitrogen). Empty vector (EV) harboring the AD or DBD served as negative control. Yeast strain PJ67-4a (James, Halladay, and Craig 1996) was prepared for competent cells. Yeast cells were grown in YPAD Medium at 28°C till an OD_{600} of 1-1.5. After washing steps, competent cells were

resuspended in TE/LiOAc for transformation. For every plasmid pair, 0.4 µg of plasmid DNA expressing the indicated proteins and 20 µg herring sperm DNA (SIGMA Aldrich) were transformed into 20 µl competent cells by PEG4000 method, which were incubated with shaking at 30°C for 1 hour. Subsequently, a heat shock was applied at 42°C for 1 hour. Transformants were resuspended in 50 µl SD-LW liquid media, and 10 µl placed onto SD-LW, SD-LWAH and SD-LWAH (50 mM 3-AT) selective plates. Yeasts were allowed to grow 2-3 days at 28°C.

2.2.10 *In vitro* kinase assay with recombinant proteins

2.2.10.1 Expression of recombinant proteins in *E. coli*

CAMTA3-WT and phospho-mutant variants, and CPK5-VK and its kinase-deficient version CPK5m-VK were expressed as His-tagged fusion proteins via *pDEST-N110* in KRX cells according to Promega guideline. After bacterial cultures grown in selective LB Medium at 37°C till an OD_{600} of 0.4-0.6, indicated proteins were induced with 0.1% Rhamnose and 1 mM IPTG. CPK5-VK and CPK5m-VK were subsequently grown at 37°C for 4 hours, and CAMTA3-WT and phospho-mutant variants were grown at 20°C for 10 hours. MPK3, MPK4 and MPK6 (provided by the host laboratory) were expressed as GST-tagged fusion proteins via pGEX4T-1 in BL21 DE3 cells. Indicated proteins were induced with 1 mM IPTG after OD_{600} reached 0.5-0.8, and cells were grown at 16°C for overnight.

2.2.10.2 Protein purification

After induction, bacteria were harvested at 6000 g, 4°C for 20 min, and the pellet was frozen in liquid nitrogen. For CAMTA3-WT and phospho-mutant variants, pellet was dissolved in lysis buffer (50 mM NaH_2PO_4; 0.3 M NaCl; 10 mM Imidazole; Protease-Inhibitor Mix HP (Serva); pH 8.0). Cells were lysed with Lysozyme (Applichem) to the final concentration of 1 mg/ml for 30 min on ice and subsequently sonicated using a SONOPULS homogenizer (Bandelin) with a VS70T probe until the lysate was clear (10 s pulse and 15 s pause each at 60% output). TritonX-100 (1%) (Serva) and DNase I (20 µg/ml) (Thermo Fisher Scientific) were added to the lysate, which incubated for 30 min on ice. After centrifugation at 16000g, 4°C for 40 min, the supernatant was incubated with equilibrated nickel affinity agarose beads Ni-NTA (Qiagen) according to the manufacturer's instruction by rotating at 4°C for at least 1 hour. Beads were spun down at 200 g for 2 min and washed twice with wash buffer (50 mM NaH_2PO_4; 0.3 M NaCl; 20 mM Imidazole; Protease-Inhibitor Mix HP; pH 8.0), once with high salt wash buffer (= wash buffer with 0.5 M NaCl) and another once with wash buffer. Proteins were finally washed with 50 mM Tris-HCl, pH8.0 buffer and

stayed on the beads. Purification of GST-tagged MPK3, MPK4 and MPK6 was based on the manufacturer's protocol of Glutathione Sepharose™ 4B (GE Healthcare). Pellet was dissolved in lysis buffer (1×PBS, Protease-Inhibitor Mix HP). After binding to GSH-Sepharose, beads were washed by wash buffer (1×PBS, 0.1% Tween) and high salt wash buffer (= wash buffer with 0.5 M NaCl), and proteins were eluted three times by elution buffer (20 mM L-Glutathione reduced in 50 mM Tris-HCl pH 8.0).

CPK5-VK and CPK5m-VK were purified by denaturing purification method. Pellet was dissolved in lysis buffer (0.1 M NaH_2PO_4; 10 mM Tris; 6 M Guanidinium chloride; pH 8.0) and left in room temperature for 1 hour. After centrifugation, supernatant was incubated with Ni-NTA at room temperature for 1 hour. Beads was washing three times with wash buffer (0.1 M NaH_2PO_4; 10 mM Tris; 8 M Urea; pH 6.3). After taking away all the wash buffer, protein on the beads was refolded on ice overnight by adding 1 M Tris-HCl, pH 7.5 and 1 mM PMSF, and gradually adding 10 mM Tris, pH 7.5 and 1 mM PMSF. Protein was eluted by elution buffer (50 mM NaH_2PO_4; 0.3 M NaCl; 0.25 M Imidazole; Protease-Inhibitor Mix HP; pH 8.0).

Eluted proteins were dialyzed at 4°C overnight using SnakeSkin dialysis tubing (Thermo Fisher Scientific) in 50 mM Tris-HCl, pH 8.0 buffer.

2.2.10.3 *In vitro* phosphorylation assay

In vitro phosphorylation assay between MPKs and CAMTA3 variants was performed in kinase substrate buffer 1 (20 mM HEPES pH 7.5; 15 mM $MgCl_2$; 5 mM EGTA; 1 mM DTT; Protease-Inhibitor Mix HP; 2 µCi [gamma-^{32}P]ATP) using recombinant His-CAMTA3 variants and GST-MPK3, 4 and 6. Samples were incubated for 30 min at 37°C, and the reactions were stopped by adding 5× loading buffer with 5 min boiling. Samples were subsequently separated on SDS-PAGE, which was stained with CBB and analyzed by autoradiography.

In vitro phosphorylation assay between CAMTA3 and CPK5-FL was performed in kinase substrate buffer 2 (20 mM HEPES pH 7.5; 15 mM $MgCl_2$; 1 mM DTT; 0.1 mM $CaCl_2$; Protease-Inhibitor Mix HP; 2 µCi [gamma-^{32}P]ATP) using recombinant His-CAMTA3 and strepII-CPK5-FL immunoprecipitated from protoplasts, and 2.4 mM EGTA was used instead of $CaCl_2$ for negative control. 0.5 µg Calmodulin was also used in one of the result. While the experiment between CAMTA3 and CPK5-VK was performed in kinase substrate buffer 1. Reactions were performed at 30°C for 30 min.

2.2.11 Phosphorylation site mapping

Mass spectrometry analysis were performed by Petra Majovsky and Domenika Thieme in the laboratory of Dr. Wolfgang Hoehenwarter (IPB, Halle). Residue-specific phosphorylation of CAMTA3 by MPK3 and MPK6 was studied by an *in vitro* phosphorylation assay and an *in vivo* approach of infiltration of 1 µM flg22 into leaves of CAMTA3 overexpression line. Amino acid residue-specific phosphorylation of CAMTA3 was mapped by liquid chromatography on-line with high resolution accurate mass MS (HR/AM LC-MS). Proteins separated by SDS-PAGE were subjected to in-gel tryptic digestion or with a combination of Glu-C. The resulting peptides were separated using C18 reverse phase chemistry employing a pre-column (EASY column SC001, length 2 cm, ID 100 µm, particle size 5 µm) in line with an EASY column SC200 with a length of 10 cm, an inner diameter (ID) of 75 µm and a particle size of 3 µm on an EASY-nLC II (all from Thermo Fisher Scientific). Peptides were eluted into a Nanospray Flex ion source (Thermo Fisher Scientific) with a 60 or 120 min gradient increasing from 5% to 40% acetonitrile in ddH_2O with a flow rate of 300 nl/min and electrosprayed into an Orbitrap Velos Pro mass spectrometer (Thermo Fisher Scientific). The source voltage was set to 1.9 kV, the S Lens RF level to 50%. The delta multipole offset was -7.00. The AGC target value was set to 1e06 and the maximum injection time (max IT) to 500 ms in the Orbitrap. The parameters were set to 1e04 and 100 ms in the LTQ with an isolation width of 2 Da for precursor isolation and MS/MS scanning. Peptides were analyzed by a targeted data acquisition (TDA) scan strategy with inclusion list to specifically select and isolate CAMTA3 phosphorylated peptides for MS/MS peptide sequencing. Multi stage activation (MSA) was applied to further fragment ion peaks resulting from neutral loss of the phosphate moiety by dissociation of the high energy phosphate bond to generate b- and y-fragment ion series rich in peptide sequence information.

MS/MS spectra were used to search the TAIR10 database (ftp://ftp.arabidopsis.org, 35394 sequences, 14486974 residues) with the Mascot software v.2.5 linked to Proteome Discoverer v.1.4. The enzyme specificity was set to trypsin and two missed cleavages were tolerated. Carbamidomethylation of cysteine was set as a fixed modification and oxidation of methionine and phosphorylation of serine and threonine as variable modifications. The precursor tolerance was set to 7 ppm and the product ion mass tolerance was set to 0.8 Da. A decoy database search was performed to determine the peptide spectral match (PSM) and peptide identification false discovery rates (FDR). Phosphorylated peptides with a score surpassing the false discovery rate threshold of 0.01 (q-value<0.01) were considered positive identifications. The phosphoRS module was used to specifically map phosphorylation to amino acid residues within the primary structure of phosphopeptides.

3 Results

3.1 CAMTA3 negatively regulates defense-related gene expression

3.1.1 Growth phenotypic comparison of Col-0, *camta3* mutants, and CAMTA3 overexpression lines

CAMTA3 was reported as a negative regulator of plant immunity, and *camta3* mutants displayed autoimmunity growth phenotype such as dwarfism, chlorotic lesions, and other enhanced disease resistance-related phenotype such as elevated accumulation of ROS, constitutively activated expression of *PR* genes, and increased SA level (Galon et al. 2008; Du et al. 2009; Nie et al. 2012). Here, we grew Col-0, two *camta3* mutant alleles, and four independent CAMTA3 overexpression lines in short day condition (8h photoperiod) at 20-22^{o}C. As shown in Fig 3-1, both *camta3* mutants displayed reduced growth and spontaneous chlorotic lesions compared with Col-0 as described in the literature. CAMTA3 expression construct driven by the native promoter and fused to EYFP (enhanced yellow fluorescent protein) tag (*pCAMTA3::CAMTA3-EYFP*) was transformed into *camta3-2* mutant, and there is no noticeable growth phenotypic difference between this complementation line (C4.6) and Col-0, which indicates that the *camta3* phenotype is due to loss of CAMTA3. Meanwhile independent CAMTA3 overexpression lines (*p35S::CAMTA3-YFP*) also grows normally like Col-0, and are, in fact, even slightly larger than Col-0.

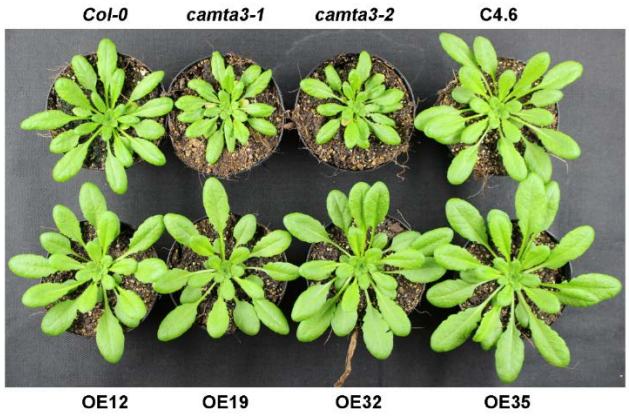

Fig 3-1. Phenotypic comparison of Col-0, *camta3* mutants and CAMTA3 overexpression lines. Col-0, two mutants (*camta3-1* and *camta3-2*), four independent CAMTA3 overexpression lines (OE12, 19, 32, and 35) grown in short day condition (8h photoperiod) at the temperature in the range of 20-22^{o}C for 4 weeks.

3.1.2 CAMTA3 expression is PAMP inducible

Global transcriptome profiling based on Genevestigator showed that besides salicylic acid, treatment with PAMPs (e.g. flg22, elf26 or chitin) induces the accumulation of *CAMTA3* transcripts. By RT-qPCR, we confirmed the increase in *CAMTA3* expression in *Arabidopsis thaliana* Col-0 seedlings stimulated with flg22 (Fig. 3-2). *CAMTA3* mRNA levels increased rapidly within 30 min of flg22 treatment, peaks around 60 min and subsided to near basal levels after about 4 h. This increased expression suggests a possible role of CAMTA3 in the control of flg22-induced transcriptional reprogramming.

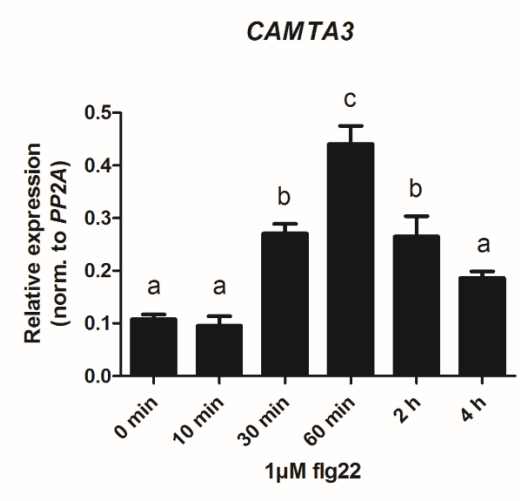

Fig 3-2. *CAMTA3* expression is induced by the bacterial PAMP, flg22. Col-0 seedlings (10 days old) were elicited by 1µM flg22, and harvested at the indicated time-points and processed for RT-qPCR. One-way ANOVA Newman-Keuls multiple comparison test was performed and bars with different letters are significantly different. Error bars represent ± SD (n=4).

3.1.3 CAMTA3 negatively regulates expression of defense related genes

CAMTA3 was reported to be a transcription factor, and it directly and specifically binds to promoter of its target genes and regulate their expression. For example, CAMTA3 negatively regulates expression of several defense related genes. This includes: (1) *EDS1*, which encodes a positive regulator of SA and SA-mediated defense immunity and is required for TIR-NBS-LRR-mediated resistance (Du et al. 2009). (2) *NDR1*, which encodes a key component in EDR2-mediated plant immunity and is required for CC-NBS-LRR-mediated resistance. (3) *EIN3*, which encodes a key component of ET signaling (Nie et al. 2012). Additionally, CAMTA3 was also reported positively regulating cold related genes expression, such as *CBF2* (Doherty et al. 2009). Notably, all of these CAMTA3 target genes promoter regions contain CGCG box.

To investigate how CAMTA3 regulates expression of its target genes and how PAMP elicitation affects this regulation, we performed a luciferase reporter assay that is based on the monitoring of defense promoter-driven luciferase activity. Several genes were selected for this assay, including three proven CAMTA3 targets (*EDS1*, *EIN3* and *CBF2)*, *ZAT10* and *WRKY33*, which are defense-related genes with up-regulated expression in *camta3* mutants, and *ZAT12*, which is a cold-responsive gene with dramatically decreased expression in *camta3* mutant. The -1.2-kb to -3-kb promoter regions (relative to the start codon) were cloned. Except for *WRKY33* promoter which does not contain any CGCG box, the others all included at least one CGCG box in the promoter region. As a negative control, the CaMV *35S* promoter was used. This promoter is weakly flg22-inducible, but lacks CGCG box. All of these promoters were fused to firefly luciferase (*LUC*) reporter gene and transiently expressed in *Arabidopsis* Col-0 mesophyll protoplasts. Either CAMTA3 or cyan fluorescent protein (CFP) overexpression constructs were co-transfected with the *promoter::LUC* constructs into protoplasts. A *GUS* reporter gene driven by *polyubiquitin10 (UBQ10)* promoter (*pUBQ10::GUS*) was also included for normalization. Unfortunately, almost no LUC activities could be detected for constructs driven by *pEDS1*, *pEIN3*, and *pCBF2* both in the presence and absence of CAMTA3 overexpression (data not shown), despite these being known targets for CAMTA3. The reason is unclear, but most likely, the chosen genomic regions are insufficient to act as active promoters. We could detect luciferase activity for constructs driven by *pZAT10*, *pZAT12*, *pWRKY33*, and *p35S*. As shown in Fig. 3-3 (A-D), all four promoters are flg22-inducible. However, CAMTA3 overexpression raised the basal activity of all promoters (Fig. 3-3 A-C). Notably, this boosting effect by CAMTA3 is seen in promoters that lack the CGCG elements, like *p35S* and *pWRKY33* (Fig. 3-3 C, D). Even the activity of the *UBQ10* promoter fused with GUS reporter was boosted by CAMTA3 (Fig. 3-3 E), so that this is not a direct effect on the luciferase enzyme. These results are likely due to the stress generated when isolating protoplasts. Hence, we used stably transformed CAMTA3 overexpression transgenic lines and quantified endogenous gene transcript levels by RT-qPCR.

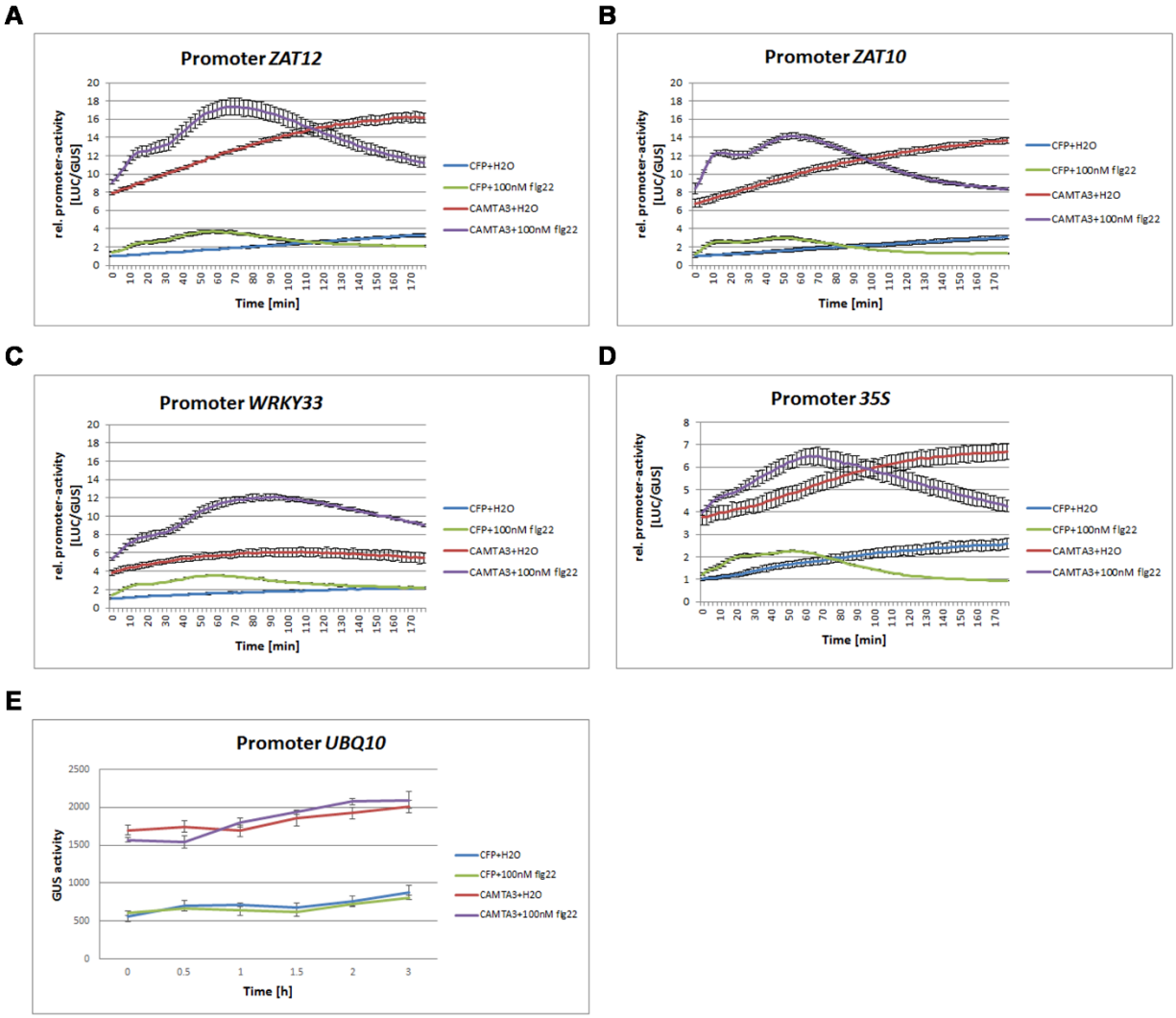

Fig 3-3. Effect of CAMTA3 on promoter activity of selected genes with reporter assay. A-D. 4 weeks Col-0 plants growing in short day condition were used for preparing protoplasts. Protoplasts were co-transfected with *promoter::LUC* and *p35S::CAMTA3-3×HA* (hemagglutinin) constructs (or as a control, an unrelated protein, *p35S::CFP:3×HA* was co-expressed). Luciferase activities in the protoplasts were monitored in the luminescence reader for continuous 180 min after treating with 100 nM flg22 or H_2O as mock treatment, in the presence of 200 µM luciferin. And luciferase activities were normalized against a constitutively expression *pUBQ10::GUS* reference and shown as the mean fold change (n=3) with the CFP-transfected controls (t = 0 min) set as a reference value of 1. Error bars indicate standard errors. **E.** Protoplasts were co-transfected with *pUBQ10::GUS* and *p35S::CAMTA3-3×HA* constructs (*p35S::CFP:3×HA* as a control). GUS activities in protoplasts were measured at indicated time points after treating with 100 nM flg22 or H_2O. Error bars indicate standard errors.

We investigated the effect of CAMTA3 on defense-related genes expression upon PAMP treatment by utilizing *Arabidopsis* adult plants with different genetic background. Col-0 together with two *camta3* mutants and two independent CAMTA3 overexpression (OE) lines were used. We first analyzed *CAMTA3* transcript levels by RT-qPCR. The basal *CAMTA3* transcript level (i.e. in the mock treated tissues) was significantly higher than Col-0 in two independent OE lines and reduced in the two *camta3* mutants. Flg22

induction of CAMTA3 expression (as shown above in Fig 3-2) further raised *CAMTA3* expression in the OE lines (Fig. 3-4 A).

Next, we analyzed the effect of CAMTA3 on *EDS1* expression, which is a known direct target of CAMTA3, but was not successfully investigated by the promoter-LUC reporter assay. Loss of *CAMTA3* resulted in high basal *EDS1* transcript levels. CAMTA3 overexpression inhibited *EDS1* transcript accumulation. Flg22-induced expression of *EDS1* was enhanced in the two *camta3* mutants and reciprocally, it was reduced in the two independent OE lines (Fig. 3-4 B). A similar effect was also shown on *NHL10*, which is a defence-related gene but not reported as a direct target of CAMTA3. Analysis of its promoter sequence revealed a typical CGCG box, which could be a potential CAMTA3-binding site, and suggests that *NHL10* may be also a potential CAMTA3 target gene (Fig. 3-4 C). These observations are in agreement to CAMTA3 functioning as a negative regulator during plant immunity response.

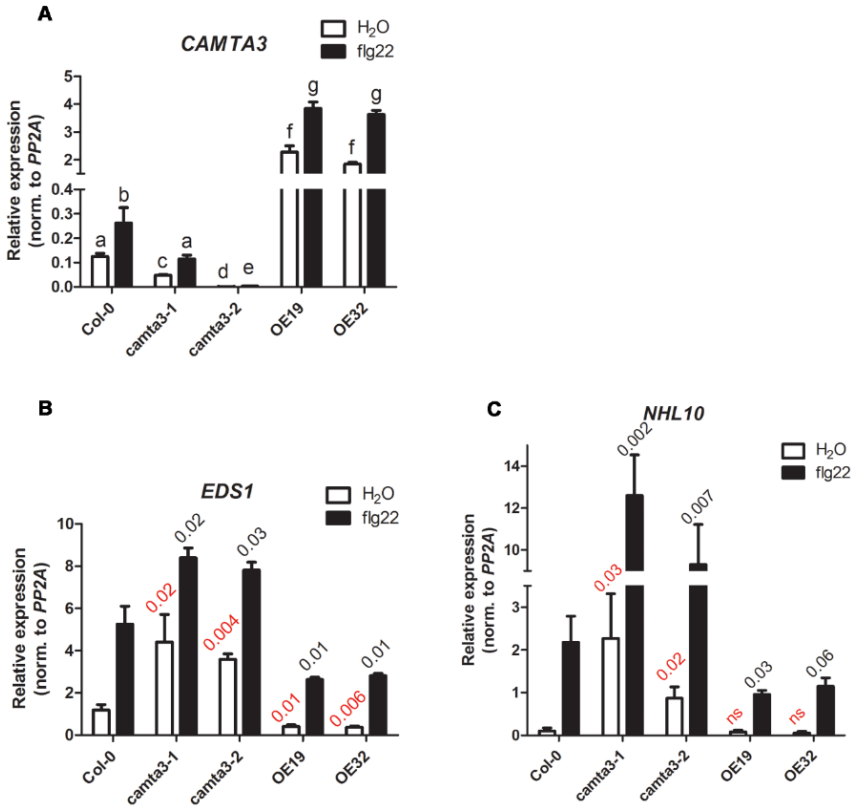

Fig 3-4. CAMTA3 negatively affects expression of defense related genes upon flg22 treatment. A. *CAMTA3* transcript levels in different genetic background upon flg22 or H_2O treatment. Adult *Arabidopsis* with indicated genetic background (4 weeks old) leaves were infiltrated with H_2O or 1 µM flg22, and harvested after 1 hour and processed for RT-qPCR. One-way ANOVA Newman-Keuls multiple comparison test was performed

and bars with different letters are significantly different. Error bars represent ± SD (n=6). **B-C.** *EDS1* and *NHL10* expression in the indicated genotype upon flg22 or H_2O treatment. RT-qPCR was performed as descript before. Pairwise t-test comparison was performed and the resulting *p*-values indicated above each column (n=3). For H_2O-treated samples, expressions of *EDS1* and *NHL10* in different genotypes are compared with that in Col-0 and marked in red, and for flg22-treated samples, it is marked in black.

3.2 flg22 induces CAMTA3 phosphorylation and destabilization *in vivo*

3.2.1 flg22 induces a proteasome-mediated CAMTA3 degradation *in vivo*

To investigate the effect of flg22 treatment on the CAMTA3 protein, we performed western blot analysis in Col-0 protoplasts transiently expressing CAMTA3 overexpression construct *p35S::CAMTA3-3×HA*. Compared to the water-treated control samples, the CAMTA3 protein level was slightly reduced upon flg22 treatment (Fig. 3-5 A), but this was not always clear in every experiment. We suspect that subtle effects on the CAMTA3 protein levels may be partially masked by the strong *35S* promoter-driven expression of *CAMTA3*. To facilitate visualization of the reduction, we co-treated the protoplasts during the flg22 elicitation with cycloheximide (CHX) to inhibit translation. In this case, the reduction in CAMTA3 levels was evidently stronger with flg22 treatment compared to the water treatment (Fig. 3-5 A). The destabilization was blocked by MG115 treatment, suggesting the involvement of the proteasome-mediated degradation pathway (Fig. 3-5 B). Hence, assuming CAMTA3 acts as a transcriptional repressor, the findings support a model where CAMTA3 degradation upon PAMP treatment may lead to its removal from promoters and the de-repression of defense gene expression. In the native context, the flg22-induced increase in *CAMTA3* expression (Fig. 3-2) may reflect the attempt to replace the degraded CAMTA3 proteins.

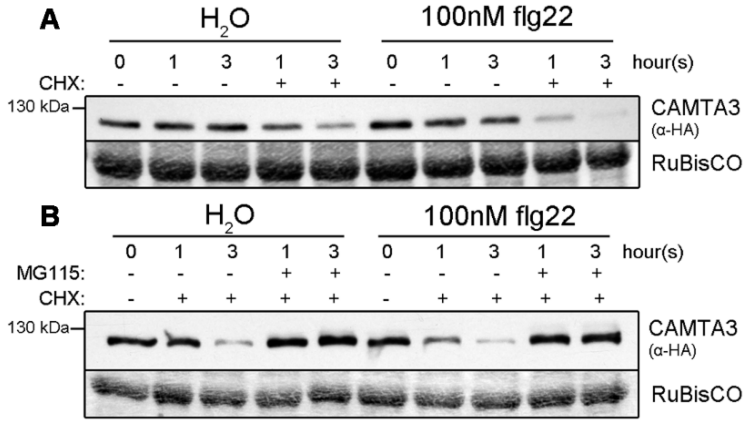

Fig 3-5. Enhanced protein destabilization by PAMP is dependent on the proteasome pathway. A. flg22 induced CAMTA3 degradation *in vivo*. Col-0 protoplasts transfected with plasmids expressing HA-epitope-tagged CAMTA3 were treated with 100 nM flg22 or H_2O (as control), and proteins were extracted for standard SDS-PAGE and western blot analysis. Co-treatment with cycloheximide (CHX, 1 µM) was used to block protein translation. **B.** flg22-induced degradation of CAMTA3 relies on proteasome pathway. Pretreatment with MG115 (50 µM for 30 min) of the transfected protoplasts was used to block proteasome-mediated protein degradation. Anti-HA antibody was used to detect CAMTA3.

3.2.2 CAMTA3 is phosphorylated upon flg22 elicitation *in vivo*

Post-translational modifications such as phosphorylation have been speculated to be involved in the destabilization of CAMTA3 after bacterial infection (Zhang et al. 2014). For this reason, we investigated phosphorylation status upon flg22 elicitation. Due to the large size of the CAMTA3 protein, we employed Manganese (II)-Phos-Tag^{TM}-based western blot analysis, which can be used to monitor phosphorylation status of proteins. Phosphorylated forms have retarded mobility in the gels compared to the non-phosphorylated proteins (Kinoshita, Kinoshita-Kikuta, and Koike 2009). Unlike the well-defined band in standard PAGE, CAMTA3 from unstressed protoplasts already appears as broad smeary bands on Phos-Tag-based western blot. This suggests that CAMTA3 is already (partially) phosphorylated prior to elicitation, which is likely resulting from the stress from handling of the protoplasts. Water treatment led to gradual increasing appearance of bands with slower migration. By contrast, the mobility shift was very rapid for flg22 treatment; all the CAMTA3 proteins shifted within 10 min of flg22 treatment (Fig. 3-6 A). λ-phosphatase treatment of the protein extracts (Fig. 3-6 B) abrogated this mobility shift, suggesting that the smeary bands or reduced mobility bands are a result of phosphorylation. Similar experiments were also performed with CAMTA3 overexpression transgenic lines. However, the large YFP tag precluded the visualization of a phospho-mobility shift even in Phos-Tag gels (Fig. 3-6 C). Nevertheless, MS analysis of the immuno-precipitated CAMTA3 from these transgenic plants allowed us to detect *in vivo* phosphorylation (see below). Taken together, the Phos-Tag analysis and the phosphatase study indicate an *in vivo* flg22-induced CAMTA3 phosphorylation.

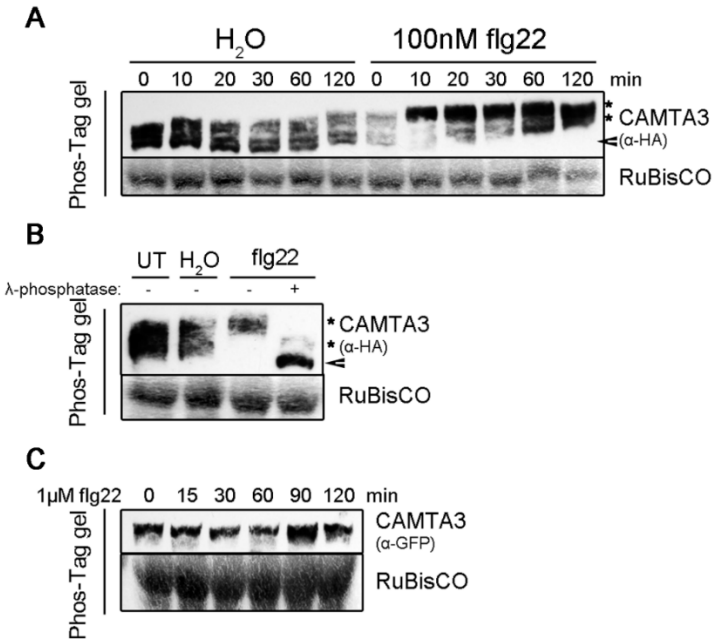

Fig 3-6. PAMP induced phospho-mobility shift of CAMTA3. A. flg22 induced mobility shift of CAMTA3. Col-0 protoplasts were transfected with plasmids expressing HA-epitope-tagged CAMTA3 and treated with 100 nM flg22 or H_2O as control. Treated protoplast samples were harvested at indicated time points, and the extracted proteins were analyzed by Western blot after separation on Manganese(II)-Phos-Tag™-based SDS-PAGE. **B.** flg22-induced CAMTA3 mobility shift was caused by phosphorylation. λ-phosphatase was incubated with protein extracts at 37°C for 10 min to verify phosphorylation. Arrowhead= "unmodified" CAMTA3; *= phosphorylated CAMTA3 forms. Amido black staining of the large subunit of RuBisCO was used as loading control for all western blot analysis. **C.** flg22-induced phospho-mobility shift was not observed within CAMTA3 overexpression line. 10 days CAMTA3 overexpression seedlings, which grew in ½ MS medium, were treated with 1 μM flg22 for indicated time, and harvested. Extracted proteins were separated and analyzed as mentioned in A.

3.3 CAMTA3 interacts with and is phosphorylated by PAMP-responsive MAPKs

3.3.1 CAMTA3 interacts with PAMP-responsive MAPKs *in vivo*

MAPKs are rapidly activated after flg22 treatment and are thus candidate kinases responsible for the CAMTA3 phosphorylation. The best studied MAPKs are MPK3, MPK4 and MPK6, which are known to be activated by pathogens infection or elicitation with PAMPs/MAMPs such as flg22 (Group et al. 2002; Pitzschke, Schikora, and Hirt 2009). Bimolecular fluorescence complementation (BiFC) assays showed that CAMTA3 can indeed interact directly with MPK3, MPK4, and MPK6. By contrast, no interaction with an

unrelated MAPK, MPK8, was seen (Fig. 3-7 A), suggesting specificity of the assay. Western blot confirmed expression of intact proteins of the expected sizes (Fig. 3-7 B). Notably, the BiFC signals are mainly nuclear, suggesting the interaction occurs predominantly in the nucleus.

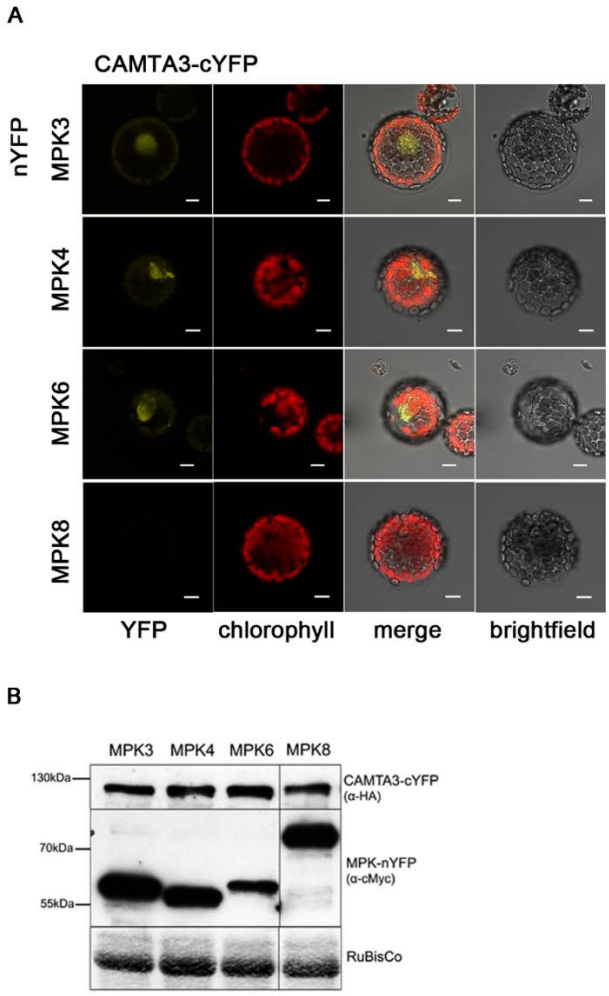

Fig 3-7. CAMTA3 interacts with stress-activated MAPKs (MPK3, MPK4, and MPK6). A. Bimolecular fluorescence complementation (BiFC) assay was performed to detect interactions between CAMTA3 and MPK3, MPK4, and MPK6. Col-0 protoplasts were transfected with constructs encoding the indicated protein fusions to cYFP or nYFP fragments. After allowing the proteins to express/accumulate overnight, the protoplasts were observed by confocal microscopy. Protein-protein interaction is visualized as reconstituted YFP fluorescence signals. MPK8, a non PAMP-responsive MAPK, was used as a negative control. Scale bar = 10 µm. **B.** Western blot showed accumulation of proteins of the expected sizes.

3.3.2 CAMTA3 is phosphorylated by PAMP-responsive MAPKs *in vitro*

To investigate whether CAMTA3 is directly targeted by flg22-regulated MAPKs, an *in vitro* kinase assay was performed. GST-tagged recombinant MPK3, MPK4 and MPK6 were used to phosphorylate purified recombinant His-tagged CAMTA3 *in vitro*. With the incorporation of the ^{32}P-radioactive labelled ATP, it showed that CAMTA3 was *in vitro* phosphorylated by MPK3 (1.00) and MPK6 (0.26), but almost not phosphorylated by MPK4 (0.01). The numbers within parenthesis represent the quantified phosphorylation intensity ratio of CAMTA3 compared with that phosphorylated by MPK3, which are normalized by corresponding phosphorylation intensity of MBP (Fig 3-8).

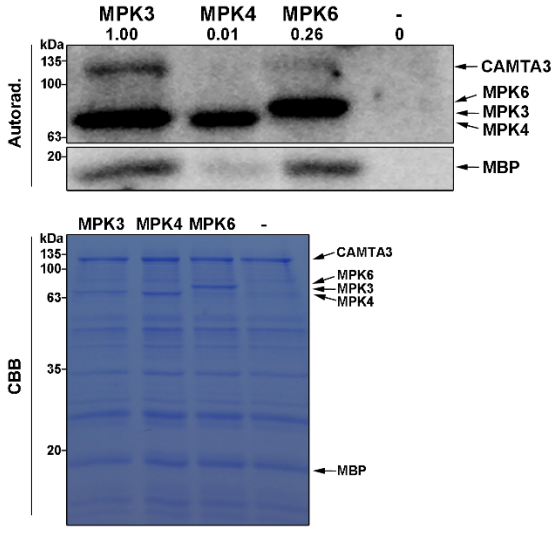

Fig 3-8. *In vitro* kinase assay of recombinant CAMTA3 by PAMP-responsive MAPKs. Recombinant His-tagged CAMTA3 was purified from *E. coli* and used as a substrate for the indicated GST-tagged MAPKs in the presence of ^{32}P-labelled ATP, and reaction was taken place at 37^{o}C for 30 min. After SDS-PAGE separation, phosphorylated proteins were visualized by autoradiography.

3.3.3 CAMTA3 is phosphorylated by MPK3 and MPK6 *in vivo*

To verify *in vivo* phosphorylation, constructs expressing constitutively active MAPKs (CA-MAPKs) (Berriri et al. 2012; Genot et al. 2017) were co-transfected with vectors expressing CAMTA3 into protoplasts. Increased kinase activities of the CA-MAPKs compared to the native kinases were proven by the auto-phosphorylation of the immunoprecipitated MAPKs. CAMTA3 phosphorylation and any effect on the protein levels were monitored by Phos-Tag or standard western blot, respectively. The results showed that CAMTA3 was phospho-shifted through co-expression with CA-MPK6 and it accumulated to lower

levels. For CA-MPK3 co-expression, some phosphorylation (but weaker compared to MPK6) was observed but a strong CAMTA3 destabilization was seen. However, CA-MPK4 co-expression did not phosphorylate CAMTA3, which is consistent with the result of *in vitro* kinase assay, and did not destabilize CAMTA3 as well (Fig. 3-9 A). Taken together, *in vivo* phosphorylation and destabilization is not mediated by MPK4 but is predominantly through MPK6 and partially by MPK3.

However, some caveats to the above interpretations include: (1) in our hands, the CA-MPK4 displayed lower autophosphorylation activity than the other two kinases; (2) it is unknown if substrate specificities or activities of these mutated MAPKs are comparable to the MAPKs natively activated through upstream MAPK kinases. For this reason, we transiently expressed in protoplasts a constitutively active MKK5 ($MKK5^{DD}$) to specifically activate endogenous MPK3 and MPK6 but not MPK4 (Lee et al. 2004; Lassowskat et al. 2014). In this case, MPK3/6 are activated "naturally" through phosphorylation of its kinase activation loop and not through mutation of secondary sites in the protein sequence. Similar to observations above for CA-MPK3 and CA-MPK6, CAMTA3 protein level was reduced through $MKK5^{DD}$ co-expression. The phosphorylated CAMTA3 proteins are difficult to visualize in the Phos-Tag gels since the reduced protein levels are further separated into smeary bands. However, the slower mobility of these fuzzy bands is in agreement with MPK3/6-mediated phosphorylation. Control transfection without any MKKs or co-transfection with a kinase-inactive MKK5 ($MKK5^{KR}$) did not show these effects (Fig. 3-9 B). Hence, the results above suggest that the flg22-responsive MAPKs, MPK3 and MPK6, phosphorylate CAMTA3, and flg22-induced destabilization of CAMTA3 may be triggered by phosphorylation via MPK3 and MPK6.

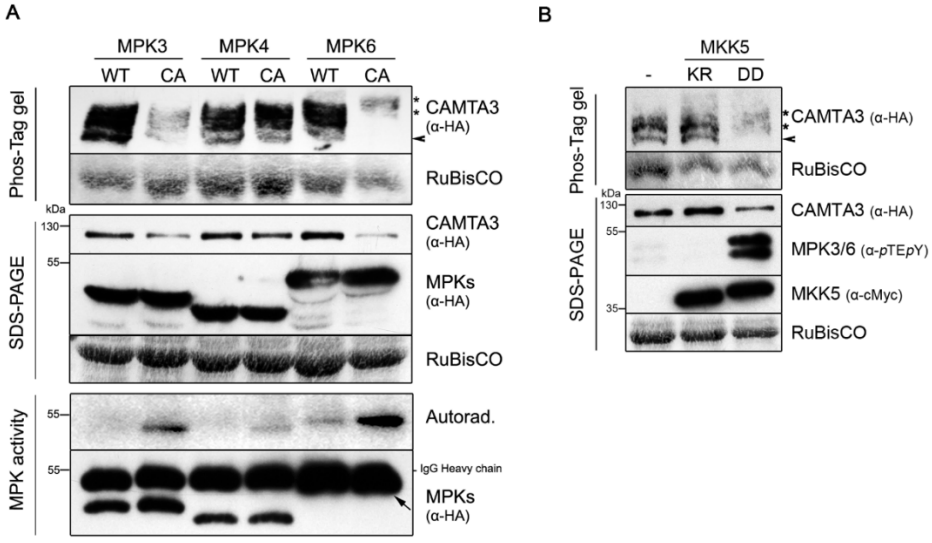

Fig 3-9. CAMTA3 is phosphorylated by MPK3 and MPK6 *in vivo*. A. Transient co-expression of constitutively-active (CA) MPK3 and MPK6, but not CA-MPK4 or wild-type (WT) MPKs, led to increased phosphorylation and destabilization of CAMTA3. Protoplasts were transfected with the indicated constructs and the extracted proteins were analyzed by western blotting after separation on Phos-Tag gel or conventional SDS-PAGE for detecting phosphorylation status (upper panel) or protein stability (middle panel) , respectively. In bottom panel, CA-MAPKs and WT-MAPKs were transfected into protoplasts, extracted and immunoprecipitated by HA antibody. Different kinase activities were determined by their auto-phosphorylation, and visualized by autoradiography. A western blot to estimate equal expression levels of the MPKs. Note that the MPK6 immunological signals are partially overlapping with the IgG heavy chain signals and indicated by a small arrow. **B.** Co-expression of a constitutive MKK5 (DD), but not its kinase-dead variant (KR), led to phospho-mobility shift and reduced protein stability of CAMTA3. CAMTA3 and $MKK5^{DD}$ were co-transfected to protoplasts ($MKK5^{KR}$ co-transfection and CAMTA3 singular transfection as control). After overnight incubation for protein expression, Phos-Tag based or conventional SDS-PAGE based western blots were performed to show CAMTA3 phosphorylation status (upper panel) or protein stability (bottom panel), respectively. Expression of CAMTA3 was monitored with anti-HA antibody, and specific MPK3 and MPK6 phosphorylation by $MKK5^{DD}$ with α-*p*TE*p*Y antibody, and MKK5 (DD and KR) with anti-cMyc antibody (note that a mobility shift was observed with $MKK5^{DD}$, which is due to its constitutive activity). Arrowhead= "unmodified" CAMTA3; *= phosphorylated CAMTA3 forms.

3.4 CAMTA3 is phosphorylated by pathogen-regulated MPK3/6 at multiple sites, which mediate CAMTA3 protein destabilization

3.4.1 CAMTA3 is phosphorylated by MPK3 and MPK6 at multiple sites

The observation that CAMTA3 is phosphorylated by MPK3 and MPK6 both *in vitro* and *in vivo* prompted us to examine the phospho-sites in CAMTA3. MAPKs phosphorylate substrate proteins on conserved motifs: serine or threonine followed by a proline (SP/TP). Among the whole sequence of CAMTA3, there are 11 potential MAPK phosphorylation sites (Fig. 3-10 A). Both *in vitro* kinase assay (with non-radioactive ATP) and infiltrating flg22 to CAMTA3 overexpression lines were used for collecting phosphorylated CAMTA3 protein samples. MPK3- or MPK6-phosphorylated CAMTA3 bands, or flg22-induced phosphorylated CAMTA3 proteins immunoprecipitated from overexpression plant extracts, were excised after SDS-PAGE separation on non-radioactive gels. After digestion and phospho-peptide enrichment, samples were subjected to mass spectrometry (MS) analysis (spectrograms for identified phospho-sites are shown in appendix Figure I). Three phospho-peptides containing phosphorylated S272, S454, or S780 respectively were detected (Fig. 3-10 A, marked in red). With this result, we generated phospho-mutant: CAMTA3-mutP1 (Alanine or glycine were used to substitute serine or threonine). However, the peptide coverage of the MS analysis did not include some regions of the protein, which may be due to insufficient trypsin digestion. PhosPhAt 4.0 database, an *Arabidopsis thaliana* phosphorylation site database incorporating experimental data from several published large- and medium-scale phosphoproteomic

analysis (Heazlewood et al. 2008), annotates two further phosphorylation sites at S8 (Hoehenwarter et al. 2013) and S587 in CAMTA3 (Fig. 3-10 A, marked in blue). Therefore, CAMTA3-mutP2 was generated containing 5 phospho-site mutations in total.

However, *in vitro* MPK3- or MPK6-mediated phosphorylation of the CAMTA3-mutP1 and mutP2 variants was not reduced compared to CAMTA3-WT (Fig. 3-10 B), suggesting additional MAPK-targeted sites exist. To overcome the low peptide coverage of MS analysis, we digested CAMTA3 by both trypsin and endoproteinase Glu-C. With this combination, the coverage of identified peptides increased to more than 60%, which covered more regions containing SP/TP motifs. Phospho-peptides covering T243, S587 and S780 were detected. Notably, T243 (Fig. 3-10 A, marked in green) is a novel phospho-site, never detected in our earlier analysis or reported in PhosPhAt. Therefore, we generated phospho-mutant CAMTA3-mutP2+, which include six phospho-sites mutations (S8, T243, S272, S454, S587 and S780). When tested with in vitro kinase assay, MPK3- or MPK6-mediated phosphorylation of the CAMTA3-mutP2+ variant was strongly reduced compared to CAMTA3-WT (Fig. 3-10 B), so that these six sites are the major MPK3/6-targeted sites. We also generated CAMTA3-mutP3, which includes all 11 potential phospho-sites mutations, and phospho-mimetic mutant CAMTA3-mimic, in which all 11 potential sites (S/T) were substituted by aspartic acids (D) (Fig. 3-10 A), and the phosphorylation of these variants were completely blocked (Fig. 3-10 B).

A

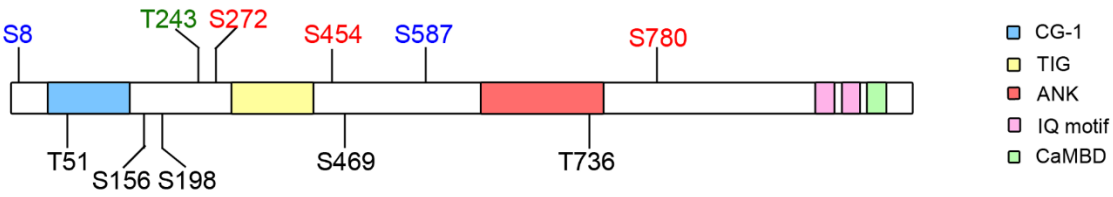

Phosphosite Mutants	Mutated Position
mutP1	S272G, S454A, S780A
mutP2	S272G, S454A, S780A, S8G, S587A
mutP2+	S272G, S454A, S780A, S8G, S587A, T243G
mutP3	all 11 putative MAPK phosphosites (S/TP) are mutated to A/GP
mimic	all 11 putative MAPK phosphosites (S/TP) are mutated to DP

B

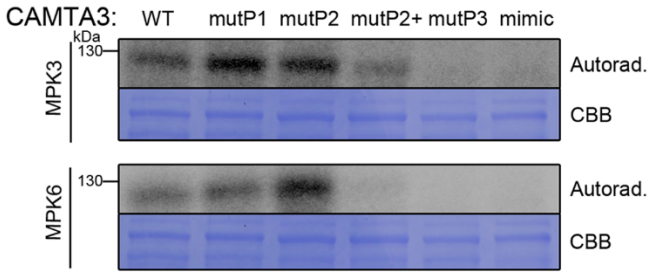

Fig 3-10. MPK3 and MPK6 drive multi-sites phosphorylation of CAMTA3. A. Structure diagram of CAMTA3, identification of phospho-sites and variants of phospho-site mutants of CAMTA3. Functional domains, and all 11 putative MAPK phospho-sites are marked in different colors in the upper panel. The bottom table shows the variants of CAMTA3 phospho-mutants, which were mutated based on MS analysis results. Three phospho-site (red) mutations (S/T were substituted for A/G) are included in mutP1, which were detected from both *in vitro* kinase assay of recombinant CAMTA3 by active MPK3 or MPK6 from (37°C for 30 min, in the presence of cold ATP), and *in vivo* approach of infiltration of 1 μM flg22 into leaves of CAMTA3-eYFP overexpression plants for 1 hour. Phosphorylated and immunoprecipitated proteins were separated in SDS-PAGE, and protein bands were cut for trypsin digestion. After phospho-peptide enrichment, samples were analyzed by LC-MS/MS. Two more phospho-site (blue) mutations were included in the mutP2 variant: S8 was reported by Höhenwarter *et al* 2013 (phosphoproteomics data on seedling after activating endogenous AtMPK3 and AtMPK6 by induction of NtMEK2 activity), and S587 was found in PhosPhAt database. T243 (green) and S587 (blue) were further detected to be phosphorylated in our subsequent MS analysis after using Glu-C and trypsin co-digestion to improve protein sequence coverage during MS. Therefore, mutP2+ was generated on the basis of all MS-based or PhosPhAt-annotated MAPK-targeted phosphosites. mutP3 includes all 11 theoretical MAPK-type phospho-sites. Meanwhile, CAMTA3-mimic was generated by mutating all 11 sites (S/T) to D. **B.** CAMTA3 phospho-sites mutant variants displayed different phosphorylation status. An *in vitro* kinase assay was performed to incubate purified recombinant CAMTA3 variants fused with His tag and activated MPK3 or MPK6, as described in Fig 3-8.

3.4.2 MPK3/6-induced phosphorylation of CAMTA3 causes its destabilization

To investigate a possible role of phosphorylation in CAMTA3 protein destabilization, we compare the stability of the different CAMTA3 phosphosite variants. As above, co-expression of $MKK5^{DD}$ was used to induce MPK3/6 activation. A quantitative western blot system (Li-COR Odyssey® CLx multiplex imaging system) was used to determine the protein levels in three independent experiments. Fig. 3-11 A shows a representative western blot from the three replicates, and the column chart from Fig. 3-11 B (upper panel) shows quantification of three replicates. In agreement with the ECL-based analysis (Fig. 3-9 B), statistically significant reduction of CAMTA3 protein level was seen when co-expressed with $MKK5^{DD}$ (Fig. 3-11). The $MKK5^{DD}$-induced destabilization of CAMTA3 is still observed with the CAMTA3-mutP1, mutP2 and mutP2+ phospho-site mutants, which may suggest that there are additional phosphosites remaining that promote destabilization. Only the CAMTA3-mutP3 mutant, which lacks T/SP motifs and therefore cannot be phosphorylated by MPK3/6, showed no significant difference in protein levels between co-expression with $MKK5^{KR}$ and $MKK5^{DD}$. Thus, the MAPK-targeted phosphosites are crucial for destabilization of the protein.

The phospho-mimic mutant behaved like the native protein in terms of protein destabilization, which probably meant that the mutations generated did not provide efficient mimicry of the phosphorylated residues. Furthermore, it should be noted that destabilization of the mutant mutP2+ variant still occurs although it is barely phosphorylatable by MPK3/6 in the *in vitro* kinase assays. Besides differences between *in vitro* and *in vivo* assays, a possible explanation for this result is that activating MPK3 and MPK6 (with $MKK5^{DD}$) may additionally stimulate proteasome activity. This notion is also supported by the destabilization of the phospho-mimic, despite it being not further phosphorylatable by MAPKs.

Generally, phosphorylation of CAMTA3 reduces the protein stability of CAMTA3, which is supported by the observation of higher basal levels of CAMTA3-mutP3 (without activation of MPK3/6 through $MKK5^{DD}$). Even the partial phosphosite mutants mutP1 to mutP3 have intermediate levels between WT and the mutP3 variant. Due to this difference in basal CAMTA3 levels, we calculated the percentage decrease within each experiment. On the level of individual experiment (differentially color-coded in Fig. 3-11 B lower panel), mutP3 always had the least percentage decrease. These results indicate that CAMTA3 destabilization induced by flg22 requires its phosphorylation mediated by MPK3/6.

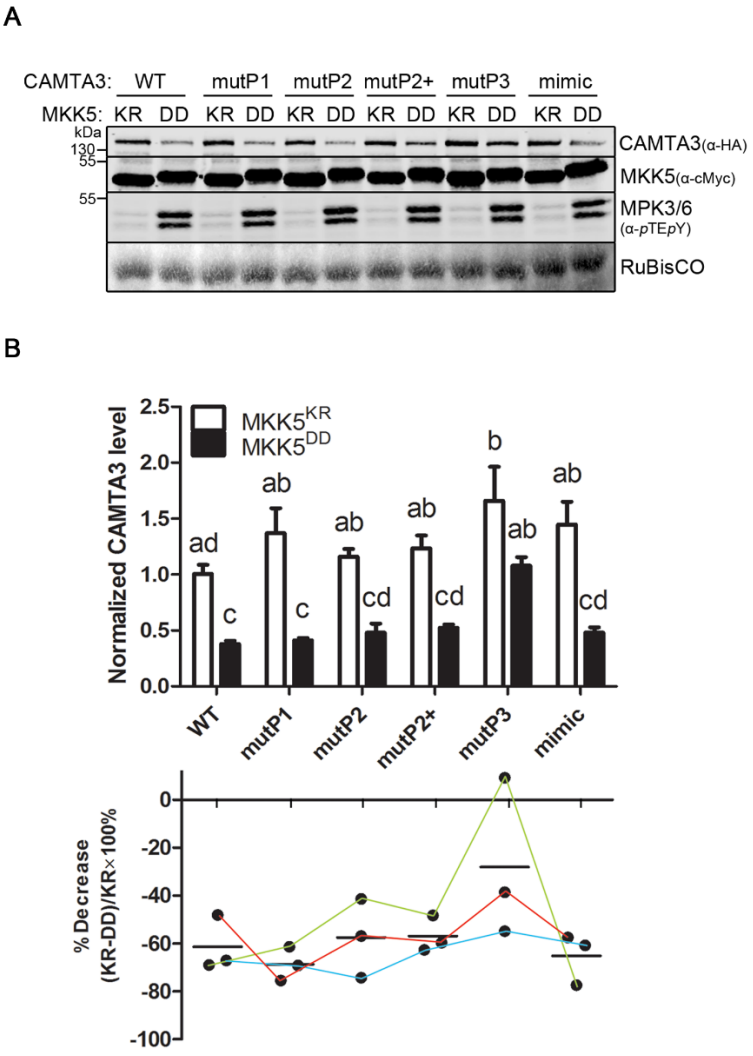

Fig 3-11. MPK3/6-mediated phosphorylation of CAMTA3 induces its degradation. A. CAMTA3 phospho-site mutant variants were transiently co-expressed in protoplasts with constitutively active MKK5 (DD) or kinase-deficient version (KR) as negative control. Extracted proteins were separated by SDS-PAGE and analyzed by quantitative western blotting to detect the CAMTA3 abundance. Anti-c-Myc antibody was used to detect expression of MKK5, and α-*p*TE*p*Y antibody was used to detect activated MPK3 and MPK6. This experiment was repeated three times independently, and a representative blot shown here. **B.** Quantification of CAMTA3 abundance and role of the phosphosites. CAMTA3 abundance was quantified as density of protein bands (as described above). For statistical analysis, the absolute values from individual experiment were normalized by the median of each dataset. One-way ANOVA ($p < 0.05$) for the normalized datasets was performed for comparison, with statistically distinct groups marked with different alphabets (upper panel). Due to different basal levels between experiments, percentage decrease comparing between KR and DD was also calculated within the same genotype for each experiment, using the formula (KR-DD)/KR. Solid black horizontal bar marks mean of the three replicates within one genotype, and the color lines connect the individual experiment.

3.5 Potential mechanism of CAMTA3 destabilization mediated by phosphorylation

From the above results, we could conclude that phosphorylation mediated by pathogen-responsive MPK3 and MPK6 triggers CAMTA3 destabilization. This presumably acts to de-repress the negative regulation of plant immune pathway by CAMTA3. The potential mechanism behind CAMTA3 destabilization through phosphorylation is still unknown. A previous study showed that SR1IP1 (AtSR1-interaction protein 1), a substrate adaptor in CUL3-based E3 ubiquitin ligase, directly interacts with full length CAMTA3 (also named as AtSR1). This recruits CAMTA3 for ubiquitination and degradation by the 26S proteasome (Zhang et al. 2014). Thus, we want to investigate the effect of phosphorylation on the SR1IP1-CAMTA3 interaction and whether it is coupled with ubiquitin-mediated degradation.

3.5.1 The reported interaction between CAMTA3 and SR1IP1 cannot be reproduced

We first wanted to confirm the interaction between SR1IP1 and CAMTA3-WT. We performed several assays including yeast two-hybrid (Fig. 3-12 A), bimolecular fluorescence complementation (BiFC) (Fig. 3-12 B), split-luciferase assay (Fig. 3-12 C) and also co-immunoprecipitation assay (co-IP) (data not shown) in *Arabidopsis* protoplast system, but none of the assays supported interaction between SR1IP1 and CAMTA3 as described in the literature.

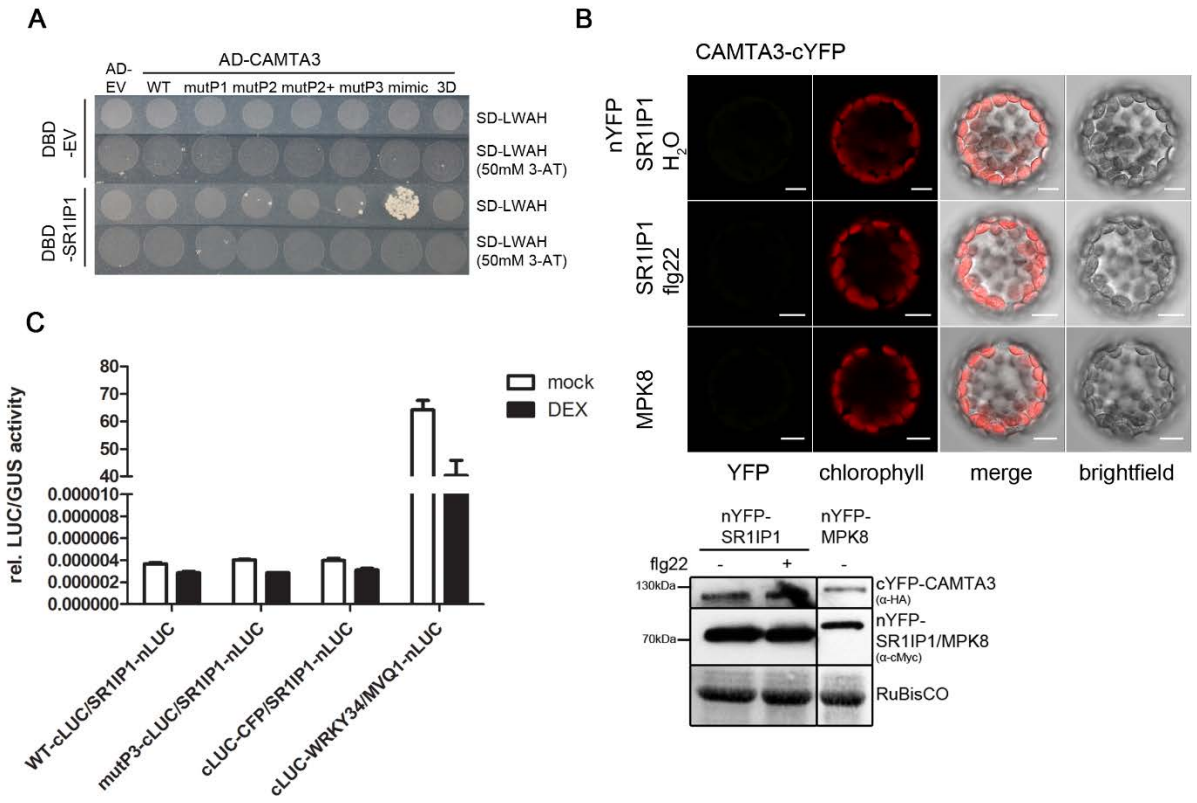

Fig 3-12. Reported interaction between CAMTA3 and SR1IP1 cannot be reproduced. A. A yeast two-hybrid analysis was performed, but failed to show any interaction between CAMTA3 and SR1IP1. CAMTA3 WT and phospho-mutant variants were fused with the activation domain (AD) and SR1IP1 was fused with DNA binding domain (DBD) of the Gal4 transcription factor, respectively. Empty vector (EV) harboring the DBD served as a negative control. The plasmid combinations expressing the indicated fusion proteins were transformed into yeast strain PJ67-4a. Transformed yeast cells were plated on nutrient-restricted media, SD-LWAH and SD-LWAH + 50 mM 3-AT (synthetic drop-out media lacking leucine, tryptophan, adenine, histidine, without or with 50 mM 3-Amino-1,2,4-triazole), and incubated in 28°C for 2 to 3 days. One out of three independent experiments is shown. None of them could show interaction between CAMTA3-WT and SR1IP1, and the interaction between CAMTA3-mimic and SR1IP1 in this figure didn't appear in the other two replicates. **B.** Bimolecular fluorescence complementation (BiFC) assay was performed in *Arabidopsis* Col-0 protoplasts. CAMTA3 fused with cYFP, and SR1IP1 fused with nYFP were co-expressed into protoplasts, and MPK8 fused with nYFP was used as a negative control. After allowing the proteins to express/accumulate overnight, the protoplasts were observed by confocal microscopy. However, YFP fluorescent signal cannot be observed either with H_2O or 100 nM flg22 treatment for 1h. Scale bar = 10 µm. Western blot showed accumulation of proteins of the expected sizes. **C.** Split luciferase assay was performed in *Arabidopsis* protoplasts derived from transgenic plants expressing $MKK5^{DD}$ driven by a dexamethasone (DEX)-inducible promoter. CAMTA3 fused with cLUC and SR1IP1 fused with nLUC fragments were co-transfected into protoplasts. An unrelated protein, CFP fused with nLUC, served as negative control, while cLUC-WRKY34 and MVQ1-nLUC co-expression served as a positive control for the split luciferase assay. *pUBQ10::GUS* was co-transfected for normalization. 2 µM DEX was added directly after transfection to induce $MKK5^{DD}$ expression, and the same amount of pure ethanol treated as mock treatment. After overnight expression and treatment, 1 mM luciferin was added and luminescence was monitored in the luminescence plate reader for 1 hour continuously. Values are the total luminescence in 1 hour normalized against the GUS assay readings. Error bars indicate standard errors (n=3).

3.5.2 CAMTA3 and SR1IP1 localize in different cell compartment

Clearly, it is important to clarify why we could not reproduce interaction between CAMTA3 and SR1IP1. As reported already, CAMTA3 is a transcription factor and mainly localized in the nucleus (Yang and Poovaiah 2002), and we could also confirm this in our results (Fig. 3-13 upper panel). However, we observed SR1IP1-CFP signals mainly in the plasma membrane of transfected protoplasts (Fig. 3-13 bottom panel). Hence, the different localization might explain why we could not detect any interaction between SR1IP1 and CAMTA3 in any of the protoplast-based assay. Compared to the protoplast transfection system, the previous published co-IP assay was performed in SR1IP1 transgenic overexpression line crossed with CAMTA3 complementation line. More proteins may accumulate or even mislocalize, and may have more chance to detect interaction. The discrepancy of the yeast two-hybrid assay is hard to explain but notably, the reported *pSOS*-based two-hybrid assay (Zhang et al. 2014) relies on myristylation of the bait proteins and hence recruitment of the reporter to the plasma membrane; interaction may possibly only occur at membranes. Taken together, the distinct localization of CAMTA3 and SR1IP1 suggests that they cannot physically interact unless there is a re-localization of either proteins from the nucleus or the plasma membrane, respectively.

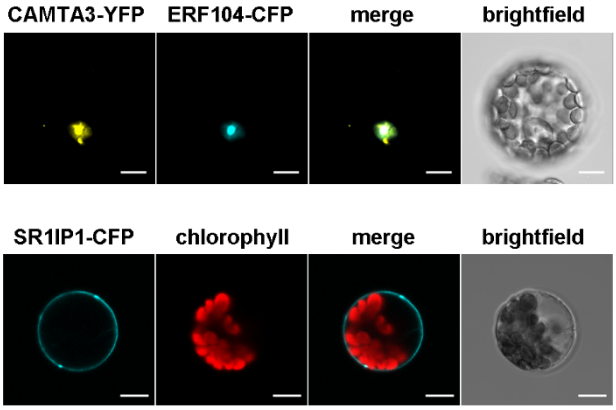

Fig 3-13. Subcellular localization of CAMTA3 and SR1IP1. CAMTA3 fused with YFP was driven by *pUBQ10*, and co-transfected with ERF104 fused with CFP (which is used as a nuclear marker protein) to Col-0 protoplasts. SR1IP1-CFP, also driven by *pUBQ10*, was expressed singly in protoplasts. After protein accumulating overnight, the protoplasts were observed by confocal microscopy. Scale bar = 10 µm.

3.5.3 Phosphorylation induces CAMTA3 subcellular localization change

Interestingly, when transiently expressed in Col-0 protoplasts, the CAMTA3-YFP signal moved out from nucleus to the cytoplasm upon flg22 elicitation (Fig. 3-14 A). Notably, flg22 treatment affected only CAMTA3 localization but not that of SR1IP1 (Fig. 3-14 A). To track the progress of the re-localization, a single Col-0 protoplast expressing YFP-tagged CAMTA3-WT was monitored over a 2 hours period after flg22 treatment. A gradual reduction of nuclear YFP signals and appearance of cytoplasmic speckles was seen after flg22 treatment (Fig. 3-14 B, upper panel) but not with H_2O treatment (Fig. 3-14 A and B). Phosphorylation status appears to be irrelevant since the CAMTA3-mutP3 mutant shows the same relocalization pattern upon flg22 treatment (Fig. 3-14 A and B). However, activation of MPK3 and MPK6 (through $MKK5^{DD}$ co-expression) caused CAMTA3 relocalization in a similar manner like the flg22 treatment. Surprisingly, the non-phosphorylatable CAMTA3-mutP3 remained nuclear-localized with the $MKK5^{DD}$ co-expression (Fig. 3-14 C); thus the phosphosites are important for the relocalization in this case. Western blot confirmed expression of intact proteins of the expected sizes so that the fluorescence signals reflect the localization of the intact proteins (Fig. 3-14 B, D). These results suggest that CAMTA3 relocalization is caused by its phosphorylation induced by MPK3/6 activation, but in the case of flg22 elicitation, there is/are alternative pathway(s) that induce relocalization.

Although the movement of CAMTA3 into the cytoplasm may permit interaction with SR1IP1 and there indeed seems to be partially co-localization between CAMTA3 and SR1IP1 (Fig. 3-14 A and C), we did not obtain any BiFC signals between CAMTA3 and SR1IP1 even upon flg22 elicitation (Fig. 3-12 B). Nevertheless, we cannot exclude that CAMTA3 does interact with SR1IP1 upon flg22 elicitation, because it is possible that upon interaction, CAMTA3 is degraded rapidly, so that no BiFC signals can be detected.

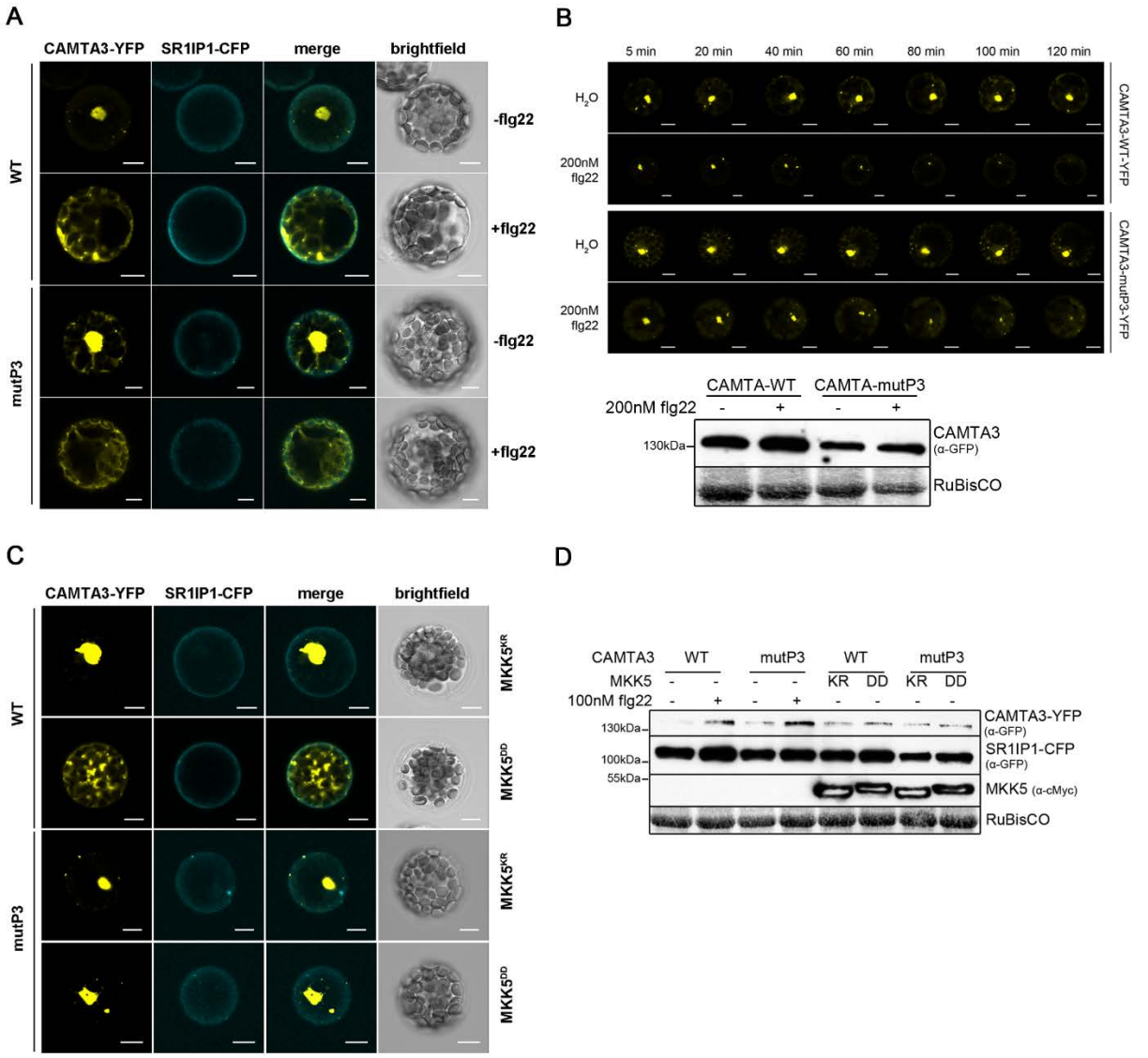

Fig 3-14. Phosphorylation induces CAMTA3 subcellular localization change. A. flg22 elicitation affects both CAMTA3-WT and mutP3 subcellular localizations, but not SR1IP1. CAMTA3-WT or mutP3 fused with YFP and SR1IP1 fused with CFP were driven by a *pUBQ10* and co-expressed in protoplasts. The protoplasts were observed by confocal microscopy in different channels before or after 100 nM flg22 (2h) elicitation. Scale bar = 10 µm. **B.** Confirmation of CAMTA3 subcellular localization change mediated by flg22. Single transfected protoplasts with CAMTA3-WT or mutP3 were continuously monitored for 2 hours after 200 nM flg22 or H_2O treatment. Scale bar = 10 µm. Western blot showed accumulation of proteins of the expected sizes. **C.** Activated MPK3 and MPK6 affect CAMTA3-WT subcellular localization, but not CAMTA3-mutP3. Protoplast transfection was as described before. Instead of flg22 elicitation, $MKK5^{DD}$ was co-transfected to activate MPK3 and MPK6. $MKK5^{KR}$ serves as a negative control. Protoplasts were observed by confocal microscopy after an overnight incubation. Scale bar = 10 µm. **D.** Western blot showed accumulation of proteins of the expected sizes for A and C.

3.6 Additional kinases may be involved in flg22-mediated phosphorylation of CAMTA3

3.6.1 Additional flg22-responsive kinases may phosphorylate CAMTA3, and CPK5 is one of the candidates

From results of the last chapter, we could show that the MAPK targeted sites are dispensable for the flg22-induced subcellular relocalization of CAMTA3 but essential for the MPK3/6-induced pathway (Fig. 3-14). We therefore conclude that flg22 activates other processes, besides MPK3/6, that mediate CAMTA3 relocalization. Using Phos-Tag-based western blot, we also proved that CAMTA3 can indeed be phosphorylated by MPK3 and MPK6 *in vivo* through co-expression of the upstream $MKK5^{DD}$ (Fig. 3-9 B). However, as illustrated in Fig. 3-15 A, flg22 elicited a further phospho-mobility shift of CAMTA3, which is stronger that induced by co-expressing $MKK5^{DD}$. This strong mobility shift was also seen for the mutP3 variant, while there was almost no difference in the mobility shift between co-expressing $MKK5^{KR}$ and $MKK5^{DD}$ (Fig. 3-15 A). Thus, besides MPK3 and MPK6, there are other flg22-responsive kinases that phosphorylate CAMTA3. The analysis with the mutP3 variant that lacks all MAPK-targeted sites also excludes MPK4 or other MAPKs known to be weakly activated by flg22 (e.g. MPK11 (Bethke et al. 2011; Nitta, Ding, and Zhang 2014)).

Besides MAPK cascade, calcium-dependent protein kinases (CDPKs or CPKs) have also been shown to be involved in plant defense responses. Several CDPKs are biochemically activated within a few minutes after exposure to PAMPs or pathogens. In *Arabidopsis*, CPK4, 5, 6, and 11 were identified to act in the innate immunity signaling mediated by PAMP receptor FLS2 (Boudsocq et al. 2010). In particular, CPK5 is phosphorylated and activated upon PAMP stimulation and is a key regulator of innate immune responses in plants (Dubiella et al. 2013). Thus, we tested if CPK5 is involved in flg22-mediated CAMTA3 phosphorylation. Removal of the autoinhibitory region and calcium-binding domain from the N-terminal variable and protein kinase domains results in a constitutively active CPK5 (CPK5-VK). Previous study has shown that CPK5-VK overexpression triggers cell death in *Nicotiana benthamiana* leaves (Dubiella et al. 2013). We transiently expressed CAMTA3-WT or mutP3 together with CPK5-VK or kinase-deficient version (CPK5m-VK) into Col-0 protoplasts. Long exposure of the western blots was necessary to visualize the low levels of CAMTA3-WT or mutP3 accumulating when co-expressed with CPK5-VK. Importantly, CPK5-VK induced a strong phospho-shift in both CAMTA3-WT and mutP3, which is comparable to the shift induced by flg22 stimulation (Fig. 3-15 B, upper panel). Thus, CPK5-VK-induced phosphorylation presumably leads

to CAMTA3 destabilization and degradation *in vivo*. Alternatively, protoplasts expressing CPK5-VK may die rapidly and there is insufficient time for CAMTA3 proteins to accumulate. However, this is unlikely because the staining of RuBisCO for loading control was not significantly different, which means most of the transfected protoplasts were alive. In any case, CPK5 is a candidate for the additional flg22-responsive kinase(s) regulating CAMTA3.

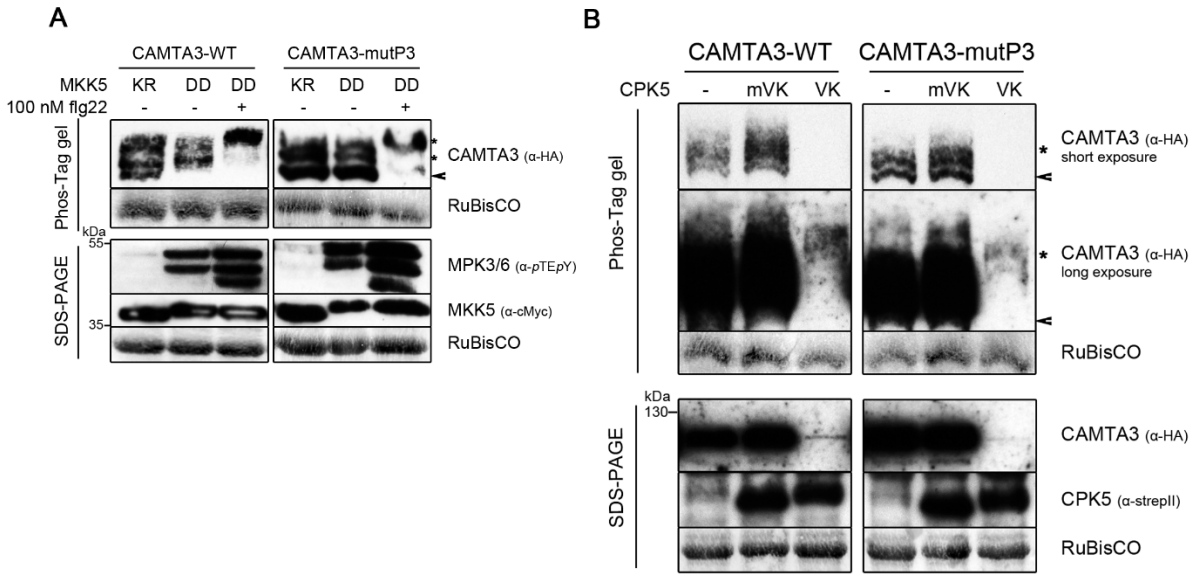

Fig 3-15. Additional kinases mediate phosphorylation of CAMTA3, for example CPK5. A. Additional kinases are involved in flg22-induced phosphorylation of CAMTA3. Col-0 protoplasts were transiently co-expressed with constitutively active $MKK5^{DD}$ or its kinase-dead variant (KR) with CAMTA3-WT or CAMTA3-mutP3, respectively. Additionally, protoplasts transfected by MKK5DD were treated with 100 nM flg22 for 10 min. The extracted proteins were analyzed by western blot after separation on Phos-Tag gel to visualize phospho-mediated mobility shift (upper panel) or conventional SDS-PAGE for MKK5 expression and MPKs activation (bottom panel). **B.** CPK5 induced CAMTA3 phosphorylation and destabilization *in vivo*. Co-transfection of a constitutively active CPK5 (VK), but not a kinase-deficient variant CPK5m-VK, led to a strong phospho-mobility shift and reduced protein stability of both CAMTA3-WT and mutP3. In upper panel, Phos-Tag based western blot displayed CAMTA3 phosphorylation status, and due to the strong protein degradation, phospho-mobility shift could only be observed under long exposure time. The standard western blot in bottom panel monitored CAMTA3 stability and also CPK5(m)-VK expression. Arrowhead= "unmodified" CAMTA3; *= phosphorylated CAMTA3 forms.

3.6.2 CPKs, mainly from subfamily I, affected CAMTA3 phosphorylation status and stability mostly

In *Arabidopsis*, CPKs are encoded by a large gene family of 34 members and classified into four subfamilies (Boudsocq et al. 2010). To assess specificity of the CAMTA3 phosphorylation induced by CPK5-VK, we tested various CPK-VK constructs selected from all four subfamilies. Direct comparison is not trivial

because some of the CPK-VK proteins cannot be reliably detected by western blot despite inducing CAMTA3 phospho-shift. However, in general, most of CPKs-VK from subfamily I can induce strong phosphorylation of CAMTA3 (Fig. 3-16 A). CPK3 from subfamily II, also caused CAMTA3 phosphorylation but since only one member from this subfamily was used, it's not possible to conclude if the other subfamily II members can phosphorylate CAMTA3. Members from subfamily III and IV only induced a slight phosphorylation, compared with the others (Fig. 3-16A).

In addition, we also quantified CAMTA3 protein levels in three independent experiments. Interestingly, CAMTA3 protein abundance was always lowest for those CPKs that trigger stronger phospho-shift. According to the quantitative western blot and statistical analysis, CAMTA3 protein stability was mostly affected by CPK1, CPK2, and CPK5, which showed significant reduction compared to negative control (without co-expressing any CPK-VK). The other members from subfamily I (CPK4, 6, 11) and CPK3 from subfamily II did not affect CAMTA3 stability significantly. And the tested members from subfamily III and IV, which only slightly phosphorylated CAMTA3, also affected CAMTA3 accumulation significantly but with increased CAMTA3 levels (Fig. 3-16 A and B). Taken together, while CPK1-VK and CPK2-VK can modulate CAMTA3 stability when overexpressed, they are not known to be activated by PAMPs and probably involved in other signaling pathways. Among the four reported flg22-responsive CPKs (CPK4, 5, 6, and 11), only CPK5 highly phosphorylated and destabilized CAMTA3. Thus, CPK5 is most likely the flg22-responsive kinase that mediates the *in vivo* flg22-induced phospho-mobility shift of CAMTA3.

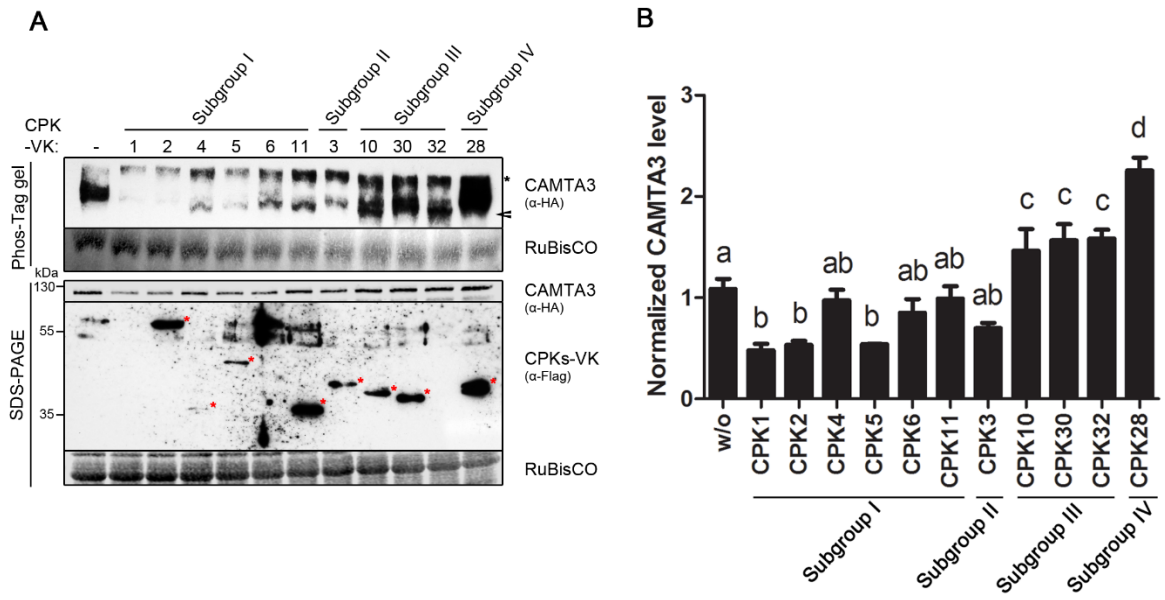

Fig 3-16. CPKs, mainly from subfamily I, affected CAMTA3 phosphorylation status and stability mostly. A. CPKs from all 4 subfamilies were picked up, and their constitutively active VK version were co-expressed in protoplasts with CAMTA3. After overnight incubation for protein expression, the extracted proteins were analyzed by western blotting after separation on Phos-Tag gel or conventional SDS-PAGE for detecting phosphorylation status (upper panel) or protein stability (bottom panel), respectively. Expression of CAMTA3 was monitored with anti-HA antibody, and anti-Flag antibody was used to detect CPKs-VK. Red * pointed indicated CPKs-VK with different size, but some of CPKs-VK were not able to be detected, such as CPK1, CPK6, and CPK32-VK, and it might be due to unstable of these active CPKs-VK. Arrowhead= "unmodified" CAMTA3; *= phosphorylated CAMTA3 forms. **B.** A quantitative western blot was used for detecting CAMTA3 stability affected by CPKs. Three independent replicates were done, and only one out of three results is shown in A (bottom panel). Data from all three replicates were analyzed statistically. The absolute numbers, which represent the density of protein bands, from individual experiment were normalized by the median of this dataset. Three independent normalized datasets were pooled together, and one-way ANOVA was performed for comparison ($p < 0.05$).

3.7 CAMTA3 is an indirect target for CPK5

3.7.1 CAMTA3 interacts with CPK5 *in vivo*

To investigate whether CAMTA3 is a direct target for CPK5, firstly, CAMTA3 interaction with CPK5 was tested. BiFC assay performed in Col-0 protoplasts showed reconstituted YFP fluorescence, suggesting that CAMTA3 can indeed interact directly with CPK5. By contrast, no interaction with MPK8, a negative control, was observed (Fig. 3-17 A, upper panel). A kinase-deficient version CPK5m was shown to interact with CAMTA3 as well (Fig. 3-17 A, upper panel), which indicates that the interaction between CAMTA3 and CPK5 is not dependent on its kinase activity. Notably, BiFC signals co-localized with a nuclear marker

protein ERF104, suggesting the interaction occurs mainly in the nucleus (Fig. 3-17 A, bottom panel). Western blot confirmed expression of intact proteins of the expected sizes (Fig. 3-17 B). All these results indicate that CAMTA3 can interact with CPK5 in the nucleus *in vivo*.

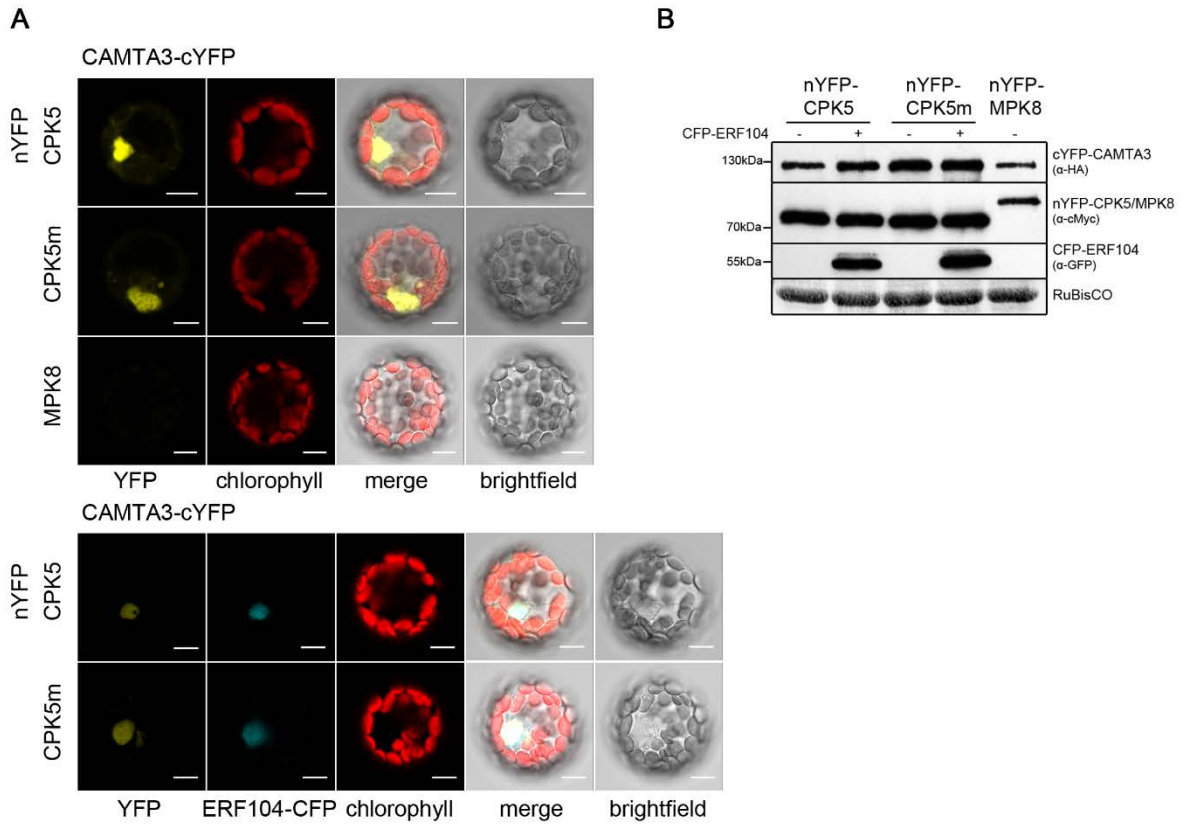

Fig 3-17. CAMTA3 *in vivo* interacts with CPK5. A. Bimolecular fluorescence complementation (BiFC) assay was performed in Col-0 protoplasts. CAMTA3 fused with cYFP fragment and CPK5 (or kinase-deficient mutant CPK5m) fused with nYFP fragment were co-expressed in protoplasts, and MPK8-nYFP fragment fusion was used as a negative control (upper panel). A nuclear marker, ERF104 fused with CFP, was co-expressed as well to study localization of the interaction (bottom panel). After allowing the proteins to express/accumulate overnight, the protoplasts were observed by confocal microscopy. Protein-protein interaction is visualized as reconstituted YFP fluorescence signals. Scale bar = 10 µm. **B.** Western blot showed accumulation of proteins of the expected sizes.

3.7.2 CPK5 does not phosphorylate CAMTA3 *in vitro*

After successfully detecting the interaction between CAMTA3 and CPK5, an *in vitro* kinase assay was performed to further investigate whether CPK5 phosphorylates CAMTA3 directly. His-tagged recombinant CPK5-VK expressed in *E.coli* was purified and was used without further activation through Ca^{2+} addition. CPK5m-VK, the inactive version, was used as a negative control. Histone, a generic kinase substrate, was

phosphorylated by CPK5-VK but not by the inactive CPK5m-VK (Fig. 3-18 A, left panel). However, no radiolabel signals was observed for CAMTA3 despite longer autoradiography exposure (Fig. 3-18 A, right panel). Note that consequently, at this exposure of the autoradiography, the CPK5-VK auto-phosphorylation band (marked with red arrow) was not visible for the gel with histone as substrate (left panel) as compared to the right panel with CAMTA3 as a substrate (Fig.3-18 A). Hence, CPK5-VK can trans-phosphorylate histone but not CAMTA3 and CAMTA3 may be not a direct target for CPK5.

However, the results above may be due to the poor solubility and yield of CPK5-VK expressed in the *E.coli* system. As an alternative source of soluble protein, strepII-tagged full length CPK5 (CPK5-FL) and its kinase-deficient version, CPK5m-FL, were transiently overexpressed and immunoprecipitated from transfected protoplasts. In the presence of Ca^{2+}, both auto-phosphorylation and trans-phosphorylation activities of CPK5-FL could be observed with histone (Fig. 3-18 B left panel) but not CAMTA3 (Fig. 3-18 B right panel) as substrates.

Ca^{2+}/CaM-binding is required for CAMTA3 to suppress plant immune response, and *camta3* mutants that lost their CaM-binding activity were compromised in their function(Du et al. 2009). Thus, calmodulin might be needed for full kinase activity. We additionally added calmodulin in the kinase reactions, but CAMTA3 was still not phosphorylated by CPK5-FL (Fig. 3-18 C). Taken together, all results indicated that CAMTA3 is not directly phosphorylated by CPK5. It is possible that the CAMTA3-CPK5 complex (as shown by BiFC) recruits additional unknown component(s), which presumably includes a kinase that can directly phosphorylate CAMTA3.

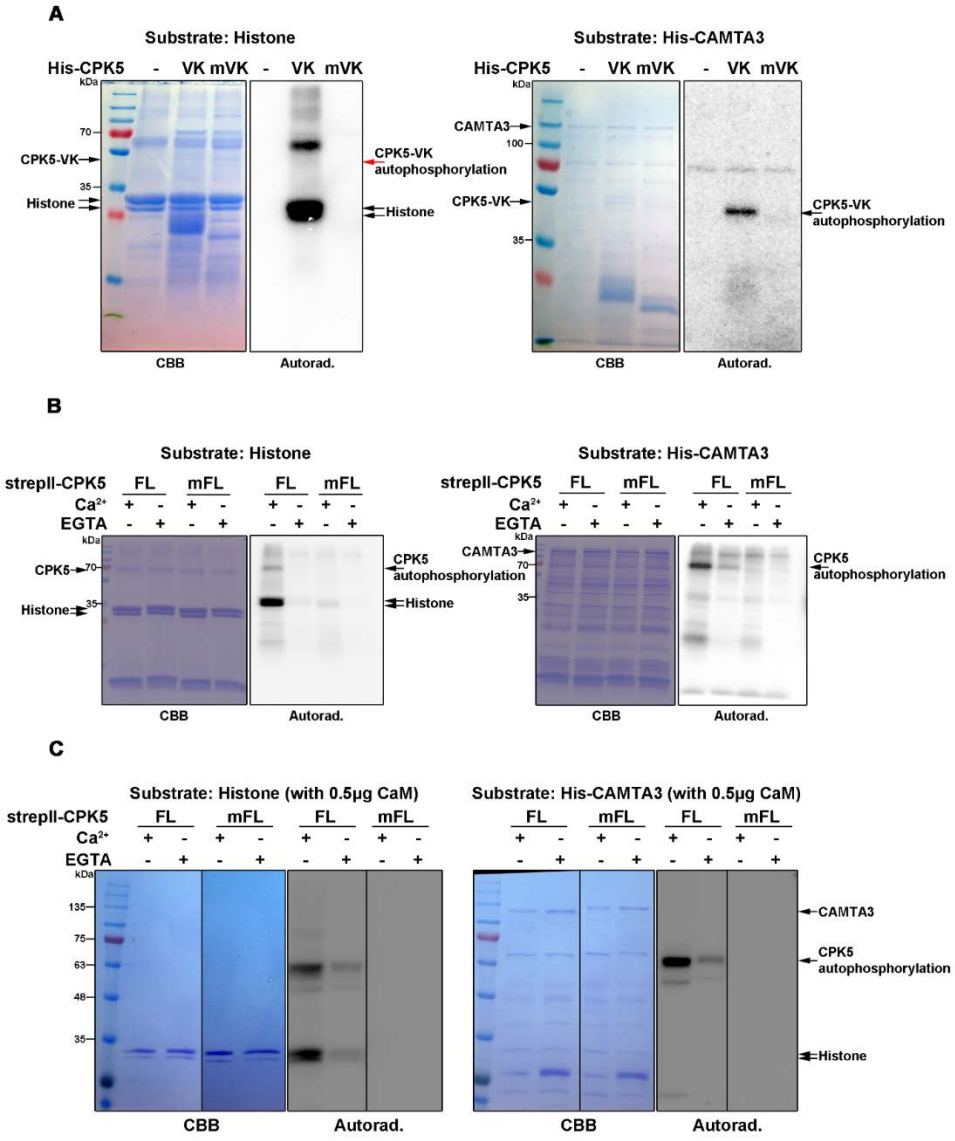

Fig 3-18. CAMTA3 is not phosphorylated by CPK5 *in vitro*. A. Constitutively active CPK5-VK does not phosphorylate CAMTA3 *in vitro*. His-tagged CPK5-VK, kinase-deficient CPK5m-VK and CAMTA3 were expressed and purified from *E.coli*. Indicated kinases were incubated with either Histone (left panel) or CAMTA3 (right panel) in the presence of ^{32}P-labelled ATP at 30ºC for 30 min. Proteins were separated by SDS-PAGE, and phosphorylated proteins were visualized by autoradiography. Note that a shorter exposure time was used for the left panel (due to the strong signals from the phosphorylated histone). **B.** Full-length CPK5 cannot phosphorylate CAMTA3 in the presence of Ca^{2+} *in vitro*. CPK5-FL and kinase-dead variant CPK5m-FL fused with strepII-tag, were natively expressed in *Arabidopsis* protoplasts. After immunoprecipitation, indicated kinases were incubated with Histone (left panel) or purified CAMTA3 (right panel). To show Ca^{2+} dependency of the reaction, EGTA was used to chelate Ca^{2+}. **C.** CaM-binding does not promote CAMTA3 phosphorylation by CPK5. *In vitro* kinase assay was performed as described in B, and additionally 0.5 µg calmodulin (purchased from Sigma) was added in each reaction. Histone (left panel) and CAMTA3 (right panel) were used as substrates, respectively.

4 Discussion

The results presented in this thesis support the notion that CAMTA3 plays a negative role in PTI. CAMTA3 (overexpression) suppresses both basal level and flg22-induced expression of defense genes (Fig 3-4). However, as a repressor of defense responses, CAMTA3 is also transcriptionally upregulated upon flg22 perception (Fig 3-2), presumably as a negative feedback regulation to shut down defense gene expression or to replace the degraded CAMTA3 proteins. Upon flg22 perception, CAMTA3 can be phosphorylated directly by MPK3 and MPK6 at multiple phosphorylation sites (Fig 3-8, 9 and 10). This phosphorylation results in CAMTA3 degradation via a proteasome-dependent pathway, and remobilization of CAMTA3 from the nucleus to cytoplasm (Fig 3-11 and 14). PAMP-responsive CDPK (CPK5) can also stimulate CAMTA3 phosphorylation via a yet unknown mechanism, which also results in CAMTA3 degradation (Fig 3-15). Thus, CAMTA3 may be a converging point downstream of both MAPK cascades and CDPKs to regulate PAMP-inducible gene expression.

4.1 CAMTA3: a hub in MAPK- and CDPK-mediated defense responses

In *Arabidopsis*, two major signaling pathways upon PAMP elicitation - MAPKs and CDPKs - are activated to induce rapid transcriptional reprogramming and mediate plant immunity. Boudsocq et al. (2010) showed that activation of both CDPKs and MAPK cascades are activated independently, which is demonstrated by the unchanged flg22-induced MPK3, MPK4, and MPK6 activation in the *cpk5 cpk6 cpk11* triple mutant or by expressing constitutively active CDPKs. Analysis of expression of selected flg22-inducible genes by RT-PCR also revealed that MAPK cascades and CDPKs can function either synergistically or independently to regulate the expression of PTI genes. There are some CDPK/MAPK synergistically regulated genes such as *NHL10*, *CYP82C2* and *PER4*, and also some MAPK or CDPK specifically regulated genes such as *FRK1* and *PHI-1*, respectively (Boudsocq and Sheen 2013). Both MAPKs and CDPKs regulate PTI signaling pathway by phosphorylating their target proteins such as transcription factors or key enzymes of biosynthetic processes. The typical phosphorylation motifs for MAPKs and CDPKs are different. The minimum MAPK target site is S/T-P, and numerous MAPK substrates have been identified in the past few years. The predicted CDPK target motif is ϕ_{-1}-$[ST]_0$-ϕ_{+1}-X-$Basic_{+3}$-$Basic_{+4}$ (ϕ is a hydrophobic residue)

(Sebastià et al. 2004), and only very few pathogen-responsive CDPK substrates have been identified. These include RBOHD, a substrate of CPK5 after PAMP stimulation (Dubiella et al. 2013), or WRKY8, 28 and 48, which are substrates of CPK4, 5, 6 and 11 involved in ETI signaling (Gao et al. 2013). It is still not known whether the indicated CDPKs phosphorylate another set of transcription factors in regulating PTI gene expression. Different phosphorylation motifs indicate that the MAPKs and CDPKs might regulate PTI signaling by targeting different substrates. However, the same target protein might also be phosphorylated by both kinases at different sites. For instance, ACS2, the key enzyme of ethylene biosynthesis, is known to be MPK3 and MPK6 substrate (Liu and Zhang 2004; Han et al. 2010). It is also possibly phosphorylated by CDPKs, because it has one CDPK phosphorylation site (Lyzenga and Stone 2012). It has been proven that tomato homolog LeACS2 is phosphorylated by LeCDPK2 at certain site, and also by MAPK at different sites in response to wound signaling (Kamiyoshihara et al. 2010).

I could show that in response to flg22, CAMTA3 is not only phosphorylated by MPK3 and MPK6 at multiple sites (Fig 3-8, 3-9), but also by the activation of CPK5 (Fig 3-15). Although a direct phosphorylation by CPK5 was not successfully detected using *in vitro* kinase assay (Fig 3-18), CAMTA3 physically interacted *in vivo* with CPK5 in the nucleus, indicating that CAMTA3 and CPK5 can form a complex (Fig 3-17). It is possible that an alternative unknown component(s) is/are involved in CPK5-mediated phosphorylation of CAMTA3, which might be another kinase that is activated downstream of CPK5. Alternatively, the unknown component is required for both the interaction with and phosphorylation of CAMTA3 by CPK5, and thus may function as a scaffold protein. As mentioned earlier, both MAPKs and CDPKs may target and regulate the same substrate by phosphorylating different sites, and the results also support this point because Fig 3-15 (A) reveals that flg22 also induced phospho-shift of the CAMTA3 phospho-mutant where all 11 potential MAPK phosphorylation sites are mutated. Thus, there might be interplay between the phosphorylation sites targeted by MAPK and CDPK.

4.2 CAMTA3 acts as either transcriptional repressor or activator

As a transcription factor, CAMTA3 is known as a transcriptional repressor in non-stressed plants by binding to the promoters of defense-related genes (e.g. *EDS1*/*NDR1*) (Nie et al. 2012; Du et al. 2009), and the derepression after pathogen infection is mediated through its removal from promoter through proteasome-mediated degradation (Zhang et al. 2014). However, in response to cold stress, CAMTA3 acts as a transcriptional activator to up-regulate cold-related genes (e.g. *CBFs*/*DREB1s*) by binding to the same

cis-element (CGCG box) in the promoters (Doherty et al. 2009). How CAMTA3 functions as a transcriptional repressor or an activator in different contexts is still unknown.

Kim *et al*. (2017) recently revealed that CAMTA3 represses defense-related gene expression (especially SA immunity pathway genes) by the N-terminal end of CAMTA3, which is named as N-terminal repression module (NRM). Du *et al.* (2009) also showed that the transcriptional repression activity of CAMTA3 required CaM binding to the CaM binding domain, which is in conflict with the observation from Kim *et al*. (2017) that only the NRM is sufficient to inhibit expression of SA immunity pathway genes. The position of NRM is consistent with CG-1 DNA-binding domain of CAMTA3, which indicates that CAMTA3 transcriptional repression activity is probably mainly dependent on DNA-binding ability. Upon pathogen infection, the expression of these defense genes are derepressed, which might be regulated by removal of transcriptional repressor CAMTA3 away from promoter. Zhang *et al.* (2014) showed that CAMTA3 is degraded in response to pathogen infection via proteasome-mediated pathway. A CAMTA3-interacting protein, SR1IP1, was identified as a substrate adaptor for cullin3 E3 ligase, which recruits CAMTA3 for ubiquitination and degradation when plants are challenged with pathogens. In agreement with this finding, my results also showed that CAMTA3 is degraded via proteasome-mediated pathway after flg22 perception (Fig 3-5), but further revealed that this decreased CAMTA3 can be induced after phosphorylation mediated by the PAMP-responsive MAPKs (MPK3 and 6) and CDPK (CPK5) (Fig 3-8, 9, 11 and 15). In order to test if phosphorylation affects recruitment of CAMTA3 to SR1IP1, various interaction assays (yeast-2-hybrid, BiFC, split-LUC and coIP) were attempted (Fig 3-12). However, in my hands, the reported interaction between CAMTA3 and SR1IP1 could not be reproduced. In fact, the two proteins are localized in different cell compartments: CAMTA3 is mainly in the nucleus, while SR1IP1 mainly localizes to the plasma membrane (Fig 3-13). Besides triggering protein degradation, phosphorylation also results in exclusion of CAMTA3 from the nucleus to cytoplasm (Fig 3-14). Thus, it is also plausible that relocalization of CAMTA3 out of the nucleus allows it to interact with SR1IP1 at the membrane. However, no BiFC or split-LUC positive signals was ever observed even after flg22 treatment (Fig 3-12). Among the six major MPK3/6-targeted sites, three of them (S8, T243 and T272) are located around CG-1 domain in NRM (Fig 3-10 A), so it would be interesting to investigate if phosphorylation event effects the DNA-binding ability and the transcriptional repression activity in the future.

CAMTA3 is reported as a transcriptional activator to regulate expression of genes responsive to several general stresses (Bjornson et al. 2014; Benn et al. 2014; Walley et al. 2007) or cold-responsive genes by recognizing typical CAMTA3 binding motif, such as *CBFs* and *DREB1s* (Doherty et al. 2009; Kidokoro et al.

2017). One study revealed that CAMTA3 regulates *CBF2* expression additionally via protein-protein interaction. A cold-induced MYB transcription factor MYB96 regulates expression of *HHP2* (*Heptahelical Protein 2*), and the encoded HHP2 protein in turn interacts with *CBF2* upstream transcriptional regulator CAMTA3 to stimulate its transcriptional activity (Lee and Seo 2015).

CAMTA3 functions differentially in different gene promoter context, which is probably mediated by diverse mechanisms. It is also known that suppression of SA immunity pathway by CAMTA3 is overcome by exposing plants to low temperature, which further increases immunity against bacterial pathogen (Kim et al. 2013). Kim *et al*. (2017) further revealed that in response to low temperature, the induction of SA immunity pathway genes is not caused by degradation of CAMTA3 or exclusion of CAMTA3 from nucleus (which is different from the case in response to PAMPs/pathogens). Rather, it results from the downregulation of NRM repression activity by CaM binding to the C-terminal region of CAMTA3, which probably leads to a conformational change (Kim et al. 2017). Thus, CAMTA3 is likely a converging point of the interplay between plant defense and cold stress responses.

4.3 CAMTA3 is a crucial regulator for both PTI and ETI in *Arabidopsis*

CAMTA3 is reported to play a negative role in plant immunity by several research groups and the observations supporting this include: (i) Up-regulated genes in *camta3* mutant are highly enriched for the GO term “defense response” (Galon et al. 2008; Prasad et al. 2016). (ii) *camta3* knockout mutant shows the temperature-related autoimmune phenotypes (Du et al. 2009). (iii) CAMTA3 is involved in *EDS1*- and *NDR1*-mediated resistance pathways, which are key components of the respective TIR-type or CC-type of NLR-mediated resistance, by directly binding to their promoters and repressing their expression (Nie et al. 2012; Du et al. 2009). (iv) CAMTA3 also negatively regulates ET signaling by directly binding to the promoter of *EIN3* and suppressing its expression (Nie et al. 2012). (v) Besides basal defense, CAMTA3 also suppresses systemic acquired resistance (SAR) via unknown mechanisms (Jing et al. 2011).

While all these results support the negative role of CAMTA3 in plant immunity, it has been challenged by a recent study that the constitutive immune activation in *camta3* mutants is caused by activation of two correlated NLRs, DSC1 and DSC2. Thus, CAMTA3 acts as a guardee to form a guard-guardee complex with DSC1 and DSC2 (Lolle et al. 2017). Moreover, CAMTA3 rapidly and transiently activates luciferase reporter activity driven by rapid stress response elements (RSREs) in response to stresses including flg22. RSRE is

overrepresented in the promoters of many general stress-responsive genes and identical to the core CAMTA3-bound element (Benn et al. 2014). Both studies challenge the transcriptional suppression activity of CAMTA3, but indicate that CAMTA3 acts as a "guardee" or even possesses transcriptional activation activity in plant immunity.

It is plausible that DSC1 and DSC2 guard CAMTA3 and trigger immunity, but the transcriptional repression activity of CAMTA3 involved in plant immunity cannot be ignored. First, the effects on immunity regulation is not restricted to the *camta3* knock-out mutants. CAMTA3 transgenic overexpression lines display compromised SAR and basal defense resistance (enhanced susceptibility to *Pst* DC3000) (Jing et al. 2011), but also reduced basal expression level of defense-related genes (*EDS1* and *NHL10*) and flg22-induced expression level of these genes (Fig 3-4). Furthermore, a CAMTA3 gain-of-function mutant, *camta3-3D* was identified as a suppressor of *edr2*-mediated resistant phenotypes and SAR, which displays opposite phenotypes to loss-of-function mutant *camta3* (Jing et al. 2011; Nie et al. 2012). Finally, unpublished results from Prof. Hillel Fromm (Israel) showed that a CAMTA3 variant lacking the CG-1 DNA binding domain cannot complement the *camta3* autoimmune phenotype. It indicates that the DNA binding activity plays a role in regulating immunity and also indirectly demonstrates that CAMTA3 regulates some gene expression during plant immunity. Furthermore, a recent publication found that the N-terminal end of CAMTA3 functions as a repression module (NRM) to suppress SA pathway genes (Kim et al. 2017). Although this work did not show how the NRM inhibits the expression of SA-related genes, it might function via directly DNA binding and repression, because this NRM overlaps with the CG-1 domain.

In analogy, RIN4 is key component of plant defense signaling, which acts as both a negative regulator of PTI and also a guardee modified by pathogen effectors, leading to triggering of ETI. RIN4 was initially identified as a target for several bacterial effectors (including AvrRpt2, AvrRpm1, and AvrB) and the modification of RIN4 by these effectors activates RPS2- and RPM1-mediated immunity (Mackey et al. 2003; Mackey et al. 2002; Axtell and Staskawicz 2003; Axtell et al. 2003). However, RIN4 is also a negative regulator of PTI. For example, overexpression of RIN4 inhibits PAMP-induced responses, which is enhanced when RIN4 is absent (Kim et al. 2005). It is known that AvrRpm1 and AvrB cause phosphorylation of RIN4 at T166, and activates RPM1-mediated immunity (Mackey et al. 2002; Chung et al. 2011). Phosphorylation of RIN4 is also induced by flg22 but at different site S141, which mediates derepressing of PTI outputs such as restriction of bacterial pathogen growth, ROS burst, callose deposition and defense gene induction (Chung et al. 2014). AvrB suppresses PTI via enhancing the phosphorylation of RIN4 at T166, and interestingly, this enhancement of RIN4 T166 phosphorylation by AvrB (and AvrRpm1)

suppresses PTI by antagonizing the phosphorylation of RIN4 at S141 that is induced by flg22 elicitation (Chung et al. 2014). Hence, there are some parallel of CAMTA3 to RIN4, with respect to differential phosphorylation, negative regulation of PTI and a guarding by NLRs.

Lolle et al. (2017) emphasized in their study that autoimmunity in *camta3* is triggered by activation of NLRs and not caused by loss of CAMTA3 as a transcriptional suppressor of defense. Despite all this, some of their notions need to be re-evaluated. For instance, to claim that *camta3*-mediated resistance to *Pst* DC3000 is repressed in the *camta3 dsc1 dsc2* triple mutant, they performed a bacterial growth assay by syringe infiltrating bacteria. They could show that after three days, bacterial growth in *camta3* is much lower than in Col-0 but the resistance in triple mutant is restored to wild-type level. It indicates that excluding the effect by two NLRs, *camta3* no longer displays enhanced pathogen resistance, suggesting that CAMTA3 does not function as a negative regulator of resistance to pathogen (Lolle et al. 2017). Similarly, *Pst* DC3000 grows equally in the double mutant *rpm1 rps2* and the triple mutant *rpm1 rps2 rin4* after syringe infiltrating (RPM1 and PRS2 are the two NLRs guarding RIN4) (Belkhadir et al. 2004). However, after spray inoculation, the growth of *Pst* DC3000 in *rpm1 rps2 rin4* is significantly reduced, suggesting that RIN4 negatively regulates the defense (Kim et al. 2005). Similar result was also reported for the *Pst* DC3000 growth in wild-type and *fls2* mutant. Again bacteria grow equally after infiltrated into leaves, but significantly reduced in wild-type after spray inoculation (Zipfel et al. 2004). The same bacterial strains with different inoculation approaches (i.e. syringe infiltration and spray) display completely different results. This mostly reflect “stomatal immunity” i.e. the ability of bacteria to enter through opened stomatal pores and subsequently multiply within the leaf intercellular spaces. Therefore, to evaluate the effect of CAMTA3 on the basal pathogen resistance, it is necessary to compare the bacterial growth in triple mutant *camta3 dsc1 dsc2* and wild-type by spray inoculation approach. Moreover, *camta3* was reported to exhibit resistance to necrotrophic fungal pathogen *Botrytis cinerea* and *Sclerotinia sclerotiorum*, biotrophic fungal pathogen powdery mildew (*Golovinomyces cichoracearum*) and *Arabidopsis* non-host bacterial pathogen *Xanthomonas oryzae pv. oryzae* (Rahman, Yang, et al. 2016; Rahman, Xu, et al. 2016; Nie et al. 2012); therefore, besides bacterial pathogen *Pst* DC3000, it may be also necessary to test these other pathogens in the triple mutant.

There are still many gaps in understanding how CAMTA3 functions in both PTI and ETI or how it can act as both a transcriptional activator and as a repressor. Post-translational modification may be part of this control. In this thesis, phosphorylation of CAMTA3 was studied and shown to induce CAMTA3 destabilization. The major phospho-sites of CAMTA3 targeted by MPK3 and MPK6 were identified (Fig 3-

10) but the phospho-sites induced by CPK5 (or other kinases) were not detected. One may assume that these CPK5-mediated phospho-sites may be more relevant than those of MPK3/6 since the phospho-shift induced by flg22 treatment resembles that induced by CPK5 (Fig 3-15), rather than the shift induced by MPK3/6. How these phosphosites can alter CAMTA3 conformationally and affect its intra- or inter-molecular interactions will help dissect the mechanism of CAMTA3 control. However, to develop these studies further, one would first have to identify the putative "intermediate" kinase acting downstream of CPK5 to phosphorylate CAMTA3. Another challenge is to identify the pathogen effector(s) that target and modify CAMTA3, and to find out the type of modifications recognized by DSC1 and DSC2. Further, it would be also interesting to investigate whether the modifications of CAMTA3 by pathogen effectors affect its phospho-status regulated by MAPKs or CDPKs and subsequently, other effects caused by phosphorylation such as phosphorylation-induced CAMTA3 destabilization (Fig 3-11) or change of subcellular localization (Fig 3-14). One likely scenario is that effector(s) may dephosphorylate CAMTA3 or suppress CAMTA3 phosphorylation (thus allowing CAMTA3 to accumulate and repress expression of immunity genes).

In conclusion, the isolation of *CAMTA3* in numerous independent genetic screens for immunity/stress-related responses coupled with its post-translational control through phosphorylation by two major stress-responsive kinase pathways, namely MAPKs and CDPKs, highlights it as a central node in immune and/or stress signaling network. The convergence between environmental (cold) and pathogen (or other biotic stresses) signaling on CAMTA3 suggests it may control the interplay and trade-offs between growth and stress response.

4.4 Working model for the function of CAMTA3 in PTI regulation

In this thesis, I showed that transcription factor CAMTA3 is a direct target of MPK3 and MPK6 upon PAMP (flg22) elicitation, and phosphorylated by indicated kinases at multiple sites. Phosphorylation event results in both degradation and change of subcellular localization of CAMTA3 (from nucleus to cytoplasm). In the literature, it is reported that pathogen infection triggered CAMTA3 degradation is mediated by the interaction with SR1IP1, a substrate adaptor in E3 ubiquitin ligase that recruits CAMTA3 for ubiquitination and degradation. However, the reported interaction between CAMTA3 and SR1IP1 cannot be reproduced in my hand, and in fact, both proteins localize in different cellular compartments (nucleus and plasma membrane, respectively). Nevertheless, phosphorylation induced movement of CAMTA3 from nucleus to cytoplasm results in a partial co-localization between CAMTA3 and SR1IP1, and may permit interaction

with SR1IP1, which needs to be further confirmed. In parallel, CPK5 also strongly induces CAMTA3 phosphorylation at different phospho-sites and destabilization upon flg22 perception. However, this appears to occur indirectly. It is possible that CAMTA3 and CPK5 form a complex and recruit additional unknown component(s), which presumably includes a kinase that can directly phosphorylate CAMTA3. Overall, two stress-responsive kinase pathways lead to phosphorylation-induced CAMTA3 re-localization and degradation, which remove the transcriptional repressor CAMTA3 from the promoter of defense genes and derepress the expression of these genes to trigger defense responses (Fig 4-1).

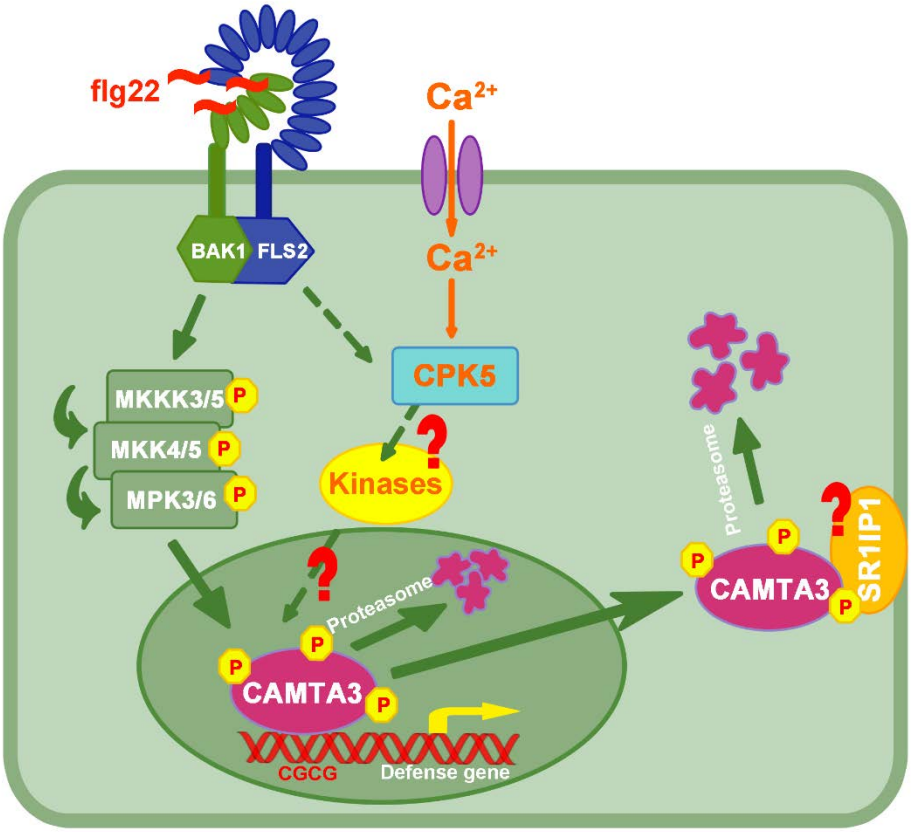

Fig 4-1. Working model for the function of CAMTA3 in regulation PTI

5 Summary

Plant innate immune responses against pathogenic microorganisms are initiated after recognition of conserved pathogen-derived molecules (typically named PAMPs, pathogen-associated molecular patterns). This recognition elicits a complex signaling network that includes early signaling events, such as activation of mitogen-activated protein kinase (MAPK) cascades and calcium-dependent pathways. The *Arabidopsis thaliana* calmodulin binding transcription activator 3 (CAMTA3) is reported to negatively regulate plant defense pathways. According to microarray analysis, many defense-related genes are upregulated in *camta3* mutants. Among these genes, CAMTA3 appears to be a direct repressor for the expression of the *EDS1*, *NDR1* and *EIN3* genes by directly binding to their promoter regions in a sequence specific manner. Phosphoproteomics studies suggested CAMTA3 to be potentially phosphorylated by PAMP-responsive MAPKs.

In this work, CAMTA3 was shown to be rapidly phosphorylated after PAMP treatment. It interacts with the PAMP-responsive MAPKs, MPK3 and MPK6, *in vivo*. Mass spectrometry, following *in vitro* phosphorylation assays, identified multiple phospho-sites in CAMTA3 that are directly phosphorylated by MAPKs. *In vivo*, MAPK-mediated phosphorylation results in subcellular re-localization (from nucleus to cytoplasm) and proteasome-mediated degradation of CAMTA3. In parallel, the PAMP-activated calcium-dependent protein kinase (CDPK), CPK5, also interacts with CAMTA3 *in vivo* and also causes CAMTA3 phosphorylation at sites distinct from those targeted by MAPKs. However, *in vitro* phosphorylation assays did not support a direct phosphorylation of CAMTA3 by CPK5. Thus, the CAMTA3-CPK5 complex may need to recruit additional component(s), which presumably includes a kinase that can directly phosphorylate CAMTA3. The proposed working model is that at least two major PAMP-activated kinase pathways (i.e. MAPKs and CDPKs) converge on CAMTA3, where phosphorylation induces CAMTA3 subcellular re-localization and degradation. CAMTA3 is released from defense-related gene promoters and expression of downstream defense genes is de-repressed. This supports the negative role of CAMTA3 in plant innate immune pathways and a phosphorylation-dependent control of its function.

6 Zusammenfassung

Die pflanzliche Immunantwort wird nach Erkennung von Pathogenen anhand konservierter Molekülstrukturen, sogenannten PAMPs (Pathogen-assoziierte molekulare Muster), ausgelöst. Dabei wird ein komplexes Signalwege-Netzwerk induziert, das frühe Antworten, wie die Aktivierung von Mitogen-aktivierten Protein Kinase (MAPK)-Kaskaden und Calcium-abhängigen Signalwegen beinhaltet. Das *Arabidopsis thaliana* Protein Calmodulin-binding Transcription Activator 3 (CAMTA3) wurde als negativer Regulator der pflanzlichen Abwehr-Signalwege beschrieben. Microarray-Analysen zeigten, dass in *camta3*-Mutanten viele Abwehr-relevante Gene induziert sind. CAMTA3 scheint ein direkter Repressor der Expression von *EDS1*, *NDR1* und *EIN3* zu sein, da es ihre Promotoren in Sequenz-spezifischer Weise bindet. Laut Phosphoproteomik-Studien könnte CAMTA3 durch PAMP-responsive MAPKs phosphoryliert werden.

In dieser Arbeit wurde gezeigt, dass CAMTA3 nach PAMP-Behandlung schnell phosphoryliert wird und mit den PAMP-responsiven MAPKs MPK3 und MPK6 *in vivo* interagiert. Mit Hilfe von Massenspektrometrie-Analysen nach *in vitro* Phosphorylierungsassays konnten mehrere MAPK-Phosphorylierungsstellen identifiziert werden. Die Phosphorylierung von CAMTA3 durch MAPKs führt *in vivo* zur Relokalisierung vom Zellkern ins Cytoplasma und zum Proteasom-abhängigen Abbau. Parallel dazu kann die PAMP-aktivierte Calcium-abhängige Protein-Kinase CPK5 mit CAMTA3 interagieren und es an Stellen phosphorylieren, die sich von den MAPK-Phosphorylierungsstellen unterscheiden. In Phosphorylierungsassays *in vitro* konnte allerdings keine direkte Phosphorylierung von CAMTA3 durch CPK5 nachgewiesen werden. Der CAMTA3-CPK5-Komplex müsste demnach weitere Interaktionspartner rekrutieren, darunter möglicherweise eine Kinase, die dann direkt CAMTA3 phosphorylieren kann. Das vorgeschlagene Arbeitsmodell sieht vor, dass wenigstens zwei unabhängige PAMP-aktivierte Kinase-Signalwege (MAPKs und CPKs) bei CAMTA3 konvergieren und durch Phosphorylierung dessen subzelluläre Relokalisierung und Abbau induzieren. Die Auflösung der Bindung von CAMTA3 an die Promotoren Abwehr-relevanter Gene resultiert in deren erhöhter Expression. Die Ergebnisse dieser Arbeit liefern weitere Hinweise auf die negative Rolle von CAMTA3 innerhalb der pflanzlichen Abwehr-Signalwege und zeigen die Kontrolle seiner Funktion durch Phosphorylierung.

7 Bibliography

Andreasson, Erik, Thomas Jenkins, Peter Brodersen, Stephan Thorgrimsen, Nikolaj H. T. Petersen, Shijiang Zhu, Jin-Long Qiu, Pernille Micheelsen, Anne Rocher, Morten Petersen, Mari-Anne Newman, Henrik Bjørn Nielsen, Heribert Hirt, Imre Somssich, Ole Mattsson, and John Mundy. 2005. 'The MAP kinase substrate MKS1 is a regulator of plant defense responses', *The EMBO Journal*, 24: 2579-89.

Asai, Tsuneaki, Guillaume Tena, Joulia Plotnikova, Matthew R. Willmann, Wan-Ling Chiu, Lourdes Gomez-Gomez, Thomas Boller, Frederick M. Ausubel, and Jen Sheen. 2002. 'MAP kinase signalling cascade in Arabidopsis innate immunity', *Nature*, 415: 977.

Axtell, Michael J., Stephen T. Chisholm, Douglas Dahlbeck, and Brian J. Staskawicz. 2003. 'Genetic and molecular evidence that the Pseudomonas syringae type III effector protein AvrRpt2 is a cysteine protease', *Molecular Microbiology*, 49: 1537-46.

Axtell, Michael J., and Brian J. Staskawicz. 2003. 'Initiation of RPS2-Specified Disease Resistance in Arabidopsis Is Coupled to the AvrRpt2-Directed Elimination of RIN4', *Cell*, 112: 369-77.

Barbashina, Violetta, Paulo Salazar, Eric C. Holland, Marc K. Rosenblum, and Marc Ladanyi. 2005. 'Allelic Losses at 1p36 and 19q13 in Gliomas: Correlation with Histologic Classification, Definition of a 150-kb Minimal Deleted Region on 1p36, and Evaluation of CAMTA1 as a Candidate Tumor Suppressor Gene', *Clinical Cancer Research*, 11: 1119-28.

Belkhadir, Youssef, Zachary Nimchuk, David A. Hubert, David Mackey, and Jeffery L. Dangl. 2004. 'Arabidopsis RIN4 Negatively Regulates Disease Resistance Mediated by RPS2 and RPM1 Downstream or Independent of the NDR1 Signal Modulator and Is Not Required for the Virulence Functions of Bacterial Type III Effectors AvrRpt2 or AvrRpm1', *The Plant Cell*, 16: 2822-35.

Benn, Geoffrey, Chang-Quan Wang, Derrick R. Hicks, Jeffrey Stein, Cade Guthrie, and Katayoon Dehesh. 2014. 'A key general stress response motif is regulated non-uniformly by CAMTA transcription factors', *The Plant journal : for cell and molecular biology*, 80: 82-92.

Benschop, Joris J., Shabaz Mohammed, Martina O'Flaherty, Albert J. R. Heck, Monique Slijper, and Frank L. H. Menke. 2007. 'Quantitative Phosphoproteomics of Early Elicitor Signaling in Arabidopsis', *Molecular & Cellular Proteomics*, 6: 1198-214.

Berriri, Souha, Ana Victoria Garcia, Nicolas Frei dit Frey, Wilfried Rozhon, Stéphanie Pateyron, Nathalie Leonhardt, Jean-Luc Montillet, Jeffrey Leung, Heribert Hirt, and Jean Colcombet. 2012. 'Constitutively Active Mitogen-Activated Protein Kinase Versions Reveal Functions of Arabidopsis MPK4 in Pathogen Defense Signaling', *The Plant Cell*, 24: 4281-93.

Bethke, Gerit, Pascal Pecher, Lennart Eschen-Lippold, Kenichi Tsuda, Fumiaki Katagiri, Jane Glazebrook, Dierk Scheel, and Justin Lee. 2011. 'Activation of the Arabidopsis thaliana Mitogen-Activated Protein Kinase MPK11 by the Flagellin-Derived Elicitor Peptide, flg22', *Molecular Plant-Microbe Interactions*, 25: 471-80.

Bethke, Gerit, Tino Unthan, Joachim F. Uhrig, Yvonne Pöschl, Andrea A. Gust, Dierk Scheel, and Justin Lee. 2009. 'Flg22 regulates the release of an ethylene response factor substrate from MAP kinase 6 in Arabidopsis thaliana via ethylene signaling', *Proceedings of the National Academy of Sciences*, 106: 8067-72.

Bi, Guozhi, Zhaoyang Zhou, Weibing Wang, Lin Li, Shaofei Rao, Ying Wu, Xiaojuan Zhang, Frank L.H. Menke, She Chen, and Jian-Min Zhou. 2018. 'Receptor-like Cytoplasmic Kinases Directly Link Diverse Pattern Recognition Receptors to the Activation of Mitogen-activated Protein Kinase Cascades in Arabidopsis', *The Plant Cell*.

Bjornson, Marta, Geoffrey Benn, Xingshun Song, Luca Comai, Annaliese K. Franz, Abhaya M. Dandekar, Georgia Drakakaki, and Katayoon Dehesh. 2014. 'Distinct Roles for Mitogen-Activated Protein Kinase Signaling and CALMODULIN-BINDING TRANSCRIPTIONAL ACTIVATOR3 in Regulating the Peak Time and Amplitude of the Plant General Stress Response', *Plant Physiology*, 166: 988-96.

Bouché, Nicolas, Ariel Scharlat, Wayne Snedden, David Bouchez, and Hillel Fromm. 2002. 'A Novel Family of Calmodulin-binding Transcription Activators in Multicellular Organisms', *Journal of Biological Chemistry*, 277: 21851-61.

Boudsocq, Marie, and Jen Sheen. 2013. 'CDPKs in immune and stress signaling', *Trends in plant science*, 18: 30-40.

Boudsocq, Marie, Matthew R. Willmann, Matthew McCormack, Horim Lee, Libo Shan, Ping He, Jenifer Bush, Shu-Hua Cheng, and Jen Sheen. 2010. 'Differential innate immune signalling via Ca2+ sensor protein kinases', *Nature*, 464: 418-22.

Boutrot, Freddy, and Cyril Zipfel. 2017. 'Function, Discovery, and Exploitation of Plant Pattern Recognition Receptors for Broad-Spectrum Disease Resistance', *Annual Review of Phytopathology*, 55: 257-86.

BROOKS, DAVID M., CAROL L. BENDER, and BARBARA N. KUNKEL. 2005. 'The Pseudomonas syringae phytotoxin coronatine promotes virulence by overcoming salicylic acid-dependent defences in Arabidopsis thaliana', *Molecular Plant Pathology*, 6: 629-39.

Brunner, Frédéric, Sabine Rosahl, Justin Lee, Jason J. Rudd, Carola Geiler, Sakari Kauppinen, Grethe Rasmussen, Dierk Scheel, and Thorsten Nürnberger. 2002. 'Pep‐13, a plant defense‐inducing pathogen‐associated pattern from Phytophthora transglutaminases', *The EMBO Journal*, 21: 6681-88.

Cao, Yangrong, Yan Liang, Kiwamu Tanaka, Cuong T. Nguyen, Robert P. Jedrzejczak, Andrzej Joachimiak, and Gary Stacey. 2014. 'The kinase LYK5 is a major chitin receptor in Arabidopsis and forms a chitin-induced complex with related kinase CERK1', *eLife*, 3: e03766.

Chen, Huamin, Yan Zou, Yulei Shang, Huiqiong Lin, Yujing Wang, Run Cai, Xiaoyan Tang, and Jian-Min Zhou. 2008. 'Firefly Luciferase Complementation Imaging Assay for Protein-Protein Interactions in Plants', *Plant Physiology*, 146: 368-76.

Cheval, Cécilia, Didier Aldon, Jean-Philippe Galaud, and Benoît Ranty. 2013. 'Calcium/calmodulin-mediated regulation of plant immunity', *Biochimica et Biophysica Acta (BBA) - Molecular Cell Research*, 1833: 1766-71.

Chinchilla, Delphine, Zsuzsa Bauer, Martin Regenass, Thomas Boller, and Georg Felix. 2006. 'The Arabidopsis Receptor Kinase FLS2 Binds flg22 and Determines the Specificity of Flagellin Perception', *The Plant Cell*, 18: 465-76.

Chinchilla, Delphine, Cyril Zipfel, Silke Robatzek, Birgit Kemmerling, Thorsten Nürnberger, Jonathan D. G. Jones, Georg Felix, and Thomas Boller. 2007. 'A flagellin-induced complex of the receptor FLS2 and BAK1 initiates plant defence', *Nature*, 448: 497.

Choi, Man Soo, Min Chul Kim, Jae Hyuk Yoo, Byeong Cheol Moon, Sung Cheol Koo, Byung Ouk Park, Ju Huck Lee, Yoon Duck Koo, Hay Ju Han, Sang Yeol Lee, Woo Sik Chung, Chae Oh Lim, and Moo Je Cho. 2005. 'Isolation of a Calmodulin-binding Transcription Factor from Rice (Oryza sativa L.)', *Journal of Biological Chemistry*, 280: 40820-31.

Chung, Eui-Hwan, Luis da Cunha, Ai-Jiuan Wu, Zhiyong Gao, Karen Cherkis, Ahmed J. Afzal, David Mackey, and Jeffery L. Dangl. 2011. 'Specific Threonine Phosphorylation of a Host Target by Two Unrelated Type III Effectors Activates a Host Innate Immune Receptor in Plants', *Cell Host & Microbe*, 9: 125-36.

Chung, Eui-Hwan, Farid El-Kasmi, Yijian He, Alex Loehr, and Jeffery L Dangl. 2014. 'A Plant Phosphoswitch Platform Repeatedly Targeted by Type III Effector Proteins Regulates the Output of Both Tiers of Plant Immune Receptors', *Cell Host & Microbe*, 16: 484-94.

Couto, Daniel, and Cyril Zipfel. 2016. 'Regulation of pattern recognition receptor signalling in plants', *Nat Rev Immunol*, 16: 537-52.

DeFalco, Thomas A., Kyle W. Bender, and Wayne A. Snedden. 2010. 'Breaking the code: Ca²⁺ sensors in plant signalling', *Biochemical Journal*, 425: 27-40.

Doherty, Colleen J., Heather A. Van Buskirk, Susan J. Myers, and Michael F. Thomashow. 2009. 'Roles for Arabidopsis CAMTA Transcription Factors in Cold-Regulated Gene Expression and Freezing Tolerance', *The Plant Cell*, 21: 972-84.

Du, Liqun, Gul S. Ali, Kayla A. Simons, Jingguo Hou, Tianbao Yang, A. S. N. Reddy, and B. W. Poovaiah. 2009. 'Ca2+/calmodulin regulates salicylic-acid-mediated plant immunity', *Nature*, 457: 1154-58.

Dubiella, Ullrich, Heike Seybold, Guido Durian, Eileen Komander, Roman Lassig, Claus-Peter Witte, Waltraud X. Schulze, and Tina Romeis. 2013. 'Calcium-dependent protein kinase/NADPH oxidase activation circuit is required for rapid defense signal propagation', *Proceedings of the National Academy of Sciences*, 110: 8744-49.

Dyson, Michael R., S. Paul Shadbolt, Karen J. Vincent, Rajika L. Perera, and John McCafferty. 2004. 'Production of soluble mammalian proteins in Escherichia coli: identification of protein features that correlate with successful expression', *BMC Biotechnology*, 4: 32.

Earley, Keith W., Jeremy R. Haag, Olga Pontes, Kristen Opper, Tom Juehne, Keming Song, and Craig S. Pikaard. 2006. 'Gateway-compatible vectors for plant functional genomics and proteomics', *The Plant Journal*, 45: 616-29.

Elmore, James Mitch, Zuh-Jyh Daniel Lin, and Gitta Coaker. 2011. 'Plant NB-LRR signaling: upstreams and downstreams', *Current Opinion in Plant Biology*, 14: 365-71.

Eschen-Lippold, Lennart, Xiyuan Jiang, James Mitch Elmore, David Mackey, Libo Shan, Gitta Coaker, Dierk Scheel, and Justin Lee. 2016. 'Bacterial AvrRpt2-Like Cysteine Proteases Block Activation of

the Arabidopsis Mitogen-Activated Protein Kinases, MPK4 and MPK11', *Plant Physiology*, 171: 2223-38.

Feilner, Tanja, Claus Hultschig, Justin Lee, Svenja Meyer, Richard G. H. Immink, Andrea Koenig, Alexandra Possling, Harald Seitz, Allan Beveridge, Dierk Scheel, Dolores J. Cahill, Hans Lehrach, Jürgen Kreutzberger, and Birgit Kersten. 2005. 'High Throughput Identification of Potential Arabidopsis Mitogen-activated Protein Kinases Substrates', *Molecular & Cellular Proteomics*, 4: 1558-68.

Felix, Georg, Juliana D. Duran, Sigrid Volko, and Thomas Boller. 1999. 'Plants have a sensitive perception system for the most conserved domain of bacterial flagellin', *The Plant Journal*, 18: 265-76.

Feng, Feng, Fan Yang, Wei Rong, Xiaogang Wu, Jie Zhang, She Chen, Chaozu He, and Jian-Min Zhou. 2012. 'A Xanthomonas uridine 5′ -monophosphate transferase inhibits plant immune kinases', *Nature*, 485: 114.

Finkler, Aliza, Ruth Ashery-Padan, and Hillel Fromm. 2007. 'CAMTAs: Calmodulin-binding transcription activators from plants to human', *FEBS Letters*, 581: 3893-98.

Furlan, Giulia, Hirofumi Nakagami, Lennart Eschen-Lippold, Xiyuan Jiang, Petra Majovsky, Kathrin Kowarschik, Wolfgang Hoehenwarter, Justin Lee, and Marco Trujillo. 2017. 'Changes in PUB22 Ubiquitination Modes Triggered by MITOGEN-ACTIVATED PROTEIN KINASE3 Dampen the Immune Response', *The Plant Cell*, 29: 726-45.

Galán, Jorge E., Maria Lara-Tejero, Thomas C. Marlovits, and Samuel Wagner. 2014. 'Bacterial Type III Secretion Systems: Specialized Nanomachines for Protein Delivery into Target Cells', *Annual Review of Microbiology*, 68: 415-38.

Galon, Yael, Roni Aloni, Dikla Nachmias, Orli Snir, Ester Feldmesser, Sarah Scrase-Field, Joy M. Boyce, Nicolas Bouché, Marc R. Knight, and Hillel Fromm. 2010. 'Calmodulin-binding transcription activator 1 mediates auxin signaling and responds to stresses in Arabidopsis', *Planta*, 232: 165-78.

Galon, Yael, Aliza Finkler, and Hillel Fromm. 2010. 'Calcium-Regulated Transcription in Plants', *Molecular Plant*, 3: 653-69.

Galon, Yael, Roy Nave, Joy M. Boyce, Dikla Nachmias, Marc R. Knight, and Hillel Fromm. 2008. 'Calmodulin-binding transcription activator (CAMTA) 3 mediates biotic defense responses in Arabidopsis', *FEBS Letters*, 582: 943-48.

Gao, Minghui, Jinman Liu, Dongling Bi, Zhibin Zhang, Fang Cheng, Sanfeng Chen, and Yuelin Zhang. 2008. 'MEKK1, MKK1/MKK2 and MPK4 function together in a mitogen-activated protein kinase cascade to regulate innate immunity in plants', *Cell Research*, 18: 1190.

Gao, Xiquan, Xin Chen, Wenwei Lin, Sixue Chen, Dongping Lu, Yajie Niu, Lei Li, Cheng Cheng, Matthew McCormack, Jen Sheen, Libo Shan, and Ping He. 2013. 'Bifurcation of Arabidopsis NLR Immune Signaling via Ca2+-Dependent Protein Kinases', *PLoS Pathogens*, 9: e1003127.

Genot, Baptiste, Julien Lang, Souha Berriri, Marie Garmier, Françoise Gilard, Stéphanie Pateyron, Katrien Haustraete, Dominique Van Der Straeten, Heribert Hirt, and Jean Colcombet. 2017. 'Constitutively Active Arabidopsis MAP Kinase 3 Triggers Defense Responses Involving Salicylic Acid and SUMM2 Resistance Protein', *Plant Physiology*, 174: 1238-49.

Gilmour, Sarah J., Daniel G. Zarka, Eric J. Stockinger, Maite P. Salazar, Jaimie M. Houghton, and Michael F. Thomashow. 1998. 'Low temperature regulation of the Arabidopsis CBF family of AP2 transcriptional activators as an early step in cold-induced COR gene expression', *The Plant Journal*, 16: 433-42.

Gómez-Gómez, Lourdes, and Thomas Boller. 2000. 'FLS2: An LRR Receptor–like Kinase Involved in the Perception of the Bacterial Elicitor Flagellin in Arabidopsis', *Molecular Cell*, 5: 1003-11.

Grefen, Christopher, Naomi Donald, Kenji Hashimoto, Jörg Kudla, Karin Schumacher, and Michael R. Blatt. 2010. 'A ubiquitin-10 promoter-based vector set for fluorescent protein tagging facilitates temporal stability and native protein distribution in transient and stable expression studies', *The Plant Journal*, 64: 355-65.

Grimm, Samuel. 2017. 'Regulation of defence gene expression by MAP-kinase targeted VQ-motif protein, MVQ8', Martin-Luther-University Halle-Wittenberg.

Group, Mapk, Kazuya Ichimura, Kazuo Shinozaki, Guillaume Tena, Jen Sheen, Yves Henry, Anthony Champion, Martin Kreis, Shuqun Zhang, Heribert Hirt, Cathal Wilson, Erwin Heberle-Bors, Brian E. Ellis, Peter C. Morris, Roger W. Innes, Joseph R. Ecker, Dierk Scheel, Daniel F. Klessig, Yasunori Machida, John Mundy, Yuko Ohashi, and John C. Walker. 2002. 'Mitogen-activated protein kinase cascades in plants: a new nomenclature', *Trends in plant science*, 7: 301-08.

Han, Junhai, Ping Gong, Keith Reddig, Mirna Mitra, Peiyi Guo, and Hong-Sheng Li. 2006. 'The Fly CAMTA Transcription Factor Potentiates Deactivation of Rhodopsin, a G Protein-Coupled Light Receptor', *Cell*, 127: 847-58.

Han, Ling, Guo-Jing Li, Kwang-Yeol Yang, Guohong Mao, Ruigang Wang, Yidong Liu, and Shuqun Zhang. 2010. 'Mitogen-activated protein kinase 3 and 6 regulate Botrytis cinerea-induced ethylene production in Arabidopsis', *The Plant Journal*, 64: 114-27.

Hayafune, Masahiro, Rita Berisio, Roberta Marchetti, Alba Silipo, Miyu Kayama, Yoshitake Desaki, Sakiko Arima, Flavia Squeglia, Alessia Ruggiero, Ken Tokuyasu, Antonio Molinaro, Hanae Kaku, and Naoto Shibuya. 2014. 'Chitin-induced activation of immune signaling by the rice receptor CEBiP relies on a unique sandwich-type dimerization', *Proceedings of the National Academy of Sciences*, 111: E404-E13.

Heazlewood, Joshua L., Pawel Durek, Jan Hummel, Joachim Selbig, Wolfram Weckwerth, Dirk Walther, and Waltraud X. Schulze. 2008. 'PhosPhAt: a database of phosphorylation sites in Arabidopsis thaliana and a plant-specific phosphorylation site predictor', *Nucleic Acids Research*, 36: D1015-D21.

Hind, Sarah R., Susan R. Strickler, Patrick C. Boyle, Diane M. Dunham, Zhilong Bao, Inish M. O'Doherty, Joshua A. Baccile, Jason S. Hoki, Elise G. Viox, Christopher R. Clarke, Boris A. Vinatzer, Frank C. Schroeder, and Gregory B. Martin. 2016. 'Tomato receptor FLAGELLIN-SENSING 3 binds flgII-28 and activates the plant immune system', *Nature Plants*, 2: 16128.

Hoehenwarter, Wolfgang, Martin Thomas, Ella Nukarinen, Volker Egelhofer, Horst Röhrig, Wolfram Weckwerth, Uwe Conrath, and Gerold J. M. Beckers. 2013. 'Identification of Novel in vivo MAP Kinase Substrates in Arabidopsis thaliana Through Use of Tandem Metal Oxide Affinity Chromatography', *Molecular & Cellular Proteomics : MCP*, 12: 369-80.

Ichimura, Kazuya, Tsuyoshi Mizoguchi, Kenji Irie, Peter Morris, Jérôme Giraudat, Kunihiro Matsumoto, and Kazuo Shinozaki. 1998. 'Isolation of ATMEKK1 (a MAP Kinase Kinase Kinase)-Interacting Proteins and Analysis of a MAP Kinase Cascade inArabidopsis', *Biochemical and Biophysical Research Communications*, 253: 532-43.

James, Philip, John Halladay, and Elizabeth A. Craig. 1996. 'Genomic Libraries and a Host Strain Designed for Highly Efficient Two-Hybrid Selection in Yeast', *Genetics*, 144: 1425-36.

Jing, Beibei, Shaohua Xu, Mo Xu, Yan Li, Shuxin Li, Jinmei Ding, and Yuelin Zhang. 2011. 'Brush and Spray: A High-Throughput Systemic Acquired Resistance Assay Suitable for Large-Scale Genetic Screening', *Plant Physiology*, 157: 973-80.

Jones, Jonathan D. G., and Jeffery L. Dangl. 2006. 'The plant immune system', *Nature*, 444: 323.

Kadota, Yasuhiro, Jan Sklenar, Paul Derbyshire, Lena Stransfeld, Shuta Asai, Vardis Ntoukakis, Jonathan DG Jones, Ken Shirasu, Frank Menke, Alexandra Jones, and Cyril Zipfel. 2014. 'Direct Regulation of the NADPH Oxidase RBOHD by the PRR-Associated Kinase BIK1 during Plant Immunity', *Molecular Cell*, 54: 43-55.

Kaku, Hanae, Yoko Nishizawa, Naoko Ishii-Minami, Chiharu Akimoto-Tomiyama, Naoshi Dohmae, Koji Takio, Eiichi Minami, and Naoto Shibuya. 2006. 'Plant cells recognize chitin fragments for defense signaling through a plasma membrane receptor', *Proceedings of the National Academy of Sciences*, 103: 11086-91.

Kamiyoshihara, Yusuke, Mineko Iwata, Tomoko Fukaya, Miho Tatsuki, and Hitoshi Mori. 2010. 'Turnover of LeACS2, a wound-inducible 1-aminocyclopropane-1-carboxylic acid synthase in tomato, is regulated by phosphorylation/dephosphorylation', *The Plant Journal*, 64: 140-50.

Kidokoro, Satoshi, Koshi Yoneda, Hironori Takasaki, Fuminori Takahashi, Kazuo Shinozaki, and Kazuko Yamaguchi-Shinozaki. 2017. 'Different Cold-Signaling Pathways Function in the Responses to Rapid and Gradual Decreases in Temperature', *The Plant Cell*, 29: 760-74.

Kim, Min Gab, Luis da Cunha, Aidan J. McFall, Youssef Belkhadir, Sruti DebRoy, Jeffrey L. Dangl, and David Mackey. 2005. 'Two Pseudomonas syringae Type III Effectors Inhibit RIN4-Regulated Basal Defense in Arabidopsis', *Cell*, 121: 749-59.

Kim, Yong Sig, Chuanfu An, Sunchung Park, Sarah J. Gilmour, Ling Wang, Luciana Renna, Federica Brandizzi, Rebecca Grumet, and Michael F. Thomashow. 2017. 'CAMTA-Mediated Regulation of Salicylic Acid Immunity Pathway Genes in Arabidopsis Exposed to Low Temperature and Pathogen Infection', *The Plant Cell*, 29: 2465-77.

Kim, YongSig, Sunchung Park, Sarah J. Gilmour, and Michael F. Thomashow. 2013. 'Roles of CAMTA transcription factors and salicylic acid in configuring the low-temperature transcriptome and freezing tolerance of Arabidopsis', *The Plant Journal*, 75: 364-76.

Kinoshita, Eiji, Emiko Kinoshita-Kikuta, and Tohru Koike. 2009. 'Separation and detection of large phosphoproteins using Phos-tag SDS-PAGE', *Nature Protocols*, 4: 1513.

Kong, Qing, Tongjun Sun, Na Qu, Junling Ma, Meng Li, Yu-ti Cheng, Qian Zhang, Di Wu, Zhibin Zhang, and Yuelin Zhang. 2016. 'Two Redundant Receptor-Like Cytoplasmic Kinases Function Downstream of Pattern Recognition Receptors to Regulate Activation of SA Biosynthesis', *Plant Physiology*, 171: 1344-54.

Koo, Sung Cheol, Man Soo Choi, Hyun Jin Chun, Dong Bum Shin, Bong Soo Park, Yul Ho Kim, Hyang-Mi Park, Hak Soo Seo, Jong Tae Song, Kyu Young Kang, Dae-Jin Yun, Woo Sik Chung, Moo Je Cho, and Min Chul Kim. 2009. 'The calmodulin-binding transcription factor OsCBT suppresses defense responses to pathogens in rice', *Molecules and Cells*, 27: 563-70.

Kunze, Gernot, Cyril Zipfel, Silke Robatzek, Karsten Niehaus, Thomas Boller, and Georg Felix. 2004. 'The N Terminus of Bacterial Elongation Factor Tu Elicits Innate Immunity in Arabidopsis Plants', *The Plant Cell*, 16: 3496-507.

Laluk, K., Kvsk Prasad, T. Savchenko, H. Celesnik, K. Dehesh, M. Levy, T. Mitchell-Olds, and A. S. N. Reddy. 2012. 'The Calmodulin-Binding Transcription Factor SIGNAL RESPONSIVE1 is a Novel Regulator of Glucosinolate Metabolism and Herbivory Tolerance in Arabidopsis', *Plant and Cell Physiology*, 53: 2008-15.

Lassowskat, Ines, Christoph Böttcher, Lennart Eschen-Lippold, Dierk Scheel, and Justin Lee. 2014. 'Sustained mitogen-activated protein kinase activation reprograms defense metabolism and phosphoprotein profile in Arabidopsis thaliana', *Frontiers in Plant Science*, 5: 554.

Lecourieux, David, Raoul Ranjeva, and Alain Pugin. 2006. 'Calcium in plant defence-signalling pathways', *New Phytologist*, 171: 249-69.

Lee, Hong Gil, and Pil Joon Seo. 2015. 'The MYB96–HHP module integrates cold and abscisic acid signaling to activate the CBF–COR pathway in Arabidopsis', *The Plant Journal*, 82: 962-77.

Lee, Jin Suk, Kyung Won Huh, Apurva Bhargava, and Brian E. Ellis. 2008. 'Comprehensive analysis of protein-protein interactions between Arabidopsis MAPKs and MAPK kinases helps define potential MAPK signalling modules', *Plant Signaling & Behavior*, 3: 1037-41.

Lee, Justin, Jason J. Rudd, Violetta K. Macioszek, and Dierk Scheel. 2004. 'Dynamic Changes in the Localization of MAPK Cascade Components Controlling Pathogenesis-related (PR) Gene Expression during Innate Immunity in Parsley', *Journal of Biological Chemistry*, 279: 22440-48.

Li, Guojing, Xiangzong Meng, Ruigang Wang, Guohong Mao, Ling Han, Yidong Liu, and Shuqun Zhang. 2012. 'Dual-Level Regulation of ACC Synthase Activity by MPK3/MPK6 Cascade and Its Downstream WRKY Transcription Factor during Ethylene Induction in Arabidopsis', *PLOS Genetics*, 8: e1002767.

Li, Lei, Meng Li, Liping Yu, Zhaoyang Zhou, Xiangxiu Liang, Zixu Liu, Gaihong Cai, Liyan Gao, Xiaojuan Zhang, Yingchun Wang, She Chen, and Jian-Min Zhou. 2014. 'The FLS2-Associated Kinase BIK1 Directly Phosphorylates the NADPH Oxidase RbohD to Control Plant Immunity', *Cell Host & Microbe*, 15: 329-38.

Liu, Yidong, and Shuqun Zhang. 2004. 'Phosphorylation of 1-Aminocyclopropane-1-Carboxylic Acid Synthase by MPK6, a Stress-Responsive Mitogen-Activated Protein Kinase, Induces Ethylene Biosynthesis in Arabidopsis', *The Plant Cell*, 16: 3386-99.

Logemann, Elke, Rainer P. Birkenbihl, Bekir Ülker, and Imre E. Somssich. 2006. 'An improved method for preparing Agrobacterium cells that simplifies the Arabidopsis transformation protocol', *Plant Methods*, 2: 16.

Lolle, Signe, Christiaan Greeff, Klaus Petersen, Milena Roux, Michael Krogh Jensen, Simon Bressendorff, Eleazar Rodriguez, Kenneth Sømark, John Mundy, and Morten Petersen. 2017. 'Matching NLR

Immune Receptors to Autoimmunity in camta3 Mutants Using Antimorphic NLR Alleles', *Cell Host & Microbe*, 21: 518-29.e4.

Lu, Dongping, Shujing Wu, Xiquan Gao, Yulan Zhang, Libo Shan, and Ping He. 2010. 'A receptor-like cytoplasmic kinase, BIK1, associates with a flagellin receptor complex to initiate plant innate immunity', *Proceedings of the National Academy of Sciences*, 107: 496-501.

Lyzenga, Wendy J., and Sophia L. Stone. 2012. 'Regulation of ethylene biosynthesis through protein degradation', *Plant Signaling & Behavior*, 7: 1438-42.

Mackey, David, Youssef Belkhadir, Jose M. Alonso, Joseph R. Ecker, and Jeffery L. Dangl. 2003. 'Arabidopsis RIN4 Is a Target of the Type III Virulence Effector AvrRpt2 and Modulates RPS2-Mediated Resistance', *Cell*, 112: 379-89.

Mackey, David, Ben F. Holt, Aaron Wiig, and Jeffery L. Dangl. 2002. 'RIN4 Interacts with Pseudomonas syringae Type III Effector Molecules and Is Required for RPM1-Mediated Resistance in Arabidopsis', *Cell*, 108: 743-54.

Mao, Guohong, Xiangzong Meng, Yidong Liu, Zuyu Zheng, Zhixiang Chen, and Shuqun Zhang. 2011. 'Phosphorylation of a WRKY Transcription Factor by Two Pathogen-Responsive MAPKs Drives Phytoalexin Biosynthesis in Arabidopsis', *The Plant Cell*, 23: 1639-53.

Mitsuda, Nobutaka, Tomomi Isono, and Masa Sato. 2003. *Arabidopsis CAMTA family proteins enhance V-PPase expression in pollen*.

Miya, Ayako, Premkumar Albert, Tomonori Shinya, Yoshitake Desaki, Kazuya Ichimura, Ken Shirasu, Yoshihiro Narusaka, Naoto Kawakami, Hanae Kaku, and Naoto Shibuya. 2007. 'CERK1, a LysM receptor kinase, is essential for chitin elicitor signaling in Arabidopsis', *Proceedings of the National Academy of Sciences*, 104: 19613-18.

Nakagawa, Tsuyoshi, Takayuki Kurose, Takeshi Hino, Katsunori Tanaka, Makoto Kawamukai, Yasuo Niwa, Kiminori Toyooka, Ken Matsuoka, Tetsuro Jinbo, and Tetsuya Kimura. 2007. 'Development of series of gateway binary vectors, pGWBs, for realizing efficient construction of fusion genes for plant transformation', *Journal of Bioscience and Bioengineering*, 104: 34-41.

Newman, Mari-Anne, Thomas Sundelin, Jon T. Nielsen, and Gitte Erbs. 2013. 'MAMP (microbe-associated molecular pattern) triggered immunity in plants', *Frontiers in Plant Science*, 4: 139.

Nie, Haozhen, Chunzhao Zhao, Guangheng Wu, Yingying Wu, Yongfang Chen, and Dingzhong Tang. 2012. 'SR1, a Calmodulin-Binding Transcription Factor, Modulates Plant Defense and Ethylene-Induced Senescence by Directly Regulating NDR1 and EIN3', *Plant Physiology*, 158: 1847-59.

Nitta, Yukino, Pingtao Ding, and Yuelin Zhang. 2014. 'Identification of additional MAP kinases activated upon PAMP treatment', *Plant Signaling & Behavior*, 9: e976155.

Palm-Forster, Mieder A. T., Lennart Eschen-Lippold, and Justin Lee. 2012. 'A mutagenesis-based screen to rapidly identify phosphorylation sites in mitogen-activated protein kinase substrates', *Analytical Biochemistry*, 427: 127-29.

Pandey, Neha, Alok Ranjan, Poonam Pant, Rajiv K. Tripathi, Farha Ateek, Haushilla P. Pandey, Uday V. Patre, and Samir V. Sawant. 2013. 'CAMTA 1 regulates drought responses in Arabidopsis thaliana', *BMC Genomics*, 14: 216.

Pitzschke, Andrea, Adam Schikora, and Heribert Hirt. 2009. 'MAPK cascade signalling networks in plant defence', *Current Opinion in Plant Biology*, 12: 421-26.

Prasad, Kasavajhala V. S. K., Amira A. E. Abdel-Hameed, Denghui Xing, and Anireddy S. N. Reddy. 2016. 'Global gene expression analysis using RNA-seq uncovered a new role for SR1/CAMTA3 transcription factor in salt stress', *Scientific Reports*, 6: 27021.

Qiu, Jin‐Long, Berthe Katrine Fiil, Klaus Petersen, Henrik Bjørn Nielsen, Christopher J Botanga, Stephan Thorgrimsen, Kristoffer Palma, Maria Cristina Suarez‐Rodriguez, Signe Sandbech‐Clausen, Jacek Lichota, Peter Brodersen, Klaus D Grasser, Ole Mattsson, Jane Glazebrook, John Mundy, and Morten Petersen. 2008. 'Arabidopsis MAP kinase 4 regulates gene expression through transcription factor release in the nucleus', *The EMBO Journal*, 27: 2214-21.

Qiu, Yongjian, Jing Xi, Liqun Du, Jeffrey C. Suttle, and B. W. Poovaiah. 2012. 'Coupling calcium/calmodulin-mediated signaling and herbivore-induced plant response through calmodulin-binding transcription factor AtSR1/CAMTA3', *Plant Molecular Biology*, 79: 89-99.

Rahman, Hafizur, You-Ping Xu, Xuan-Rui Zhang, and Xin-Zhong Cai. 2016. 'Brassica napus Genome Possesses Extraordinary High Number of CAMTA Genes and CAMTA3 Contributes to PAMP Triggered Immunity and Resistance to Sclerotinia sclerotiorum', *Frontiers in Plant Science*, 7: 581.

Rahman, Hafizur, Juan Yang, You-Ping Xu, Jean-Pierre Munyampundu, and Xin-Zhong Cai. 2016. 'Phylogeny of Plant CAMTAs and Role of AtCAMTAs in Nonhost Resistance to Xanthomonas oryzae pv. oryzae', *Frontiers in Plant Science*, 7: 177.

Ranf, Stefanie, Lennart Eschen-Lippold, Katja Fröhlich, Lore Westphal, Dierk Scheel, and Justin Lee. 2014. 'Microbe-associated molecular pattern-induced calcium signaling requires the receptor-like cytoplasmic kinases, PBL1 and BIK1', *BMC Plant Biology*, 14: 374.

Ranty, Benoît, Didier Aldon, and Jean-Philippe Galaud. 2006. 'Plant Calmodulins and Calmodulin-Related Proteins: Multifaceted Relays to Decode Calcium Signals', *Plant Signaling & Behavior*, 1: 96-104.

Rao, Shaofei, Zhaoyang Zhou, Pei Miao, Guozhi Bi, Man Hu, Ying Wu, Feng Feng, Xiaojuan Zhang, and Jian-Min Zhou. 2018. 'Roles of receptor-like cytoplasmic kinase VII members in pattern-triggered immune signaling', *Plant Physiology*.

Rasmussen, Magnus W., Milena Roux, Morten Petersen, and John Mundy. 2012. 'MAP Kinase Cascades in Arabidopsis Innate Immunity', *Frontiers in Plant Science*, 3: 169.

Robatzek, Silke, Pascal Bittel, Delphine Chinchilla, Petra Köchner, Georg Felix, Shin-Han Shiu, and Thomas Boller. 2007. 'Molecular identification and characterization of the tomato flagellin receptor LeFLS2, an orthologue of Arabidopsis FLS2 exhibiting characteristically different perception specificities', *Plant Molecular Biology*, 64: 539-47.

Roitinger, Elisabeth, Manuel Hofer, Thomas Köcher, Peter Pichler, Maria Novatchkova, Jianhua Yang, Peter Schlögelhofer, and Karl Mechtler. 2015. 'Quantitative Phosphoproteomics of the Ataxia Telangiectasia-Mutated (ATM) and Ataxia Telangiectasia-Mutated and Rad3-related (ATR) Dependent DNA Damage Response in Arabidopsis thaliana', *Molecular & Cellular Proteomics*, 14: 556-71.

Roux, Milena Edna, Magnus Wohlfahrt Rasmussen, Kristoffer Palma, Signe Lolle, Àngels Mateu Regué, Gerit Bethke, Jane Glazebrook, Weiping Zhang, Leslie Sieburth, Martin R Larsen, John Mundy, and Morten Petersen. 2015. 'The mRNA decay factor PAT1 functions in a pathway including MAP kinase 4 and immune receptor SUMM2', *The EMBO Journal*, 34: 593-608.

Roux, Milena, Benjamin Schwessinger, Catherine Albrecht, Delphine Chinchilla, Alexandra Jones, Nick Holton, Frederikke Gro Malinovsky, Mahmut Tör, Sacco de Vries, and Cyril Zipfel. 2011. 'The Arabidopsis Leucine-Rich Repeat Receptor–Like Kinases BAK1/SERK3 and BKK1/SERK4 Are Required for Innate Immunity to Hemibiotrophic and Biotrophic Pathogens', *The Plant Cell*, 23: 2440-55.

Saijo, Yusuke, Eliza Po-iian Loo, and Shigetaka Yasuda. 2018. 'Pattern recognition receptors and signaling in plant–microbe interactions', *The Plant Journal*, 93: 592-613.

Schulze, Birgit, Tobias Mentzel, Anna K. Jehle, Katharina Mueller, Seraina Beeler, Thomas Boller, Georg Felix, and Delphine Chinchilla. 2010. 'Rapid Heteromerization and Phosphorylation of Ligand-activated Plant Transmembrane Receptors and Their Associated Kinase BAK1', *Journal of Biological Chemistry*, 285: 9444-51.

Schwessinger, Benjamin, and Pamela C. Ronald. 2012. 'Plant Innate Immunity: Perception of Conserved Microbial Signatures', *Annual Review of Plant Biology*, 63: 451-82.

Sebastià, Cinta Hernández, Shane C. Hardin, Steven D. Clouse, Joseph J. Kieber, and Steven C. Huber. 2004. 'Identification of a new motif for CDPK phosphorylation in vitro that suggests ACC synthase may be a CDPK substrate', *Archives of Biochemistry and Biophysics*, 428: 81-91.

Shan, Libo, Ping He, Jianming Li, Antje Heese, Scott C. Peck, Thorsten Nürnberger, Gregory B. Martin, and Jen Sheen. 2008. 'Bacterial Effectors Target the Common Signaling Partner BAK1 to Disrupt Multiple MAMP Receptor-Signaling Complexes and Impede Plant Immunity', *Cell Host & Microbe*, 4: 17-27.

Shi, Hua, Qiujing Shen, Yiping Qi, Haojie Yan, Haozhen Nie, Yongfang Chen, Ting Zhao, Fumiaki Katagiri, and Dingzhong Tang. 2013. 'BR-SIGNALING KINASE1 Physically Associates with FLAGELLIN SENSING2 and Regulates Plant Innate Immunity in Arabidopsis', *The Plant Cell*, 25: 1143-57.

Shi, Hua, Haojie Yan, Juan Li, and Dingzhong Tang. 2013. 'BSK1, a receptor-like cytoplasmic kinase, involved in both BR signaling and innate immunity in Arabidopsis', *Plant Signaling & Behavior*, 8: e24996.

Shibuya, N., and E. Minami. 2001. 'Oligosaccharide signalling for defence responses in plant', *Physiological and Molecular Plant Pathology*, 59: 223-33.

Song, Kunhua, Johannes Backs, John McAnally, Xiaoxia Qi, Robert D. Gerard, James A. Richardson, Joseph A. Hill, Rhonda Bassel-Duby, and Eric N. Olson. 2006. 'The Transcriptional Coactivator CAMTA2 Stimulates Cardiac Growth by Opposing Class II Histone Deacetylases', *Cell*, 125: 453-66.

Southern, Ed. 2006. 'Southern blotting', *Nature Protocols*, 1: 518.

Suarez-Rodriguez, Maria Cristina, Lori Adams-Phillips, Yidong Liu, Huachun Wang, Shih-Heng Su, Peter J. Jester, Shuqun Zhang, Andrew F. Bent, and Patrick J. Krysan. 2007. 'MEKK1 Is Required for flg22-Induced MPK4 Activation in Arabidopsis Plants', *Plant Physiology*, 143: 661-69.

Sun, Chih-Wen, and Judy Callis. 1997. 'Independent modulation of Arabidopsis thaliana polyubiquitin mRNAs in different organs and in response to environmental changes', *The Plant Journal*, 11: 1017-27.

Sun, Tongjun, Yukino Nitta, Qian Zhang, Di Wu, Hainan Tian, Jin Suk Lee, and Yuelin Zhang. 2018. 'Antagonistic interactions between two MAP kinase cascades in plant development and immune signaling', *EMBO reports*, 19.

Sun, Yadong, Zhifu Han, Jiao Tang, Zehan Hu, Chengliang Chai, Bin Zhou, and Jijie Chai. 2013. 'Structure reveals that BAK1 as a co-receptor recognizes the BRI1-bound brassinolide', *Cell Research*, 23: 1326-29.

Sun, Yadong, Lei Li, Alberto P. Macho, Zhifu Han, Zehan Hu, Cyril Zipfel, Jian-Min Zhou, and Jijie Chai. 2013. 'Structural Basis for flg22-Induced Activation of the Arabidopsis FLS2-BAK1 Immune Complex', *Science*, 342: 624-28.

Takken, F. L. W., and W. I. L. Tameling. 2009. 'To Nibble at Plant Resistance Proteins', *Science*, 324: 744-46.

Thulasi Devendrakumar, Karen, Xin Li, and Yuelin Zhang. 2018. 'MAP kinase signalling: interplays between plant PAMP- and effector-triggered immunity', *Cellular and Molecular Life Sciences*, 75: 2981-89.

Umezawa, Taishi, Naoyuki Sugiyama, Fuminori Takahashi, Jeffrey C. Anderson, Yasushi Ishihama, Scott C. Peck, and Kazuo Shinozaki. 2013. 'Genetics and Phosphoproteomics Reveal a Protein Phosphorylation Network in the Abscisic Acid Signaling Pathway in Arabidopsis thaliana', *Science Signaling*, 6: rs8-rs8.

van der Hoorn, Renier A. L., and Sophien Kamoun. 2008. 'From Guard to Decoy: A New Model for Perception of Plant Pathogen Effectors', *The Plant Cell*, 20: 2009-17.

Vogel, Jonathan T., Daniel G. Zarka, Heather A. Van Buskirk, Sarah G. Fowler, and Michael F. Thomashow. 2005. 'Roles of the CBF2 and ZAT12 transcription factors in configuring the low temperature transcriptome of Arabidopsis', *The Plant Journal*, 41: 195-211.

Walley, Justin W., Sean Coughlan, Matthew E. Hudson, Michael F. Covington, Roy Kaspi, Gopalan Banu, Stacey L. Harmer, and Katayoon Dehesh. 2007. 'Mechanical Stress Induces Biotic and Abiotic Stress Responses via a Novel <italic>cis</italic>-Element', *PLoS Genet*, 3: e172.

Walter, Michael, Christina Chaban, Katia Schütze, Oliver Batistic, Katrin Weckermann, Christian Näke, Dragica Blazevic, Christopher Grefen, Karin Schumacher, Claudia Oecking, Klaus Harter, and Jörg Kudla. 2004. 'Visualization of protein interactions in living plant cells using bimolecular fluorescence complementation', *The Plant Journal*, 40: 428-38.

Xiang, Tingting, Na Zong, Yan Zou, Yong Wu, Jie Zhang, Weiman Xing, Yan Li, Xiaoyan Tang, Lihuang Zhu, Jijie Chai, and Jian-Min Zhou. 2008. 'Pseudomonas syringae Effector AvrPto Blocks Innate Immunity by Targeting Receptor Kinases', *Current Biology*, 18: 74-80.

Xin, Xiu-Fang, and Sheng Yang He. 2013. 'Pseudomonas syringae pv. tomato DC3000: A Model Pathogen for Probing Disease Susceptibility and Hormone Signaling in Plants', *Annual Review of Phytopathology*, 51: 473-98.

Yamada, Kenta, Koji Yamaguchi, Tomomi Shirakawa, Hirofumi Nakagami, Akira Mine, Kazuya Ishikawa, Masayuki Fujiwara, Mari Narusaka, Yoshihiro Narusaka, Kazuya Ichimura, Yuka Kobayashi, Hidenori Matsui, Yuko Nomura, Mika Nomoto, Yasuomi Tada, Yoichiro Fukao, Tamo Fukamizo, Kenichi Tsuda, Ken Shirasu, Naoto Shibuya, and Tsutomu Kawasaki. 2016. 'The Arabidopsis CERK1 ‐ associated kinase PBL27 connects chitin perception to MAPK activation', *The EMBO Journal*, 35: 2468-83.

Yamaguchi, Koji, Kenta Yamada, Kazuya Ishikawa, Satomi Yoshimura, Nagao Hayashi, Kouhei Uchihashi, Nobuaki Ishihama, Mitsuko Kishi-Kaboshi, Akira Takahashi, Seiji Tsuge, Hirokazu Ochiai, Yasuomi Tada, Ko Shimamoto, Hirofumi Yoshioka, and Tsutomu Kawasaki. 2013. 'A Receptor-like Cytoplasmic Kinase Targeted by a Plant Pathogen Effector Is Directly Phosphorylated by the Chitin Receptor and Mediates Rice Immunity', *Cell Host & Microbe*, 13: 347-57.

Yan, Haojie, Yaofei Zhao, Hua Shi, Juan Li, Yingchun Wang, and Dingzhong Tang. 2018. 'BRASSINOSTEROID-SIGNALING KINASE1 Phosphorylates MAPKKK5 to Regulate Immunity in Arabidopsis', *Plant Physiology*.

Yang, Tianbao, and B. W. Poovaiah. 2000. 'An Early Ethylene Up-regulated Gene Encoding a Calmodulin-binding Protein Involved in Plant Senescence and Death', *Journal of Biological Chemistry*, 275: 38467-73.

———. 2002. 'A Calmodulin-binding/CGCG Box DNA-binding Protein Family Involved in Multiple Signaling Pathways in Plants', *Journal of Biological Chemistry*, 277: 45049-58.

Yoo, Sang-Dong, Young-Hee Cho, and Jen Sheen. 2007. 'Arabidopsis mesophyll protoplasts: a versatile cell system for transient gene expression analysis', *Nature Protocols*, 2: 1565.

Yuan, Peiguo, Kiwamu Tanaka, Liqun Du, and B. W. Poovaiah. 2018. 'Calcium Signaling in Plant Autoimmunity: A Guard Model for AtSR1/CAMTA3-Mediated Immune Response', *Molecular Plant*, 11: 637-39.

Zhang, Hongtao, Houjiang Zhou, Lidija Berke, Albert J. R. Heck, Shabaz Mohammed, Ben Scheres, and Frank L. H. Menke. 2013. 'Quantitative Phosphoproteomics after Auxin-stimulated Lateral Root Induction Identifies an SNX1 Protein Phosphorylation Site Required for Growth', *Molecular & Cellular Proteomics*, 12: 1158-69.

Zhang, Jie, Wei Li, Tingting Xiang, Zixu Liu, Kristin Laluk, Xiaojun Ding, Yan Zou, Minghui Gao, Xiaojuan Zhang, She Chen, Tesfaye Mengiste, Yuelin Zhang, and Jian-Min Zhou. 2010. 'Receptor-like Cytoplasmic Kinases Integrate Signaling from Multiple Plant Immune Receptors and Are Targeted by a Pseudomonas syringae Effector', *Cell Host & Microbe*, 7: 290-301.

Zhang, Jie, Feng Shao, Yan Li, Haitao Cui, Linjie Chen, Hongtao Li, Yan Zou, Chengzu Long, Lefu Lan, Jijie Chai, She Chen, Xiaoyan Tang, and Jian-Min Zhou. 2007. 'A Pseudomonas syringae Effector Inactivates MAPKs to Suppress PAMP-Induced Immunity in Plants', *Cell Host & Microbe*, 1: 175-85.

Zhang, Lei, Liqun Du, Chenjia Shen, Yanjun Yang, and B. W. Poovaiah. 2014. 'Regulation of plant immunity through ubiquitin-mediated modulation of Ca2+–calmodulin–AtSR1/CAMTA3 signaling', *The Plant Journal*, 78: 269-81.

Zhang, Tong, Sixue Chen, and Alice C. Harmon. 2016. 'Protein–protein interactions in plant mitogen-activated protein kinase cascades', *Journal of Experimental Botany*, 67: 607-18.

Zhang, Xiuren, Rossana Henriques, Shih-Shun Lin, Qi-Wen Niu, and Nam-Hai Chua. 2006. 'Agrobacterium-mediated transformation of Arabidopsis thaliana using the floral dip method', *Nature Protocols*, 1: 641.

Zhang, Zhibin, Yanan Liu, Hao Huang, Minghui Gao, Di Wu, Qing Kong, and Yuelin Zhang. 2017. 'The NLR protein SUMM2 senses the disruption of an immune signaling MAP kinase cascade via CRCK3', *EMBO reports*, 18: 292-302.

Zhang, Zhibin, Yaling Wu, Minghui Gao, Jie Zhang, Qing Kong, Yanan Liu, Hongping Ba, Jianmin Zhou, and Yuelin Zhang. 2012. 'Disruption of PAMP-Induced MAP Kinase Cascade by a Pseudomonas syringae Effector Activates Plant Immunity Mediated by the NB-LRR Protein SUMM2', *Cell Host & Microbe*, 11: 253-63.

Zipfel, Cyril, Gernot Kunze, Delphine Chinchilla, Anne Caniard, Jonathan D. G. Jones, Thomas Boller, and Georg Felix. 2006. 'Perception of the Bacterial PAMP EF-Tu by the Receptor EFR Restricts Agrobacterium-Mediated Transformation', *Cell*, 125: 749-60.

Zipfel, Cyril, Silke Robatzek, Lionel Navarro, Edward J. Oakeley, Jonathan D. G. Jones, Georg Felix, and Thomas Boller. 2004. 'Bacterial disease resistance in Arabidopsis through flagellin perception', *Nature*, 428: 764.

8 Appendix

8.1 Tables

Table I: Primers for cloning to entry vector *pENTR/D*

Description	Sequence
CAMTA3 forward	CACCATGGCGGAAGCAAGACGA
CAMTA3 no stop reverse	ACTGGTCCACAAAGATGAGGAC
CAMTA3 stop reverse	TTAACTGGTCCACAAAGATGAGGAC
SR1IP1 forward	CACCATGTCAGCAAAGAAGAAAGATCTTT
SR1IP1 no stop reverse	AGAAATAGAGTGTCTCCGATCTTTTG
SR1IP1 stop reverse	CTATCAAGAAATAGAGTGTCTCCGATC
CPK5 forward	CACCATGGGCAATTCTTGCCG
CPK5-FL no stop reverse	CGCGTCTCTCATGCTAATGTTTAG
CPK5-FL stop reverse	CTA CGCGTCTCTCATGCTAATGTTTAG
CPK5-VK no stop reverse	AACACCATTCTCACAGATCCATG
CPK5-VK stop reverse	CTA AACACCATTCTCACAGATCCATG

Table II: Primers for promoters using in the reporter activity assays

Description	Sequence
***pEDS1*-BH5**	CATGGGATCCTGCATGTCCTGATTCTTTCG
***pEDS1*-Nco3**	CGCCATGGATCTATATCTATTCTCTTTTCTTTAGTGG
***pEIN3*-BH5**	CATGGGATCCTCACCTCTTGAGAACAGATTTG
***pEIN3*-Nco3**	CGCCATGGTAACCTGTAACAAATCAAATACAC
***pZAT10*-Pst5**	CATGCTGCAGCGTCAAGATTTGTTTCCCAGC
***pZAT10*-Nco3**	CGCCATGGAGTTAAAGATTCTGAGGATTTCTTG
***pZAT12*-BH5**	CATGGGATCCTGATTGGCCGTATACTCTG
***pZAT12*-Nco3**	CGCCATGGTTCTTCTGATGATGATGATTAAAACG
***pCBF2*-BH5**	CATGGGATCACCGAAACAACCGATTCAGC
***pCBF2*-Nco3**	CGCCATGGATCAGAAGAGTACTCTGTTTCAAG
***pWRKY33*-BH5**	CATGGGATCCAGTCTTCACTCGATCGGAC
***pWRKY33*-Nco3**	CGCCATGGGAAAAATGGAAGTTTGTTTTATAAAAG
***pUBQ10*-BH5**	CATGGGATCCCGACGAGTCAGTAATAAACG
***pUBQ10*-Nco3**	CGCCATGGTGTTAATCAGAAAAACTCAG

Table III: Primers used for SDM on CAMTA3 in entry vectors

Mutation	Sequence	Enzyme	Diagnostic
S8G forward	AATTGGTCTCGTTCATGAATTAGATGTTGGACAAATAC	ApaI	BsaI
S8G reverse	AATTGGTCTCATGAACGGGCCCGAATCGTCTTGC		
T51A forward	AATTGGTCTCGGCGCCATCAAGTGGGTCTGTTTTTATG	KasI	BsaI
T51A reverse	AATTGGTCTCGGCGCCGTAGGTGGCTCAGTAGAAATTTG		
S156A forward	AATTGGTCTCGGCGCCTCAAGAAACTGGGGACGC	KasI	BsaI
S156A reverse	AATTGGTCTCGGCGCCCGAGCCGCGTCTTCAG		
S198G forward	AATTGGTCTCCGGGCCCGAACTTGAAGATGCTGAATC	ApaI	BsaI
S198G reverse	AATTGGTCTCGGCCCGTGAAAACCATTGACACTTGCTG		
T243G forward	AATTGGTCTCGGGGCCCAGGGATAGTTATCAAAAAGAGC	ApaI	BsaI
T243G reverse	AATTGGTCTCGGCCCCAAAGAGATTTGATAGTAAGGATCAAAAC		
S272G forward	AATTGGTCTCGGAGTAACAAATGGGTTAAAAAACAG	ApaI	BsaI
S272G reverse	TTAAGGTCTCTACTCCGGGCCCGTTGATAGTTTTGCTTTTG		
S454A forward	AATTGGTCTCGGCGCCTTCCCTCTCAAAGGAAC	KasI	BsaI
S454A reverse	AATTGGTCTCGGCGCCATAACATATCCATCCATG		
S469G forward	AATTGGTCTCCGGGCCCAGCTGGGCTTATGTGGGTTG	ApaI	BsaI
S469G reverse	AATTGGTCTCGGCCCGAAGTCATTGATGCTAAAGAGCTG		
S587A forward	AATTGGTCTCGGCGCCTGTTTCTGGGAATGACAG	KasI	BsaI
S587A reverse	AATTGGTCTCGGCGCCGTATTTTCAGATTTCGAGCAC		
T736G forward	AATTGGTCTCCGGGCCCTCTGATCTAGCCTATGCTAATGGTC	ApaI	BsaI
T736G reverse	AATTGGTCTCGGCCCGCTTCCTGATGGGAAATCTG		
S780A forward	AATTGGTCTCGGCGCCATCCAGCTCATCATTGAC	KasI	BsaI
S780A reverse	AATTGGTCTCGGCGCCGGAGCCATCTCAACAG		

Table IV: Primers for genotyping

Description	Sequence	Purpose
Basta-F	AACTTCCGTACCGAGCCGCA	*BAR* gene
Basta-R	GCTGAAGTCCAGCTGCCAGAAAC	
petC-F	TAAGACTCATGGTCCCGGTGAC	Genomic PCR of single copy gene
petC-R	ACCATGGAGCATCACCAGTCCT	

Table V: Primers and probes for RT-qPCR

Description	Sequence
EDS1 forward	TCATTTGGATGGAGAAAACTCA
EDS1 reverse	CCTCTAATGCAGCTTGAACGTA
EDS1 probe	FAM-AGTCTACGCTCAATGACCTTGGAGT-BHQ
NHL10 forward	ACGCCGGACAGTCTAGGA
NHL10 reverse	CCCTAAGCCTGAACTTGATCTC
NHL10 probe	FAM-ACGCGGAGAGGATATCCGGTGT-BHQ
CAMTA3 forward	GACGATTCAGCCCAGTTCAT
CAMTA3 reverse	AGAAATTTGAAATCTTTGGTAATTCTG
CAMTA3 probe	FAM-TCTCAGAAGCACGACATCGATGGC-BHQ
PP2A forward	GACCGGAGCCAACTAGGAC
PP2A reverse	AAAACTTGGTAACTTTTCCAGCA
PP2A probe	CY5-GATCTGGTGCCTGCATATGCTCGTC-BBQ

Table VI: List of constructs used in this study

Construct	Point mutations	Vector type	Fusion protein	Size [kDa]	Selection in bacteria [µg/ml]
pENTR/D-CAMTA3	-	Gateway entry	-	-	Kanamycin [50]
pENTR/D-CAMTA3-mutP1	S272G, S454A, S780A	Gateway entry	-	-	Kanamycin [50]
pENTR/D-CAMTA3-mutP2	S8G, S272G, S454A, S587A, S780A	Gateway entry	-	-	Kanamycin [50]
pENTR/D-CAMTA3-mutP2+	S8G, S243G, S272G, S454A, S587A, S780A	Gateway entry	-	-	Kanamycin [50]
pENTR/D-CAMTA3-mutP3	All S/TP are mutated to A/GP	Gateway entry	-	-	Kanamycin [50]
pDONR221-CAMTA3-mimic	All S/TP are mutated to DP	Gateway entry	-	-	Kanamycin [50]
pENTR/D-SR1IP1	-	Gateway entry	-	-	Kanamycin [50]
pENTR/D-CPK5-VK	-	Gateway entry	-	-	Kanamycin [50]
pENTR/D-CPK5m-VK	D221A	Gateway entry	-	-	Kanamycin [50]
pUGW14-CAMTA3	-	Plant expression	CAMTA3-3×HA	120	Ampicillin [100]
pUGW14-CAMTA3-mutP1	S272G, S454A, S780A	Plant expression	CAMTA3-mutP1-3×HA	120	Ampicillin [100]
pUGW14-CAMTA3-mutP2	S8G, S272G, S454A, S587A, S780A	Plant expression	CAMTA3-mutP2-3×HA	120	Ampicillin [100]
pUGW14-CAMTA3-mutP2+	S8G, S243G, S272G, S454A, S587A, S780A	Plant expression	CAMTA3-mutP2+-3×HA	120	Ampicillin [100]
pUGW14-CAMTA3-mutP3	All S/TP are mutated to A/GP	Plant expression	CAMTA3-mutP3-3×HA	120	Ampicillin [100]
pUGW14-CAMTA3-mimic	All S/TP are mutated to DP	Plant expression	CAMTA3-mimic-3×HA	120	Ampicillin [100]
pUGW18-SR1IP1	-	Plant expression	4×cMyc-SR1IP1	73	Ampicillin [100]
pE-SPYCE-CAMTA3	-	Plant expression	HA-cYFP-CAMTA3	128	Ampicillin [100]
pUC-SPYCE-CAMTA3	-	Plant expression	CAMTA3-HA-cYFP	128	Ampicillin [100]
pE-SPYNE-SR1IP1	-	Plant expression	cMyc-nYFP-SR1IP1	87	Ampicillin [100]
pUC-SPYNE-SR1IP1	-	Plant expression	SR1IP1-cMyc-nYFP	87	Ampicillin [100]
pE-SPYNE-CPK5	-	Plant expression	cMyc-nYFP-CPK5	59	Ampicillin [100]
pE-SPYNE-CPK5m	D221A	Plant expression	cMyc-nYFP-CPK5m	59	Ampicillin [100]
pUBC-CAMTA3-YFP	-	Plant expression	CAMTA3-YFP	145	Spectinomycin [50]
pUBC-CAMTA3-mutP3-YFP	All S/TP are mutated to A/GP	Plant expression	CAMTA3-mutP3-YFP	145	Spectinomycin [50]
pUBC-SR1IP1-CFP	-	Plant expression	SR1IP1-CFP	99	Spectinomycin [50]
pCambia1300-CAMTA3-cLUC	-	Plant expression	CAMTA3-cLUC	135	Kanamycin [50]
pCambia1300-CAMTA3-mutP3-cLUC	All S/TP are mutated to A/GP	Plant expression	CAMTA3-mutP3-cLUC	135	Kanamycin [50]
pCambia1300-cLUC-CFP	-	Plant expression	cLUC-CFP	50	Kanamycin [50]

pCambia1300-SR1IP1-nLUC	-	Plant expression	SR1IP1-nLUC	112	Kanamycin [50]
pEDS1-LUC	-	Plant expression	-	-	Ampicillin [100]
pEIN3-LUC	-	Plant expression	-	-	Ampicillin [100]
pZAT10-LUC	-	Plant expression	-	-	Ampicillin [100]
pZAT12-LUC	-	Plant expression	-	-	Ampicillin [100]
pCBF2-LUC	-	Plant expression	-	-	Ampicillin [100]
pWRKY33-LUC	-	Plant expression	-	-	Ampicillin [100]
p35S-LUC	-	Plant expression	-	-	Ampicillin [100]
pEarleyGate101-CAMTA3	-	Plant expression	CAMTA3-YFP-HA	146	Kanamycin [50] Rifampicin [75] Gentamycin [15] Basta (1:2500)
pDEST-N110-CAMTA3	-	Bacterial expression	His10-CAMTA3	118	Ampicillin [100]
pDEST-N110-CAMTA3-mutP1	S272G, S454A, S780A	Bacterial expression	His10-CAMTA3-mutP1	118	Ampicillin [100]
pDEST-N110-CAMTA3-mutP2	S8G, S272G, S454A, S587A, S780A	Bacterial expression	His10-CAMTA3-mutP2	118	Ampicillin [100]
pDEST-N110-CAMTA3-mutP2+	S8G, S243G, S272G, S454A, S587A, S780A	Bacterial expression	His10-CAMTA3-mutP2+	118	Ampicillin [100]
pDEST-N110-CAMTA3-mutP3	All S/TP are mutated to A/GP	Bacterial expression	His10-CAMTA3-mutP3	118	Ampicillin [100]
pDEST-N110-CAMTA3-mimic	All S/TP are mutated to DP	Bacterial expression	His10-CAMTA3-mimic	118	Ampicillin [100]
pDEST-N110-CPK5-VK	-	Bacterial expression	His10-CPK5-VK	42	Ampicillin [100]
pDEST-N110-CPK5m-VK	D221A	Bacterial expression	His10-CPK5m-VK	42	Ampicillin [100]
pDEST^{TM}22-CAMTA3	-	Yeast expression	AD-CAMTA3	-	Ampicillin [100]
pDEST^{TM}22-CAMTA3-mutP1	S272G, S454A, S780A	Yeast expression	AD-CAMTA3-mutP1	-	Ampicillin [100]
pDEST^{TM}22-CAMTA3-mutP2	S8G, S272G, S454A, S587A, S780A	Yeast expression	AD-CAMTA3-mutP2	-	Ampicillin [100]
pDEST^{TM}22-CAMTA3-mutP2+	S8G, S243G, S272G, S454A, S587A, S780A	Yeast expression	AD-CAMTA3-mutP2+	-	Ampicillin [100]
pDEST^{TM}22-CAMTA3-mutP3	All S/TP are mutated to A/GP	Yeast expression	AD-CAMTA3-mutP3	-	Ampicillin [100]
pDEST^{TM}22-CAMTA3-mimic	All S/TP are mutated to DP	Yeast expression	AD-CAMTA3-mimic	-	Ampicillin [100]
pDEST^{TM}32-SR1IP1	-	Yeast expression	DBD-SR1IP1	-	Gentamycin [15]

8.2 Figures

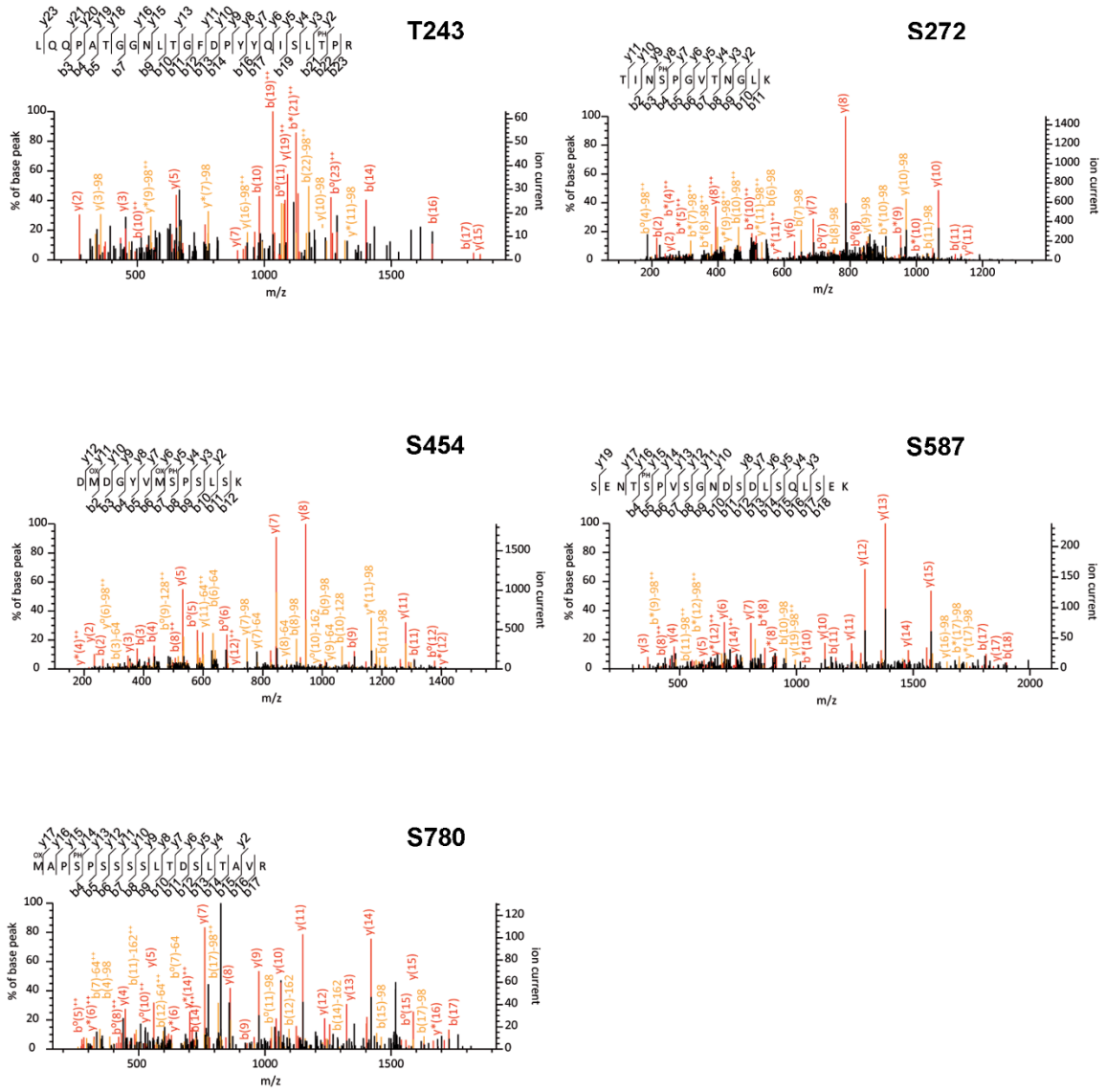

Figure I. MS spectra of peptides with phosphorylated site found in CAMTA3. Purified His-CAMTA3 was used for *in vitro* phosphorylation assay with MPK3 and MPK6 for 30 min at 37°C. After SDS-PAGE separation, excised bands were analyzed by LC-MS/MS.

Acknowledgements

Firstly, I would like to express my special thanks of gratitude to my supervisors Prof. Dierk Scheel and Dr. Justin Lee for providing me this opportunity to work on this project, and supporting me throughout my entire doctorate studies. Also, I would like to appreciate Prof. Hillel Fromm and Prof. Tina Romeis for all the supports and experimental materials that they provided to me. Moreover, I would like to thank the thesis committee for spending their precious time to evaluate my work.

I also would like to appreciate all the people I mentioned in my thesis. Especially as colleagues and friends, I would like to thank Lennart and Nicole for helping me in the lab and in the life, since I came to Germany. I would also like to thank all the other lab members in AG LEE and AG Rosahl for materials, protocols and ideas sharing, and for the nice working atmosphere, and we had a lot of fun during these years.

In the end, a special thanks from my heart goes to all my friends and my family. Five year PhD time is almost finished, and filled full of joys and sorrows. When everything did not go well, they put a lot of patience to listen to my complaint, and give me a lot of support. Especially my parents are the persons who support me the most in the world, and respect all the decisions I have made. Although we leave far away with each other, I could feel all the encouragement from you.

Curriculum Vitae

Personal Information

Name: Xiyuan Jiang
Date of birth: 31/12/1986
Date of place: Xi'an (China)
Nationality: Chinese
Address: Weinberg 3, 06120, Halle (Saale)
E-mail: xiyuan.jiang@gmail.com

Education and Working Experience

Since May 2014 **Ph.D. degree in Natural Sciences – Plant Biology**
Leibniz Institute of Plant Biochemistry (IPB) and Martin-Luther Universität Halle-Wittenberg (MLU), Germany
Thesis title: Calcium-regulated transcription in plant innate immunity: Interplay between CAMTA3 and MAPKs/CDPKs
Thesis supervisors: Prof. Dierk Scheel, Dr. Justin Lee

Dec 2011 to Dec 2013 **Assistant Research Officer – Plant Biology**
Temasek Life Sciences Laboratory (TLL), Singapore
Supervisors: Prof. Nam Hai Chua, Dr. Jian Ye and Dr. Junlin Yin

Sep 2009 to July 2011 **Master degree – Applied Biotechnology**
Uppsala University (UU), Sweden
Thesis title: Investigation antibacterial properties during hardening of dental cements
Supervisors: Prof. Håkan Engqvist, Dr. Jesper Lööf

Sep 2005 to July 2009 **Bachelor degree in Biological Sciences – Biochemistry and Molecular Biology**
China Agricultural University (CAU), China
Thesis title: Functional analysis of Millet Late Embryogenesis Abundant Protein (TiLEA)
Supervisor: Prof. Jingjuan Yu

Sep 2002 to July 2005 **High School diploma**
Xi'an Middle School of Shaanxi Province (Xi'an, China)

Publications

Furlan, G., Nakagami, H., Eschen-Lippold, L., Majovsky, P., Kowarschik, K., **Jiang, X.**, Hoehenwarter, W., Lee, J., and Trujillo, M., **Dampening of the immune response by changes in PUB22 ubiquitination modes triggered by MPK3** (2017) The Plant Cell, Vol.29: 726-745, https://doi.org/10.1105/tpc.16.00654

Sun, Y., Wang, C., Wang, N., **Jiang, X.**, Mao, H., Zhu, C., Wen, F., Wang, X., Lu, Z., Yue, G., Xu, Z., and Ye, J., **Manipulation of *Auxin Response Factor 19* affects seed size in the woody perennial *Jatropha curcas*** (2017) Scientific Reports, Vol.7: 40844, doi: 10.1038/srep40844

Eschen-Lippold, L., **Jiang, X.**, Elmore, JM., Mackey, D., Shan, L., Coaker, G., Scheel, D., Lee, J., **Bacterial AvrRpt2-Like Cysteine Proteases Block Activation of the Arabidopsis Mitogen-Activated Protein Kinases, MPK4 and MPK11** (2016) Plant Physiology, Vol.171: 2223-38, doi: 10.1104/pp.16.00336

Wang, M., Li, P., Li, C., Pan, Y., **Jiang, X.**, Zhu, D., Zhao, Q., Yu, J., **SiLEA14, a novel atypical LEA protein, confers abiotic stress resistance in foxtail millet** (2014) BMC Plant Biology, Vol.14: 290, https://doi.org/10.1186/s12870-014-0290-7

Unosson, E., Cai, Y., **Jiang, X.**, Lööf, J., Welch, K., and Engqvist, H., **Antibacterial Properties of Dental Luting Agents: Potential to Hinder the Development of Secondary Caries** (2012) International journal of dentistry, Vol.2012, Article ID 529495, 7 pages, doi:10.1155/2012/529495

Halle (Saale) Xiyuan Jiang

Declaration

I hereby declare that I have written this dissertation independently and the content contained within is solely based on my work as a Ph.D. student of Martin-Luther-Universität Halle-Wittenberg. All resources that were utilised during this study were cited and any assistance received is acknowledged accordingly.

I hereby submit this dissertation for examination for Dr.rer.nat. exclusively to the Martin-Luther-Universität Halle-Wittenberg. I also certify that it has never been submitted to other faculties or universities for examination.

Halle (Saale) Xiyuan Jiang